FELIPE VON GLEHN SILVA

“Espectro da Neuromielite Óptica: estudo clínico, imunológico e de neuroimagem.”

CAMPINAS

2013

UNIVERSIDADE ESTADUAL DE CAMPINAS
Faculdade de Ciências Médicas

FELIPE VON GLEHN SILVA

"Espectro da Neuromielite Óptica: estudo clínico, imunológico e de neuroimagem."

Orientadora: Profa. Dra. Leonilda Maria Barbosa dos Santos

Co-orientador: Prof. Dr. Benito Pereira Damasceno

Tese de Doutorado apresentada ao Curso de Pós- Graduação da Faculdade de Ciências Médicas da Universidade de Campinas- UNICAMP para obtenção do título de Doutor em Ciências Médicas, área de concentração Neurologia.

ESTE EXEMPLAR CORRESPONDE À VERSÃO FINAL DA TESE DEFENDIDO PELO ALUNO FELIPE VON GLEHN SILVA E ORIENTADO PELA PROFA. DRA. LEONILDA M.B. DOS SANTOS.

Assinatura do Orientador

CAMPINAS

2013

FICHA CATALOGRÁFICA ELABORADA POR
MARISTELLA SOARES DOS SANTOS – CRB8/8402
BIBLIOTECA DA FACULDADE DE CIÊNCIAS MÉDICAS
UNICAMP

Si38e

Silva, Felipe von Glehn, 1978-
Espectro da neuromielite óptica: estudo clínico, imunológico e de neuroimagem / Felipe von Glehn Silva. -- Campinas, SP : [s.n.], 2013.

Orientador : Leonilda Maria Barbosa dos Santos.
Coorientador : Benito Pereira Damasceno.
Tese (Doutorado) - Universidade Estadual de Campinas, Faculdade de Ciências Médicas.

1. Neuromielite óptica. 2. Paraparesia espástica tropical. 3. Aquaporina 4. 4. Neurite óptica. 5. Neuroimagem. I. Santos, Leonilda Maria Barbosa dos, 1950-. II. Damasceno, Benito Pereir, 1942-. III. Universidade Estadual de Campinas. Faculdade de Ciências Médicas. IV. Título.

Informações para Biblioteca Digital

Título em inglês: Neuromyelitis optica spectrum disorders: study of the clinical, immunological and neuroimaging aspects.

Palavras-chave em inglês:

Neuromyelitis optica

Paraparesis, Tropical spastic

Aquaporin 4

Optic Neuritis

Neuroimaging

Área de concentração: Neurologia

Titulação: Doutor em Ciências Médicas

Banca examinadora:

Leonilda Maria Barbosa dos Santos [Orientador]
Marco Aurélio Ramirez Vinolo

Li Li Min

Dagoberto Callegaro

Doralina Guimarães Brum Souza

Data da defesa: 15-05-2013

Programa de Pós-Graduação: Ciências Médicas

BANCA EXAMINADORA DA DEFESA DE DOUTORADO

FELIPE VON GLEHN SILVA

Orientador (a) PROF(A). DR(A). LEONILDA MARIA BARBOSA DOS SANTOS

MEMBROS:

1. **PROF(A). DR(A). LEONILDA MARIA BARBOSA DOS SANTOS** _____
2. **PROF(A). DR(A). MARCO AURÉLIO RAMIREZ VINOLO** _____
3. **PROF(A). DR(A). LI LI MIN** _____
4. **PROF(A).DR(A). DAGOBERTO CALLEGARO** _____
5. **PROF(A).DR(A). DORALINA GUIMARÃES BRUM SOUZA** _____

Programa de Pós-Graduação em Ciências Médicas da Faculdade de Ciências Médicas da Universidade Estadual de Campinas

Data: 15/05/2013

Trabalho realizado com apoio recebido da:

COORDENAÇÃO DE APERFEIÇOAMENTO DE PESSOAL DE NÍVEL SUPERIOR (CAPES)

FUNDAÇÃO DE AMPARO A PESQUISA DO ESTADO DE SAO PAULO (FAPESP)

Dedicatória

Dedico este trabalho à minha família: meus pais Elisabete e Xavier, minha esposa Fádua e meu filho Henrique, que sempre me ensinaram que o maior investimento que existe é o da educação; à minha orientadora Leonilda e aos pacientes.

À Profa. Leonilda M. B. dos Santos por toda a orientação e formação ao longo destes 7 anos que vai além da área cientifica, ficando como uma referência pessoal, profissional e educadora para minha vida. Agradeço a oportunidade de trabalhar em seu laboratório, fazer parte do grupo de neuroimunologia e ter me ensinado a ser um pesquisador.

Aos amigos do laboratório de Neuroimunologia pelo apoio, ensinamentos e trocas de experiências no laboratório: Alessandro Farias, Adriel Moraes, Elaine Oliveira, Rosemeire de Paula, Marília de Andrade, Alliny Lima, Walkyria Volpini, Lidiane Campos, Daniela Camilo, Fernando Pradella, Marina e Ana Leda Longhini.

Ao Prof. Benito Damasceno pela co-orientação e pela oportunidade de trabalhar no ambulatório de Esclerose Múltipla.

À equipe multidisciplinar do ambulatório de Esclerose Múltipla pelo apoio e ajuda no atendimento dos pacientes: Dr. Leonardo de Deus, Dr. Alfredo Damasceno, Juan Cabanillas, Marcos Barg, Isilda, Solaine, Sônia, Ivonilde, Cida e os residentes de neurologia.

À Dra. Clarissa Yasuda, Prof. Fernando Cendes, Dra. Fádua Hedjazi Ribeiro, Guilherme Beltramini, Felipe Bergo e ao grupo do laboratório de Neuroimagem pela ajuda imprescindível no processamento e análise das imagens do neuro-eixo dos pacientes avaliados.

Ao Prof. Augusto C. Penalva de Oliveira, Prof. Jorge Casseb, equipe de enfermagem do Hospital Dia, Rosa Marcusso e equipe da Neuroinfectologia do

Instituto de Infectologia Emílio Ribas/ Instituto de Medicina Tropical da USP pelo apoio incondicional e ajuda no atendimento aos pacientes infectados pelo HTLV-1.

Aos professores do departamento de Neurologia, que me ensinaram muito e passaram experiências valiosas durante a residência de Neurologia.

Ao Prof. Rodrigo P. Cavalcanti Lira, Dra. Maria Carolina Ferreira, Stella M. Castro e Costa e departamento de Oftalmologia pelo apoio e ajuda nas avaliações oftalmológicas e de Tomografia de Coerência Óptica dos pacientes.

A Profa. Brigitte Wildemann, Prof. Jürgen Haas, Dr. Sven Jarius e ao grupo do laboratório de Neuroimunologia da Universidade de Heidelberg (Alemanha), pelo apoio e ajuda nas análises do anticorpo anti-Aquaporina 4.

Ao Dr. Carlos Otávio Brandão pelo apoio e ensinamentos na coleta e análise do líquido cefalorraquiano.

À FAPESP e CAPES pelo apoio financeiro na realização deste estudo.

“O melhor médico é aquele que recebe os que foram desenganados por todos os outros.”

Aristóteles

A Neuromielite óptica (NMO) é uma doença inflamatória e desmielinizante do SNC, de natureza autoimune, caracterizada por surtos graves de neurite óptica e mielite transversa, de evolução mais freqüente na forma recidivante-remitente, com pouca remissão dos déficits entre as crises, altamente incapacitante. A presença do anticorpo anti-aquaporina 4 (anti-AQP4) foi descrito em 73% a 91% dos pacientes com diagnóstico de NMO. Doenças autoimunes podem frequentemente ser desencadeadas após infecções por micro-organismos, como agentes virais. A NMO e a infecção pelo HTLV-1 possuem prevalência coincidentemente elevada em certas áreas do globo, como o Brasil. Com o objetivo de avaliar a associação do HTLV-1 com a NMO, foi pesquisada a presença de anti-AQP4 e anti-HTLV-1 em 34 pacientes com DENMO, 43 pacientes infectados com HTLV-1, assintomáticos ou com a doença mielopatia associada ao HTLV-1 (HAM/TSP) e 23 controles sadios. Nenhum paciente com DENMO apresentou sorologia positiva para HTLV-1. Nenhum paciente infectado pelo HTLV-1 apresentou soropositividade para anti-AQP4. 60% dos casos de DENMO foram positivos para anti-AQP4. Esses resultados sugerem que a mielopatia associada à variante aguda da HAM/TSP e aquela associada ao anticorpo anti-AQP4 são entidades clínicas distintas, e provalvemente, não relacionadas de forma patogênica ao HTLV-1 em nosso meio.

O cérebro humano expressa amplamente AQP4, mas estudos anatomopatológicos e de neuroimagem não detectaram lesões corticais desmielinizantes ou infiltrados inflamatórios no DENMO. A fim de avaliar melhor a presença de alterações estruturais nas substâncias cinzenta e branca encefálicas no

DENMO, foram estudados 34 pacientes por RNM de 3T e tomografia de coerência óptica retiniana pareados com controles sadios, divididos nas apresentações NMO, mielite transversa longitudinal extensa (MTLE) e neurite óptica (NO), além de soropositivos versus soronegativo para anti-AQP4 e 5 anos ou menos de doença versus mais de 5 anos de doença. Houve maior grau de atrofia retiniana nos grupos NMO e NO, além dos grupos anti-AQP4+ e mais de 5 anos de doença. Foi constatado maior grau de atrofia cortical cerebral e estruturas da substância branca nos grupos NMO e MTLE, anti-AQP4+ e mais de 5 anos de doença. A atrofia retiniana se correlacionou positivamente com a atrofia do lobo occipital. Esses dados sugerem que o DENMO está associado à atrofia de estruturas das substâncias cinzenta e branca cerebrais; que a atrofia não se limita apenas às áreas das vias sensorial, motora e visual, mas é mais difusa; que quanto maior o tempo de doença e a presença do anticorpo anti-AQP4, maior é o grau de atrofia cortical, configurando estes fatores, tempo e anti-AQP4+, como de pior prognóstico; e a correlação positiva entre atrofia da camada de fibras nervosas retinianas e atrofia pericalcarina, além da escala de incapacidade funcional expandida (EDSS), sugere que a degeneração neuronal retrógrada e/ou anterógrada do tipo Walleriana é um importante causador da atrofia cortical no DENMO.

Neuromyelitis optica (NMO) is an inflammatory disease of the central nervous system (CNS) of putative autoimmune aetiology, which is characterized by severe attacks of myelitis and optic neuritis (ON). A relapsing course with rapid accumulation of neurological deficits with little or no remission is common. The NMO is autoimmune in nature and antibodies to Aquaporin 4 (AQP4) are associated with the development of the disease. AQP4 is the most common water channel protein of CNS, present in astrocytes processes, endothelium and piamater meninges. It predominates at some sites of the CNS, as optic nerve, brain stem and gray matter of medulla, the same sites of the usual inflammatory lesions. Autoimmune diseases may be triggered by microorganism infections and NMO and HTLV-1 infection have coincidentally high prevalence in certain areas of the world including Brazil. To study a possible relationship between these two diseases, we determined the seroprevalence of antibodies to AQP4 in 43 patients with HTLV-1 infection, asymptomatic or with HTLV-1 associated myelopathy (HAM/TSP) and that of HTLV-1 antibodies in patients with neuromyelitis optica spectrum disorders (NMOSD). AQP4ab positivity was found in 60% of NMOSD patients, but in none of the HAM/TSP patients and none of the asymptomatic HTLV-1 infected individuals. Conversely, all AQP4-Ab-positive NMOSD patients were negative for HTLV-1 antibodies. The results argue both against a role of antibodies to AQP4 in the pathogenesis of HAM/TSP and against an association between HTLV-1 infection and the development of AQP4-Ab. Moreover, the absence of HTLV-1 in all patients with NMOSD suggests that HTLV-1 is not a common trigger of acute attacks in patients with AQP4-Ab positive NMOSD in

populations with high HTLV-1 seroprevalence. Although AQP4 is also expressed widely in the human brain cortex, beyond the common sites of lesions in NMO, recent studies have found no MRI or histopathological evidence for cortical demyelination. To investigate magnetic resonance imaging (MRI) patterns of gray matter (GM) and white matter (WM) abnormalities in patients with NMO and its incomplete forms, isolated longitudinally extensive transverse myelitis and optic neuritis, and to assess the prognostic impact of GM and WM abnormalities in these conditions, we performed both 3T high-resolution T1-weighted and diffusion tensor MRI in thirty-four patients with NMO spectrum disorders (NMOSD) and 34 matched healthy controls. Voxel-based morphometry (SPM8/MATLAB2012b), cortical analyses (Freesurfer), and diffusion tensor imaging analyses (TBSS-FSL) were used to investigate brain abnormalities. In addition, retinal nerve fiber layer was measured by means of optic coherence tomography (OCT). These analyses resulted in following findings: (1) NMOSD is associated with GM and WM atrophy, which encompasses more brain structures than the motor, sensory, and visual pathways; (2) this atrophy is more widespread in patients with NMO and LETM than in patients with ON; (3) the extent of GM atrophy correlates with disease duration, and (4) GM/WM atrophy in NMOSD is more pronounced in AQP4 antibody-seropositive than in -seronegative patients. Furthermore, it was demonstrated for the first time in NMOSD a correlation between RNFL atrophy and GM atrophy in the occipital lobes as assessed by OCT, indicating a role for retrograde degeneration in GM atrophy and suggesting that the extent of brain GM/WM atrophy may be of prognostic relevance in NMOSD.

AQP4 – aquaporina 4

BOC – bandas oligoclonais

DENMO – distúrbios do espectro da neuromielite óptica

DTI – imagem por tensor de difusão

EDSS – escala de incapacidade funcional de Kurzke

EM – esclerose múltipla

EMRR – esclerose múltipla forma recorrente remitente

HAM – mielopatia associada ao HTLV-1

HLA – antígeno leucocitário humano

HIV – vírus da imunodeficiência humana

HTLV-1 – vírus linfotrópico de células T tipo 1

INF - interferon

IgG – imunoglobulina G

IgM – imunoglobulina M

IL - Interleucinas

LCR – líquido cefalorraquiano

MHC – complexo de histocompatibilidade principal

MTLE – mielite transversa longitudinal extensa

NMO – neuromielite óptica

NO – neurite óptica

OCT – tomografia de coerência óptica

SNC – sistema nervoso central

RNFL- camada de fibras nervosas retinianas

RNM – ressonância nuclear magnética

TBSS – *tract-based spatial statistics*

TCR – receptor de célula T

Th – linfócitos T auxiliadores

TSP – Paraparesia espástica tropical

VBM – *voxel-based morphometry*

Introdução

NEUROMIELITE ÓPTICA

A neuromielite óptica (NMO) ou Doença de Devic é uma doença inflamatória autoimune primária do sistema nervoso central (SNC) de etiologia ainda não bem esclarecida, definida por surtos, recorrente ou não, de mielite transversa e neurite óptica (1,2). A remissão espontânea é rara, sendo frequente a progressão rápida e o acúmulo de deficiências neurológicas. A média de idade do início dos sintomas é 37 anos, apesar de existirem relatos de casos ocorrendo na infância e entre idosos (3,4).

Devic e Gault no final do século XIX descreveram a neurite óptica bilateral e a mielite aguda ocorrendo ao mesmo tempo ou numa rápida sucessão, como condição *sine qua non* para o diagnóstico da NMO (5). Por muito tempo, foi discutido se a NMO era uma variante da EM, uma vez que a neurite ótica, a mielite e a inflamação desmielinizante estão relatadas nas duas doenças (4). No entanto, a apresentação clínica mais comum envolvendo os nervos ópticos e a medula; a evolução não progressiva, mas com surtos mais graves, incapacitantes e com pouca recuperação; a extensão da lesão medular, envolvendo mais de 3 corpos vertebrais vistas na ressonância nuclear magnética (RNM) de medula (1); e a descoberta do anticorpo anti-NMO em 2004 (6), com posterior descoberta do auto antígeno contra o qual ele reagia, a aquaporina 4 (AQP4) em 2005 (7), tornou possível a distinção entre NMO e EM como entidades clínicas com fisiopatogêneses diferentes(4).

A NMO está associada à presença de anticorpos contra a AQP4 em 60 a 80% dos casos (6,7). A AQP4 é o principal canal que regula a homeostase da água no

SNC, e está distribuída em alta densidade nas regiões perivasculares e subpial nos pés dos astrócitos. Ela é encontrada também nas membranas das células ependimárias, mas não nos neurônios, oligodendrócitos ou células epiteliais coroidais; acumula-se nos nervos ópticos, tronco encefálico e substância cinzenta da medula espinhal, correlacionando com os locais preferidos das lesões (8). A expressão e regulação da AQP4 tem sido estudada no sentido de entender sua fisiologia em várias condições patológicas como a NMO (9,10).

A associação da NMO com outras doenças auto-imunes como as tireoidites, lúpus eritematoso sistêmico (LES) e síndrome de Sjögren forneceu evidências sobre a natureza autoimune dessa doença (1,11). Estudos iniciais mostraram que o anticorpo anti-AQP4 foi detectado em 14 de 85.000 amostras de pacientes suspeitos de autoimunidade paraneoplásica. Posteriormente, a NMO foi confirmada em 12 dos 14 pacientes soropositivos inicialmente para os anticorpos anti-AQP4 (6). Este auto-anticorpo também foi descrito em 12 soros de 19 pacientes diagnosticados com a forma optico-espinhal de EM em asiáticos (12). Estudos realizados na Espanha, Reino Unido, França, Turquia e em um estudo multicêntrico europeu, mostraram que o anticorpo anti-AQP4 detectado pelas técnicas de Imunofluorescência e Imunoprecipitação era 91-100% específico para diferenciar a NMO ou a forma optico-espinhal da Esclerose Múltipla (13). No entanto, mesmo utilizando ensaios extremamente sensíveis cerca de 10-25% dos pacientes diagnosticados para NMO são soronegativos para os anticorpos anti-AQP4 (2). Essa observação pode indicar problemas no diagnóstico, sensibilidade dos testes ainda inadequados para quantificar esses auto-anticorpos ou a resposta imune dirigida a outro neuroantígeno que não a AQP4.

A observação de casos de síndromes agudas isoladas de mielite transversa longitudinal extensa (MTLE), com lesões contínuas envolvendo mais de 3 corpos vertebrais vistas pela RNM de medula, ou de neurite optica recorrente (NOr), associado ou não à presença de anticorpos anti-AQP4 levaram a uma nova classificação em 2006, proposta por Wingerschuk e colaboradores (4,11). Estas síndromes (NMO, MTLE e NOr) foram classificadas de uma forma mais ampla como Distúrbios do Espectro da Neuromielite Optica (DENMO). A MTLE e a NOr, formas incompletas de NMO, apresentam soropositividade para o anticorpo anti-AQP4 em aproximadamente 60% (14) e em 5-25% dos casos (15-17), respectivamente, e a sua presença determina um alto risco para evolução para forma clássica da NMO. Por este motivo, alguns autores denominam as formas incompletas de NMO soropositivos para o anti-AQP4 como síndrome de alto risco (2,4).

No Brasil, os estudos com NMO e a detecção do anticorpo anti-AQP4 estão em sua fase inicial, e em trabalho recentemente publicado pelo grupo da Universidade de São Paulo com uma casuística de 28 pacientes, os autores determinaram os níveis de anticorpo anti-AQP4 em 64% dos pacientes com NMO (18). Vários estudos estão sendo feitos no sentido de verificar se o anticorpo anti-AQP4 é apenas um marcador biológico da NMO ou se esse anticorpo atua na patogênese da doença. Trabalho recente sugere que o anticorpo anti-AQP4 deve participar da destruição tecidual observada na NMO (19), e os surtos são precedidos por um aumento sérico dos níveis deste anticorpo (20). Nos sítios lesionais são encontrados predominantemente desmielinização da substância branca medular, tronco cerebral e nervos ópticos, com infiltrado de neutrófilos e eosinófilos e deposição perivascular de imunoglobulinas IgG e IgM e componentes ativados do

complemento (21). Estas lesões podem evoluir para necrose tecidual, associado à formação de cavidade, e coincidem com as áreas de maior concentração da AQP4 no SNC (10).

ATROFIA CORTICAL, LESÃO RETINIANA, NEURITE ÓPTICA E LESÃO MEDULAR

O cérebro humano expressa amplamente AQP4, incluindo o seu córtex. Como estudos por RNM de crânio demonstraram lesões desmielinizantes corticais no cérebro de pacientes com EM forma recorrente-remitente (EMRR) desde os primeiros anos de doença (22), Calebrese e colaboradores investigaram também a existência de lesões corticais em pacientes com NMO, comparando-os com EMRR, e de forma intrigante, não encontraram lesões desmielinizantes (23). Anteriormente, um trabalho por necropsia havia estudado o córtex de pacientes com NMO e não detectou infiltrados inflamatórios e nem perda da expressão de AQP4 cortical, um achado comum nos sítios de lesões medulares e da substância branca cerebral (21,24). Entretanto, dois estudos independentes de neuroimagem detectaram atrofia de estruturas cerebrais, principalmente, em regiões ligadas aos sistemas visual, sensorial e motor (23,25). Como não existiam desmielinizações ou infiltrados inflamatórios corticais, foi levantado à hipótese de estas atrofias focais poderem estar relacionadas a um processo de degeneração retrógrada desencadeada pelas típicas lesões axonais nos nervos ópticos e medula espinhal, com repercussão nos respectivos córtex das vias lesadas (23,24,26).

Nesse sentido, estudos com tomografia de coerência óptica (OCT) demonstraram uma importante redução da espessura da camada de fibras nervosas

retinianas como consequência das lesões axonais das células ganglionares retinianas e atrofia do nervo óptico que se seguem após episódios de NO na NMO (27-30).

A fim de aprofundar o estudo das atrofias das estruturas da substância cinzenta e substância branca cerebrais, e estudar a presença de alterações precoces, analisamos através de três métodos automatizados e validados na literatura, morfometria baseada em voxel (VBM), segmentação cerebral por Freesurfer e estatística espacial baseada em tracto (TBSS) (31-33), as imagens volumétricas em T1 e em tensor de difusão do crânio adquiridas através de aparelho de RNM de alto campo (3T) de pacientes com DENMO, divididos conforme apresentação da doença (NMO, MTLE, NO), tempo de doença (5 anos ou menos do primeiro surto ou mais de 5 anos de duração) e detecção sérica do anticorpo anti-AQP4 (seropositivo ou seronegativo). Além disso, realizamos a análise retiniana dos pacientes através de OCT de última geração SOCT Spectralis OCT™ (Heidelberg Engineering, Heidelberg, Alemanha), e correlacionamos o grau de atrofia da camada de fibras nervosas retiniana com a espessura do córtex visual pericalcarino e a escala de incapacidade funcional expandida (EDSS) a fim de verificar se os fatores apresentação clinica, tempo e presença da anti-AQP4 teriam valor prognóstico.

HTLV-1 E O ANTICORPO ANTI-AQUAPORINA 4

Outro ponto a ser destacado é a existência de alguns relatos de casos associando mielite infecciosa, lesões centro medulares multi-segmentares e anticorpo anti-AQP4. Em países com alta incidência de mielite infecciosa, por vírus, fungo ou bactéria, e coincidente alta prevalência de NMO, a especificidade da

pesquisa do anticorpo anti-AQP4 pode ser comprometida (34). Além disso, não se sabe qual seria a importância destes anticorpos nestes pacientes com mielite infecciosa.

Recentemente, surgiram na literatura casos de indivíduos portadores assintomáticos do HTLV-1 ou com a forma clássica de HAM/TSP, que apresentavam uma evolução aguda de mielite transversa acompanhada ou não de neurite óptica, uma apresentação considerada típica da NMO (35-39). Consequentemente, estas síndromes clinicas receberam a denominação de HAM/TSP variante aguda. Estes relatos levantaram a possibilidade de o vírus HTLV-1 estar relacionado a surtos de NMO, pelo fato de doenças autoimunes frequentemente serem desencadeadas após infecções por micro-organismos, como agentes virais, através de mimetismo molecular com antígenos próprios em indivíduos geneticamente susceptíveis (3,4); e por ambas as doenças apresentarem prevalências elevadas, coincidentemente, em certas áreas do globo (40,41), incluindo também o Brasil (42-48).

Por esse motivo, na primeira parte do nosso trabalho, determinamos os níveis do anticorpo anti-HTLV-1 em pacientes com DENMO com o objetivo de avaliar se existia uma correlação entre a infecção viral e esta síndrome neurológica. Também foi pesquisada a presença de anticorpos anti-AQP4 nesta população de pacientes através da técnica de Imunofluorescência indireta em células HEK293 transfectadas com o gene da AQP4 humana, método mais sensível (70%) e específico (100%) disponível atualmente no mercado internacional (49,50).

A seguir, encontra-se um artigo de revisão caracterizando e comparando às mielopatias associada ao HTLV-1 e associada ao DENMO, publicada na revista Latin American Multiple Sclerosis Journal em 2013.

Latin American Multiple Sclerosis Journal | LAMSJ

REVISÃO/REVIEW/REVISIÓN

Características distintivas entre mielite transversa associada à neuromielite óptica e mielopatia associada ao HTLV-1: uma revisão sobre aspectos clínicos e imunológicos

Distinguishing characteristics between transverse myelitis associated with neuromyelitis optica and HTLV-1-associated myelopathy: a review on clinical and immunological features

Características distintivas entre mielitis transversa asociada a neuromielitis óptica y mielopatía referente al HTLV-1: una revisión de los aspectos clínicos e inmunológicos

Felipe von Glehn[1,2],
Jorge Casseb[3,4],
Carlos O Brandão[1,2],
Alessandro S Farias[5],
Augusto C P de Oliveira[4,5]
Leonilda M B Santos[1]

[1]Unidade de Neuroimunologia, Departamento de Genética, Evolução e Bioagentes, Universidade Estadual de Campinas-UNICAMP, Campinas, Brasil.
[2]Departamento de Neurologia, Universidade Estadual de Campinas-UNICAMP, Campinas, Brasil.
[3]Instituto de Medicina Tropical de São Paulo, Faculdade de Medicina da USP, São Paulo, Brasil.
[4]Unidade de Doenças Neuroinfecciosas, Departamento de Medicina Interna, Universidade Estadual de Campinas-UNICAMP, Campinas, Brasil.

Corresponding: Felipe von Glehn and Leonilda M. B. Santos.
Neuroimmunology Unit, Departamento de Genética, Evolução e Bioagentes – UNICAMP, Rua Monteiro Lobato, 255, Campinas, SP Brazil, CEP 13083-970, E-mail: fglehn@terra.com.br, leonilda@unicamp.br

Received 15 December 2012
Received in revised form 18 January 2013
Accepted 20 January 2013

Resumo

A neuromielite óptica (NMO) e a mielopatia associada ao HTLV-1/paraparesia espástica tropical (do inglês, HAM/TSP) são doenças inflamatórias do sistema nervoso central. A NMO é uma síndrome de etiologia autoimune, ainda não muito bem definida, e a HAM/TSP é considerada uma doença imunomediada associada à infecção pelo retrovírus HTLV-1, evoluindo com apresentações clínicas distintas. Recentemente, alguns casos agudos de mielite transversa e/ou neurite óptica durante o curso da HAM/TSP foram descritos, com evolução clínica semelhante à NMO, e denominados variante aguda da HAM/TSP. Estes relatos levantaram a possibilidade do HTLV-1 estar relacionado a surtos de NMO, pelo fato de doenças autoimunes frequentemente serem desencadeadas por infecções virais em indivíduos geneticamente susceptíveis, e ambas as doenças apresentarem prevalências elevadas, coincidentemente, em certas áreas do globo. O presente estudo tem como objetivo revisar os casos agudos de HAM/TSP e discutir os aspectos clínicos, patológicos e laboratoriais da mielopatia associada ao HTLV-1 e da NMO.

Palavras-chave: Neuromielite óptica; paraparesia espástica tropical, vírus 1 linfotrópico T humano.

Abstract

Neuromyelitis optica (NMO) and HTLV-1-associated myelopathy/tropical spastic paraparesis (HAM/TSP) are inflammatory diseases of the central nervous system. NMO is a syndrome of autoimmune etiology still not well defined and HAM/TSP is considered an immune-mediated disease associated with the infection of the HTLV-1 retrovirus, evolving with different clinical presentations. Recently, some acute cases of transverse myelitis and/or optic neuritis during the course of HAM/TSP were described, with a clinical evolution similar to NMO and were called acute variant of HAM/TSP. These reports raised the possibility that HTLV-1 is related to NMO attacks due to the fact that autoimmune diseases are frequently triggered by viral infections in genetically susceptible individuals and that both diseases present high prevalences, coincidently, in certain areas of the world. The objective of the present study is to review acute cases of HAM/TSP and discuss clinical, pathological and laboratory features of HTLV-1-associated myelopathy and NMO.

Keywords: *Neuromyelitis optica; tropical spastic paraparesis, human T-lymphotropic virus 1.*

Resumen

La neuromielitis óptica (NMO) y la mielopatía vinculada al HTLV-1/paraparesia espástica tropical (del inglés, HAM/TSP) son enfermedades inflamatorias del sistema nervioso central. La NMO es un síndrome de etiología autoinmune, todavía no definida muy bien, y la HAM/TSP es considerada como siendo una enfermedad inmunomediada vinculada a la infección por el retrovirus HTLV-1, evolucionando con diferentes presentaciones clínicas. Recientemente, se describieron algunos casos agudos de mielitis transversal y/o neuritis ópticas durante el curso de la HAM/TSP, con evolución clínica semejante a la NMO y denominados variación aguda de la HAM/TSP. Estos relatos indicaron la posibilidad de que el HTLV-1 pueda estar relacionado con ataques de NMO, por el hecho de que las enfermedades autoinmunes son desencadenadas, frecuentemente, por infecciones virales en individuos genéticamente susceptibles, y ambas enfermedades mostraron preponderancias altas, como coincidencia, en ciertas regiones del mundo. Este estudio tiene como objetivo revisar los casos agudos de HAM/TSP y analizar los aspectos clínicos, patológicos y de laboratorio de la mielopatía vinculada al HTLV-1 y de la NMO.

Palabras-clave: *Neuromielitis óptica; paraparesia espástica tropical, virus 1 linfotropico T humano.*

Introdução

Neuromielite óptica (NMO) é uma doença inflamatória autoimune primária do sistema nervoso central (SNC) de etiologia ainda não bem esclarecida, definida por surto, recorrente ou não, de mielite transversa e neurite óptica.[1,2] Em 60 a 80% dos casos, a NMO está associada à presença de anticorpos contra o principal canal de água do SNC, a aquaporina 4 (AQP4), considerada não apenas um biomarcador, mas um importante agente na fisiopatologia da doença.[3,4] A observação de casos de síndromes agudas isoladas de mielite transversa longitudinalmente extensa (MTLE), com lesões contínuas envolvendo três ou mais corpos vertebrais vistas pela imagem por ressonância magnética (IRM) de medula, ou de neurite óptica recorrente (NOr), associados ou não à presença de anticorpos anti-AQP4, levou a uma nova classificação em 2006, proposta por Wingerchuk e colaboradores. Essas síndromes (NMO, MTLE e NOr) foram classificadas de uma forma mais ampla como distúrbios do espectro da neuromielite óptica (DENMO)[5]. As formas incompletas de NMO (MTLE e NOr) apresentam soropositividade para o anticorpo anti-AQP4 em aproximadamente 60%[6] e em 5-25% dos casos,[7-9] respectivamente, e a sua presença determina um alto risco para evolução para forma clássica da NMO.

Paraparesia espástica tropical e mielopatia associada ao HTLV-1 (HAM/TSP) é uma doença inflamatória imunomediada predominantemente do SNC, porém relacionada a um retrovirus, o vírus linfotrópico de células T tipo 1 (HTLV-1). A manifestação clínica mais frequente é caracterizada por uma paraparesia espástica com evolução progressiva e crônica, com graus variáveis de alterações sensoriais, distúrbios urinários, constipação intestinal e disfunção erétil.[10] A fisiopatologia da HAM/TSP não está completamente elucidada, mas um dos principais mecanismos sugeridos envolve uma reação inflamatória mediada por linfócitos T citotóxicos, induzida ou não por antígenos do HTLV-1 expressos pelas células T $CD4^+$ infectadas. Essa resposta imune atua na eliminação do vírus, mas ao mesmo tempo, a inflamação resultante contribui para a lesão do tecido nervoso ao nível medular.[11-12-13]

Recentemente, surgiram casos na literatura de indivíduos portadores assintomáticos do HTLV-1 ou com a forma clássica de HAM/TSP, que apresentavam uma evolução aguda de mielite transversa acompanhada ou não de neurite óptica, uma apresentação considerada atípica da forma clássica de mielopatia associada ao HTLV-1.[14-19] Consequentemente, essas síndromes clínicas receberam a denominação de HAM/TSP variante aguda. Esses relatos levantaram a possibilidade do vírus HTLV-1 estar relacionado a surtos de NMO, pelo fato de doenças autoimunes frequentemente serem desencadeadas por infecções por micro-organismos, como agentes virais, em indivíduos geneticamente susceptíveis, através de mimetismo molecular com antígenos próprios; e ambas as doenças apresentarem prevalências elevadas, coincidentemente, em certas áreas do globo. O presente estudo objetiva revisar os casos agudos de HAM/TSP e discutir os aspectos clínicos, patológicos e laboratoriais da mielopatia associado ao HTLV-1 e aos DENMO.

Epidemiologia

Estudos epidemiológicos estimam 15 a 20 milhões de indivíduos infectados pelo HTLV-1 no mundo,[20,21] sendo as maiores prevalências observadas em alguns países da Ásia, África e América Latina.[13] Coincidentemente, apesar de poucos estudos populacionais epidemiológicos, a prevalência de DENMO é maior em pacientes asiáticos, afrodescendentes e hispânicos quando comparados com caucasianos.[8,22,23] É observada também uma predileção, em ambas as doenças, pelo sexo feminino.[13,24]

No Brasil, a infecção pelo vírus HTLV-1 já foi demonstrada em todas as regiões geográficas. Estudos nacionais com doadores de sangue demonstraram uma prevalência total de 0,45%, estimando-se que cerca de um milhão de brasileiros são portadores do HTLV-1.[25-27] Os casos registrados no Brasil de HAM/TSP, assim como de DENMO, predominam em afrodescendentes e pacientes do sexo feminino.[28-32]

Revisão de casos relacionados com síndromes agudas associadas à infecção pelo HTLV-1

Ao revisarmos a literatura na base de dados Pubmed, encontramos seis relatos de casos escritos na língua inglesa. O primeiro caso registrou um surto de neurite óptica à esquerda em uma paciente de 50 anos, que vinha em acompanhamento por HAM/TSP clássica, com anticorpos anti-HTLV-1 detectados no LCR e soro. A paciente apresentou súbita diminuição da acuidade visual, com exame clínico e imagem por IRM de crânio confirmando neurite óptica retrobulbar e excluindo outras possíveis etiologias. Na época, não existia a pesquisa do anticorpo anti-AQP4.[14] O segundo caso foi publicado em 2003 e apresentou o primeiro estudo anatomopatológico de um caso de HAM/TSP aguda. Um paciente de 52 anos desenvolveu um quadro clínico de mielite transversa associada à presença de anti-HTLV-1 no LCR e soro. Evoluiu a óbito por sepse após 11

meses de acompanhamento e o estudo anatomopatológico demonstrou infiltrados inflamatórios perivasculares e parenquimatosos envolvendo a coluna lateral da medula torácica baixa, associados à vacuolização da substância branca, características anatomopatológicas dos pacientes com HAM/TSP clássica. Ainda não existia pesquisa de anti-AQP4.[15] O caso foi descrito como variante aguda da HAM/TSP.

Puccioni-Sohler e colaboradores descreveram o terceiro caso relatando uma paciente com surto de mielite transversa, que evoluiu com óbito por sepse após três meses de seguimento. Na investigação, foram detectados anticorpos anti-HTLV e carga proviral para o HTLV-1 maior no LCR que no soro. O estudo anatomopatológico evidenciou lesões características da HAM/TSP na medula torácica e infiltrados linfocitários perivasculares envolvendo não só medula, mas também encéfalo, fígado, músculos e glândula adrenal.[16]

O quarto caso apresentou um paciente portador assintomático de HTLV-1 que evoluiu para MTLE, envolvendo seis corpos vertebrais, com anticorpo anti-HTLV-1 positivo no LCR e soro. O paciente foi tratado inicialmente com corticosteroides e na evolução, com interferon alfa. Após três anos, evoluiu com neurite óptica e novo surto medular. Na investigação, foram detectados altos títulos séricos do anticorpo anti-AQP4.[17] O quinto caso foi de um paciente de 51 anos com antecedente de neurite óptica bilateral grave e atrofia importante da camada de fibras nervosas retinianas avaliada pela tomografia de coerência óptica (do inglês, OCT). Após cinco anos, apresentou quadro medular agudo, envolvendo medula de C2 a T1 demonstrado pela imagem por IRM, com pesquisa sérica do anticorpo anti-AQP4 negativa e presença de títulos de anti-HTLV-1 maior no LCR que no soro. Houve remissão parcial dos sinais e sintomas após pulsoterapia com corticosteroides.[18] O sexto e último caso relatou a síndrome clínica de uma paciente de 19 anos, com episódios de neurite óptica recorrente, que evoluiu, posteriormente, com encefalopatia. A carga proviral do HTLV-1 foi maior no LCR que no soro e a avaliação dos anticorpos anti-AQP4 mostrou títulos elevados. Uma biópsia cerebral demonstrou lesões desmielinizantes ativas necrotizantes e ausência de AQP4, padrão característico de NMO[19] (tabela 1).

Analisando os seis casos, o estudo anatomopatológico foi o que melhor definiu o diagnóstico final, se variante aguda de HAM/TSP ou DENMO. São características da HAM/TSP infiltrados linfomonocitários parenquimatosos e perivasculares, com predomínio de linfócitos T $CD8^+$, T $CD4^+$ e B, na substância branca e cinzenta medular, mais localizados nas colunas laterais e posteriores da medula torácica, com vacuolização da substância branca circunferencial. Pode ser encontrada também inflamação sistêmica com infiltrados linfomonocitários envolvendo músculos, glândulas e fígado.[15,16,33] Por outro lado, nos DENMO, predominam lesões desmielinizantes na substância branca medular, tronco cerebral e nervos ópticos, com infiltrado de neutrófilos e eosinófilos e deposição perivascular de imunoglobulinas IgG e IgM e componentes ativados do complemento.Essas lesões podem evoluir para necrose tecidual, associada à formação de cavidade, e coincidem com as áreas de maior concentração de AQP4.[34,35] Portanto, a existência de dois padrões histopatológicos distintos, um imunocelular e outro imuno-humoral, facilita a definição diagnóstica dos casos atípicos.[35]

A carga proviral do HTLV-1 foi também um parâmetro muito utilizado. Os achados da literatura demonstraram que pacientes

Tabela 1. Relatos de caso sobre infecção pelo HTLV-1 e quadro clínico de mielite e/ ou neurite optica.

Estudos	idade, sexo	Apresentação clínica	anti-HTLV-1/ou carga pro-viral	anti-AQP4
Yoshida Y. et al., 1998[14]	50,M	HAM/TSP tipico durante 3 anos. Evoluiu com neurite óptica aguda, confirmada pela IRM de cranio.	LCR>Soro	ND
Kasahata N. et al., 2003[15]	52,H	Mielite transversa aguda com lesão medular extensa maior que 6 corpos vertebrais. Depois do óbito, estudo anatomopatológico indicou lesões tipicas de HAM/TSP.	LCR>Soro	ND
Puccioni-Sohler M. et al., 2003[16]	41, M	Mielite transversa aguda. TC de crânio normal. Depois do óbito, estudo antomopatológico indicou lesões típicas de HAM/TSP.	LCR>Soro	ND
Koga M. et al., 2009[17]	56, M	NO e mielite transversa recorrente, IRM de medula com lesão extensa maior que 6 corpos vertebrais. IRM de crânio demonstrou leões desmielinizantes periventriculares.	LCR>Soro	positivo/titulo alto 1:32.768
Olindo S. et al., 2009[18]	51, M	NO e mielite, IRM de medula indicou lesão extensa envolvendo 7 corpos vertebrais. OCT indicou atrofia de camada de fibras nervosas retiniana bilateral e assimetrica. IRM de cranio normal.	LCR>Soro	Negativo
Symmonds M. et al., 2012[19]	19, M	Neurite optica recorrente e encefalopatia subaguda. IRM de cranio demonstrou leões desmielinizantes periventriculares. Biopsia cerebral compatível com NMO.	LCR>Soro	positivo/titulo alto 1:45.000

N.D.: não disponível; LCR: liquido cefalorraquiano; IRM: Imagem por ressonância magnética; OCT: Tomografia de coerência óptica; HAM/TSP: paraplegia espástica tropical

com a doença HAM/TSP apresentam maior carga proviral nos linfócitos do sangue periférico do que portadores assintomáticos. Um grupo francês demonstrou ainda que mesmo entre os pacientes com HAM/TSP, aqueles com uma evolução do quadro clínico motor mais rápida, apresentaram maior carga proviral em comparação aos que possuíam progressão mais lenta.[36] Entretanto, alguns autores sugerem que uma carga proviral mais elevada no LCR em relação ao sangue periférico reflete melhor a inflamação que ocorre no SNC dos pacientes com HAM/TSP.[37,38] Em 2001, um interessante estudo propôs um protocolo de investigação diagnóstica para pacientes infectados pelo HTLV-1 e com distúrbios neurológicos. Esse protocolo envolveu a combinação dos resultados do índice de IgG de anticorpos específicos anti-HTLV-1 no LCR e soro, detecção de bandas oligoclonais de IgG restritas ao LCR e a pesquisa da carga proviral do HTLV-1 no LCR. A associação desses dados no algoritmo proposto resultou em sensibilidade de 96% e especificidade de 100% para o diagnóstico de HAM/TSP,[39] e, portanto, pode auxiliar na definição diagnóstica entre casos de portadores assintomáticos de HTLV-1, acometidos pelos DENMO e casos de variante aguda de HAM/TSP.

Estudo de anti-AQP4 em pacientes com HAM/TSP

O HTLV-1 é um vírus de baixa virulência e a maioria dos indivíduos infectados não desenvolve doença, permanecendo assintomática pelo resto das suas vidas. Não está claro ainda porque menos de 5% dos pacientes infectados poderão desenvolver HAM/TSP, leucemia/linfoma de células T do adulto (do inglês, ATL), uveíte e/ou outras manifestações inflamatórias. Devido à ausência de marcadores específicos correlacionando lesões do SNC e o HTLV-1, fica difícil associar apresentações clínicas atípicas de HAM/TSP ou outras manifestações neurológicas com a sua simples infecção. Assim, nos casos de evolução aguda/subaguda de mielite transversa, tem-se tentado associar o HTLV-1 como agente etiológico, após detecção de títulos mais elevados de anticorpos específicos ou carga proviral no LCR do que no sangue periférico ou ainda, utilizando a combinação do índice de IgG para anticorpos específicos anti-HTLV-1.[40] Porém, existem casos de portadores assintomáticos com elevada carga proviral no sangue periférico, sem qualquer manifestação neurológica,[40,41] ou ainda, dificuldades técnicas e financeiras para a realização da pesquisa da carga proviral em áreas distantes dos grandes centros. Esses aspectos indicam a necessidade de mais estudos na busca de possíveis biomarcadores específicos para compreensão dos fenômenos envolvidos na infecção pelo HTLV-1 e lesões do SNC, assim como ocorreu nos DENMO após a descoberta do anticorpo anti-AQP4.[4]

No caso da NMO, já foram demonstrados casos de aparecimento de anticorpo anti-AQP4 precedidos por infecções virais e bacterianas.[42,43] Para verificar se o HTLV-1 poderia agir como desencadeador dos DENMO, nosso grupo investigou a presença de anticorpos anti-AQP4 em 22 indivíduos portadores assintomáticos de HTLV-1 e 26 com HAM/TSP, sendo que três deles eram coinfectados com HIV e/ou vírus da hepatite C. Um paciente apresentou HAM/TSP aguda, com história de NO de repetição e mielite transversa. Não detectamos anti-AQP4 nos casos estudados[32]. Fizemos também a pesquisa de anticorpo anti-HTLV-1 em um grupo de pacientes com diagnóstico de DENMO clínico e soropositivo para anti-AQP4 e nenhum desses pacientes apresentou anticorpo anti-HTLV-1 detectável.[32] Esses achados nos permitiram concluir que o HTLV-1 não parece ser um agente viral comum desencadeador de DENMO; que anti-AQP4 não está comumente envolvido na fisiopatogenia da mielopatia associada ao HTLV-1; que em áreas com alta prevalência de infecção pelo HTLV-1 e casos de DENMO, como o Brasil, pacientes com quadro clínico atípico de HAM/TSP deveriam ser investigados para presença do anticorpo anti-AQP4 para melhor definição diagnóstica e proposta terapêutica adequada.

O teste de linfoproliferação espontânea é outro teste laboratorial que pode ajudar a diagnosticar HAM/TSP.[44] Como o HTLV-1 promove a hiperativação das células T, induzindo-as a secretarem citocinas inflamatórias como IL-2, IL-15, TNF-alfa e INF-gama, além de aumentarem a expressão do receptor de IL-2[45], o teste de linfoproliferação detecta aumento significativo da proliferação espontânea, sem estímulo, de linfócitos em cultura de pacientes com HAM/TSP quando comparados a controles sadios, portadores assintomáticos do HTLV-1 e na coinfecção HIV/HTLV-1, ao mesmo tempo em que apresentam uma menor resposta aos estímulos inespecíficos, como a fito hemaglutinina (PHA) e aos específicos, como o antígeno candidina (CMA). Existe também um aumento da linfoproliferação espontânea em menor grau, mas significativo, dos portadores assintomáticos comparados com os controles. Interessante é que o HIV provoca uma menor resposta proliferativa de linfócitos T, e na coinfecção HTLV-1/HIV, os linfócitos voltam a ficar hiper-reativos.[44] No caso da NMO, não existe aumento da resposta linfoproliferativa espontânea quando comparado a controles sadios.[46]

Outros dados que poderiam auxiliar na diferenciação diagnóstica entre os casos de HAM/TSP aguda e DENMO com clínica de neurite óptica seria o estudo da camada de fibras nervosas retinianas pela OCT. A literatura tem demonstrado uma atrofia retiniana importante e específica logo após os primeiros episódios de NO nos pacientes com DENMO independente da presença do anticorpo anti-AQP4[47-50] (figura 1). Dos seis casos revisados da literatura, em quatro foram relatados episódios de neurite óptica. Apenas o caso do grupo francês[18] realizou investigação complementar com OCT e o padrão apresentado foi de atrofia importante da camada de fibras nervosas de forma assimétrica, semelhante ao padrão de NO de DENMO. Não encontramos estudos de OCT em pacientes com HAM/TSP, provavelmente devido à apresentação oftalmológica mais comum relacionada ao HTLV-1 ser predominantemente a uveíte e não as alterações próprias do nervo óptico. Como a atrofia da camada de fibras nervosas retinianas é maior nos DENMO mesmo após comparação com a atrofia observada na esclerose múltipla remitente-recorrente,[50] a OCT pode ser uma boa ferramenta para ajudar no diagnóstico diferencial com a HAM/TSP aguda.

Os dados apresentados indicam que o HTLV-1 não seria um desencadeador de DENMO, uma doença autoimune, porém a coexistência das duas doenças poderia alterar a evolução natural delas, piorando a sua apresentação clínica. Nos dois únicos casos que apresentaram o anticorpo anti-AQP4, eles foram detectados em altos níveis, ultrapassando o limite máximo de titulação do método utilizado. Níveis elevados de anti-AQP4 estão associados a pior evolução clínica e riscos de surtos de mielite e/ou NO.[2,43] Além disso, os pacientes apresentaram múltiplas lesões desmielinizantes na substância branca encefálica

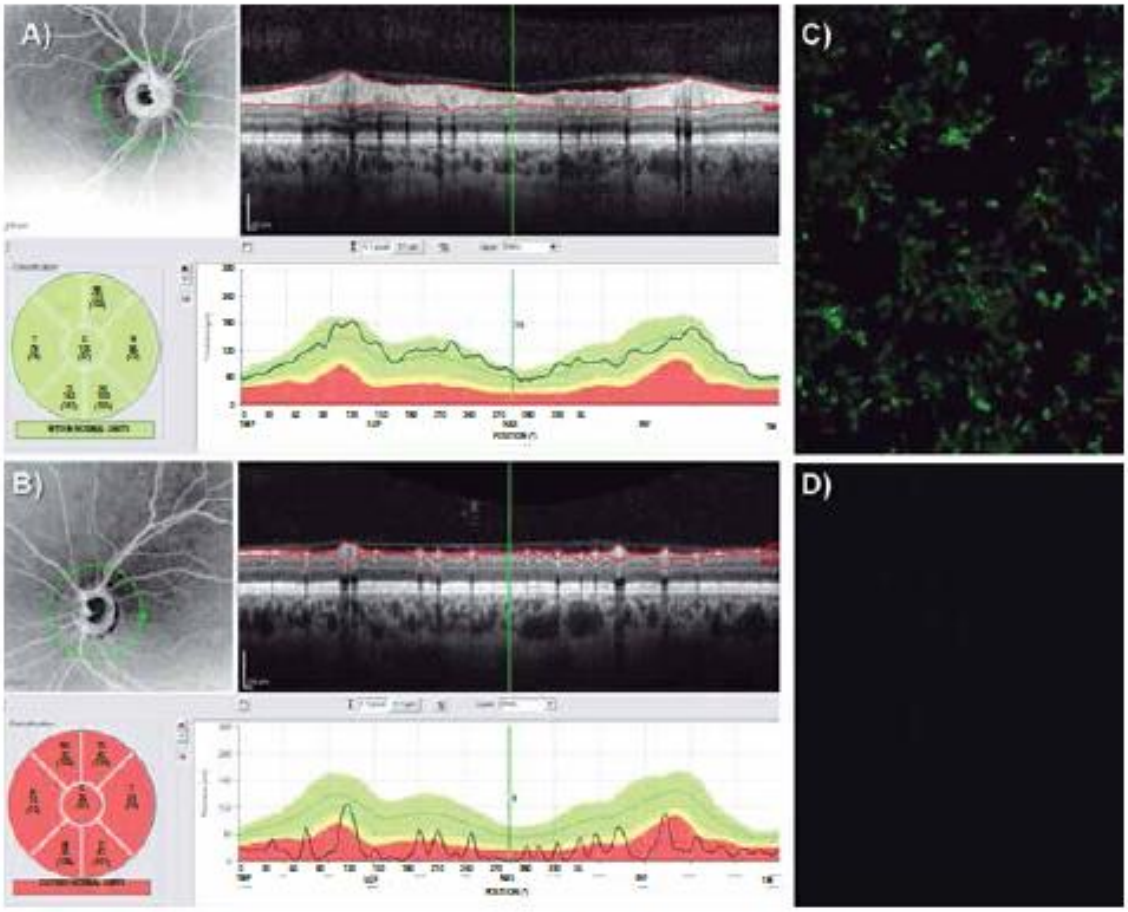

Figura 1. Exames paraclínicos utilizados para diferenciação entre DENMO e HAM/TSP. A e B representam exame de OCT de paciente com DENMO. A) Demonstra um exame normal. B) Representa uma retina com atrofia importante da camada de fibras nervosas. Comparando os exames A e B, nota-se uma atrofia envolvendo todos os seis campos retinianos (temporal, temporal superior, temporal inferior, nasal, nasal superior e nasal inferior) do olho afetado (fotos do ambulatório de Retinopatia, UNICAMP). C e D representam o estudo de Imunofluorescência indireta em células HEK293 transfectadas com o gene da aquaporina 4 humano. C) Demonstra exame positivo para o anticorpo anti-AQP4 em um paciente com DENMO. D) Representa um exame normal, sem a presença do anticorpo anti-AQP4 (fotos do laboratório de Neuroimunologia, UNICAMP).

vista na IRM de crânio.[17,19] Esses níveis elevados de anti-AQP4 poderiam estar relacionados à coestimulação de linfócitos B por células T hiperativadas pela infecção pelo HTLV-1, através do seu aumento da expressão de receptores de TNF-alfa, dentre outros mecanismos, o que levaria à maior produção de anticorpos derivados dessas células B estimuladas.[51] Porém, mais estudos são necessários para definir se a infecção pelo HTLV-1 se traduz em um fator de pior prognóstico para DENMO. Diante do exposto, a mielopatia associada à variante aguda da HAM/TSP e aquela associada ao anticorpo anti-AQP4 são entidades clínicas distintas, porém existe a possibilidade da infecção pelo HTLV-1 piorar a evolução e determinar um pior prognóstico dos pacientes com DENMO.

Conflito de interesse

Os autores declaram que não há conflito de interesses na realização deste trabalho. Este estudo recebeu apoio financeiro das agências FAPESP (Fundação de Amparo à Pesquisa do Estado de São Paulo), CAPES (Coordenação de Aperfeiçoamento de Pessoal de Nível Superior) e CNPq (Comissão Nacional de Pesquisas). Os financiadores não possuem qualquer influência no desenho do estudo, preparo do manuscrito e submissão do artigo.

Referências

1. Wingerchuk DM, Hogancamp WF, O'Brien PC, Weinshenker BG. The clinical course of neuromyelitis optica (Devic's syndrome). *Neurology.* 1999; 53(5):107-14.
2. Jarius S, Ruprecht K, Wildemann B, et al. Contrasting disease patterns in seropositive and seronegative neuromyelitis optica: A multicentre study of 175 patients. *J Neuroinflammation.*2012;9:14. Disponível em: Acesso em (10/12/2012).
3. Lennon VA, Wingerschuk DM, Kryzer TJ et al. A serum autoantibody marker of neuromyelitis optica: distinction from multiple sclerosis. *Lancet.* 2004;364(9451):106-12.
4. Jarius S, Wildemann B. AQP4 antibodies in neuromyelitis optica: diagnostic and pathogenetic relevance. *Nat Rev Neurol.* 2010;6(7):383-92.
5. Wingerchuk DM, Lennon VA, Lucchinetti CF, Pittock SJ, Weinshenker BG. The spectrum of neuromyelitis optica. *Lancet Neurol.* 2007; 6(9):805-15.
6. Pittock SJ, Lennon VA, de Seze J et al. Neuromyelitis optica and non-organ-specific autoimmunity. *Arch Neurol.* 2008; 65(1):78-83.
7. Matiello M, Lennon VA, Jacob A et al. NMO-IgG predicts the outcome of recurrent optic neuritis. *Neurology.* 2008;70 (23):2197-200.

8. Jarius S, Frederikson J, Waters P et al. Frequency and prognostic impact of antibodies to aquaporin-4 in patients with optic neuritis. *J Neurol Sci.* 2010(1-2);298:158-62.

9. Petzold A, Pittock S, Lennon V et al. Neuromyelitis optica-IgG (aquaporin-4) autoantibodies in immune mediated optic neuritis. *J Neurol Neurosurg Psychiatry.* 2010;81:109-11.

10. Osame M, Usuku K, Izumo S et al. HTLV-I associated myelopathy, a new clinical entity. *Lancet.*1986;1(8488):1031-2.

11. Jacobson S, Shida H, McFarlin DE, Fauci AS, Koenig S. Circulating CD8+ cytotoxic T lymphocytes specific for HTLV-I pX in patients with HTLV-I associated neurological disease. *Nature.*1990;348(6298):245-8.

12. Hanon E, Hall S, Taylor GP et al. Abundant tax protein expression in CD4+ T cells infected with human T-cell lymphotropic virus type I (HTLV-I) is prevented by cytotoxic T lymphocytes. *Blood.*2000;95(4):1386-92.

13. Verdonck K, Gonzalez E, Van Dooren S et al. Human T-lymphotropic virus 1: recent knowledge about an ancient infection. *Lancet Infect Dis.* 2007;7(4):266-81.

14. Yoshida Y, Saiga T, Takahashi H, Hara A. Optic neuritis and human T-lymphotropic virus type 1-associated myelopathy: a case report. *Ophthalmologica.* 1998; 212(1):73-6.

15. Kasahata N, Shiota J, Miyazawa Y, Nakano I, Murayama S. Acute human T-lymphotropic virus type 1-associated myelopathy: a clinicopathologic study. *Arch Neurol.* 2003;60(6):873-6.

16. Puccioni-Sohler M, Chimelli L, Merçon M et al. Pathological and virological assessment of acute HTLV-I-associated myelopathy complicated with encephalopathy and systemic inflammation. *J Neurol Sci.* 2003;207(1-2):87-93.

17. Koga M, Takahashi T, Kawai M, Negoro K, Kanda T. Neuromyelitis optica with HTLV-1 infection: different from acute progressive HAM? *Intern Med.* 2009; 48(13):1157-9.

18. Olindo S, Bonnan M, Merle H et al. Neuromyelitis optica associated with subacute human T-lymphotropic virus type 1 infection. *J Clin Neurosci.* 2010;17(11):1449-51.

19. Symmonds M, Nirmalananthan N, Taylor GP, Bridges LR, Schon F. Devastating aquaporin-4 and HTLV-1-associated necrotizing encephalopathy. *J Neurol.* 2012; 259 (12):2732-5.

20. Matsuoka M, Jeang KT. Human T-cell leukaemia virus type 1 (HTLV-1) infectivity and cellular transformation. *Nat Rev Cancer.* 2007;21(7):270-80.

21. Gessain A, Cassar O. Epidemiological Aspects and World Distribution of HTLV-1 Infection. *Front Microbiol.* 2012;3:388. Acesso em (01/02/2013).

22. Kira J. Multiple sclerosis in the Japanese population. *Lancet Neurol.* 2003;2(2):117-27.

23. Cabre P, Heinzlef O, Merle H et al. MS and neuromyelitis optica in Martinique (French West Indies). *Neurology.* 2001;56(4):507-14.

24. Wingerchuk DM. *Neuromyelitis optica*: effect of gender. *J Neurol Sci.* 2009;286(2-1):18-23.

25. Galvão-Castro B, Loures L, Rodrigues LG et al. Distribution of human T-lymphotropic virus type I among blood donors: a nationwide Brazilian study. *Transfusion.* 1997;37(2) : 242-3.

26. Catalan-Soares B, Carneiro-Proietti AB, Proietti FA. Interdisciplinary HTLV Research Group. Heterogeneous geographic distribution of human T-cell lymphotropic viruses I and II (HTLV-I/II): serological screening prevalence rates in blood donors from large urban areas in Brazil. *Cad Saude Publica.* 2005;21(3):926-31.

27. Kaplan JE, Osame M, Kubota H et al. The risk of development of HTLV-I-associated myelopathy/tropical spastic paraparesis among persons infected with HTLV-I. *J Acquir Immune Defic Syndr.* 1990;3(11):1096-101.

28. Lana-Peixoto MA, Lana Peixoto MI. Is multiple sclerosis in Brazil and Asia alike? *Arq Neuropsiquiatr.* 1992;50(4):419-25.

29. Papais-Alvarenga RM, Miranda-Santos CM, Puccioni-Sohler M et al. Optic neuromyelitis syndrome in Brazilian patients. *J Neurol Neurosurg Psychiatry.* 2002;73(4):429-35.

30. Kashima S, Alcantara LC, Takayanagui OM et al. Distribution of human T cell lymphotropic virus type 1 (HTLV-1) subtypes in Brazil: genetic characterization of LTR and tax region. *AIDS Res Hum Retroviruses.* 2006;22(10):953-59.

31. Adoni T, Lino AM, da Gama PD et al. Recurrent neuromyelitis optica in Brazilian patients: clinical, immunological, and neuroimaging characteristics. *Mult Scler.* 2010;16 (1):81-6.

32. von Glehn F, Jarius S, Penalva de Oliveira AC et al. Aquaporin-4 antibodies are not related to HTLV-1 associated myelopathy. *PLoS One.* 2012;7(7):e39372.

33. Iwasaki Y. Pathology of chronic myelopathy associated with HTLV-I infection (HAM/TSP). *J Neurol Sci.* 1990;96(1):103-23.

34. Lucchinetti CF, Mandler RN, McGavern D et al. A role for humoral mechanisms in the pathogenesis of Devic's neuromyelitis optica. *Brain.* 2002;125(Pt 7):1450-61.

35. Roemer SF, Parisi JE, Lennon VA et al.Pattern-specific loss of aquaporin-4 immunoreactivity distinguishes neuromyelitis optica from multiple sclerosis. *Brain.* 2007;130(Pt 5):1194-205.

36. Olindo S, Lézin A, Cabre P et al. HTLV-1 proviral load in peripheral blood mononuclear cells quantified in 100 HAM/TSP patients: a marker of disease progression. *J Neurol Sci.* 2005;237(1-2):53-9.

37. Moritoyo T, Izumo S, Moritoyo H et al. Detection of human T-lymphotropic virus type I p40tax protein in cerebrospinal fluid cells from patients with human T-lymphotropic virus type I-associated myelopathy/tropical spastic paraparesis. *J Neurovirol.*1999;5(3):241-8.

38. Nagai M, Yamano Y, Brennan MB, Mora CA, Jacobson S. Increased HTLV-I proviral load and preferential expansion of HTLV-I Tax-specific CD8+ T cells in cerebrospinal fluid from patients with HAM/TSP.*Ann Neurol.* 2001;50(6):807-12.

39. Puccioni-Sohler M, Rios M, Carvalho SM et al. Diagnosis of HAM/TSP based on CSF proviral HTLV-I DNA and HTLV-I antibody index. *Neurology.* 2001; 57(4):725-7.

40. Lezin A, Olindo S, Oliere S et al. Human T lymphotropic virus type I (HTLV-I) proviral load in cerebrospinal fluid: a new criterion for the diagnosis of HTLV-I-associated myelopathy/tropical spastic paraparesis? *J Infect Dis.* 2005;191(11):1830-4.

41. Furtado Mdos S, Andrade RG, Romanelli LC et al. Monitoring the HTLV-1 proviral load in the peripheral blood of asymptomatic carriers and patients with HTLV-associated myelopathy/tropical spastic paraparesis from a Brazilian cohort: ROC curve analysis to establish the threshold for risk disease. *J Med Virol.* 2012;84(4):664-71.

42. Wingerchuk DM. Diagnosis and treatment of neuromyelitis optica. *Neurologist.* 2007;13 (2):2-11.

43. Jarius S, Aboul-Enein F, Waters P et al. Antibody to aquaporin-4 in the long-term course of neuromyelitis optica. *Brain.* 2008;131(Pt 11):3072-80.

44. Olah I, Fukumori LM, Montanheiro P et al. Patterns of in vitro lymphoproliferative responses among HTLV-1-infected subjects: upregulation by HTLV-1 during HIV-1 co-infection. *Scand J Immunol.* 2007;65(6):577-80.

45. Matsumoto M, Sugimoto M, Nakashima H et al. Spontaneous T cell proliferation and release of soluble interleukin-2 receptors in patients with HTLV-I-associated myelopathy. *Am J Trop Med Hyg.* 1990;42(4):365-73.

46. Linhares UC, Schiavoni PB, Barros PO et al. The Ex Vivo Production of IL-6 and IL-21 by CD4(+) T Cells is Directly Associated with Neurological Disability in Neuromyelitis Optica Patients. *J Clin Immunol.* 2013;33(1):179-89.

47. Merle H, Olindo S, Donnio A, Richer R, Smadja D, Cabre P. Retinal peripapillary nerve fiber layer thickness in neuromyelitis optica. *Invest Ophthalmol Vis Sci.* 2008;49(10): 4412-7.

48. de Seze J, Blanc F, Jeanjean L et al. Optical coherence tomography in neuromyelitis optica. *Arch Neurol.* 2008;65(7):920-3.

49. Green AJ, Cree BA. Distinctive retinal nerve fibre layer and vascular changes in neuromyelitis optica following optic neuritis. *J Neurol Neurosurg Psychiatry.* 2009;80(9):1002-5.

50. Ratchford JN, Quigg ME, Conger A et al. Optical coherence tomography helps differentiate neuromyelitis optica and MS optic neuropathies. *Neurology.* 2009;73(4):302-8.

51. Higuchi M, Nagasawa K, Horiuchi T, et al. Membrane tumor necrosis factor-alpha (TNF-alpha) expressed on HTLV-I-infected T cells mediates a costimulatory signal for B cell activation--characterization of membrane TNF-alpha. *Clin Immunol Immunopathol.* 1997;82(2):133-40.

Copyright – Autorização da revista Latin American Multiple Sclerosis Journal para inclusão do artigo na tese de doutorado.

From: Marcos Moreira
Sent: Wednesday, May 22, 2013 17:36
To: Felipe von Glehn
Subject: Permissão para publicação em tese de doutorado

Prezado Dr. Felipe von Glehn,

A Latin American Multiple Sclerosis Journal (LAMSJ) autoriza a inclusão do artigo **"Distinguishing characteristics between transverse myelitis associated with neuromyelitis optica and HTLV-1 associated myelopathy: a review on clinical and immunological features"** em sua tese de doutorado.

Atenciosamente,

--
Marcos Moreira
Editor-Chefe, Latin American Multiple Sclerosis Journal
Prof. Adjunto de Neurologia, Faculdade de Ciências Médicas e da Saúde de Juiz de Fora

Objetivos

Objetivos gerais:

Estudar aspectos clínicos, imunológicos e de neuroimagem por ressonância nuclear magnética de pacientes com Distúrbios do Espectro da Neuromielite Óptica e estudar se pacientes com NMO apresentam anticorpos anti-HTLV-1, no nosso meio.

Objetivos específicos:

1. Determinar a prevalência de anticorpos anti-AQP4 no soro de pacientes acometidos pelo DENMO e pacientes infectados pelo HTLV-1, assintomáticos ou acometido pela HAM/TSP, e controles sadios.
2. Determinar a presença de anticorpos anti-HTLV-1 em pacientes com DENMO, HAM/TSP e controles sadios.
3. Determinar a espessura da camada de fibras nervosas retinianas dos pacientes com DENMO através de OCT e compará-las conforme apresentação clinica (NMO, MTLE e NO), tempo de doença (5 anos ou menos do primeiro surto ou mais de 5 anos de duração) e detecção sérica do anticorpo anti-AQP4 (seropositivo ou seronegativo).
4. Determinar a presença de alterações estruturais da substancia cinzenta e substancia branca cerebral através das análises das imagens encefálicas dos pacientes com DENMO por VBM, Freesurfer e TBSS, e compará-las conforme apresentação clinica (NMO, MTLE e NO), tempo de doença (5 anos ou menos

do primeiro surto ou mais de 5 anos de duração) e detecção sérica do anticorpo anti-AQP4 (seropositivo ou seronegativo).

5. Correlacionar o grau de atrofia da camada de fibras nervosas retiniana com a espessura do córtex visual pericalcarino e a escala clinica EDSS a fim de verificar se os fatores apresentação clinica, tempo e presença da anti-AQP4 teriam valor como fator de mal prognóstico e indicariam degeneração neuronal retrograda e/ou anterógrada.

Capítulo 1

Artigo publicado em 10 de julho 2012 na revista PLoS ONE.

OPEN ACCESS Freely available online

PLoS one

Aquaporin-4 Antibodies Are Not Related to HTLV-1 Associated Myelopathy

Felipe von Glehn[1,2]*, Sven Jarius[3], Augusto C. Penalva de Oliveira[4,5], Carlos Otávio Brandão[1,2], Alessandro S. Farias[1], Alfredo Damasceno[2], Jorge Casseb[5], Adriel S. Moraes[1], Ana Leda F. Longhini[1], Klaus-Peter Wandinger[6], Benito P. Damasceno[2], Brigitte Wildemann[3], Leonilda M. B. Santos[1]*

1 Neuroimmunology Unit, Department of Genetics, Evolution and Bioagents, University of Campinas, Campinas, Brazil, **2** Department of Neurology, University of Campinas, Campinas, Brazil, **3** Division of Molecular Neuroimmunology, Department of Neurology, University of Heidelberg, Heidelberg, Germany, **4** Neuroinfectious Disease Unit, Department of Internal Medicine, University of Campinas, Campinas, Brazil, **5** Department of Neurology, Emilio Ribas Institute of Infectious Diseases, Sao Paulo, Brazil, **6** Institute for Experimental Immunology, affiliated to Euroimmun, Luebeck, Germany

Abstract

Introduction: The seroprevalence of human T-cell leukemia virus type 1 (HTLV-1) is very high among Brazilians (~1:200). HTLV-1 associated myelopathy or tropical spastic paraparesis (HAM/TSP) is the most common neurological complication of HTLV-1 infection. HAM/TSP can present with an acute/subacute form of longitudinally extensive myelitis, which can be confused with lesions seen in aquaporin-4 antibody (AQP4-Ab) positive neuromyelitis optica spectrum disorders (NMOSD) on MRI. Moreover, clinical attacks in patients with NMOSD have been shown to be preceded by viral infections in around 30% of cases.

Objective: To evaluate the frequency of AQP4-Ab in patients with HAM/TSP. To evaluate the frequency of HTLV-1 infection in patients with NMOSD.

Patients and Methods: 23 Brazilian patients with HAM/TSP, 20 asymptomatic HTLV-1+ serostatus patients, and 34 with NMOSD were tested for AQP4-Ab using a standardized recombinant cell based assay. In addition, all patients were tested for HTLV-1 by ELISA and Western blotting.

Results: 20/34 NMOSD patients were positive for AQP4-Ab but none of the HAM/TSP patients and none of the asymptomatic HTLV-1 infected individuals. Conversely, all AQP4-Ab-positive NMOSD patients were negative for HTLV-1 antibodies. One patient with HAM/TSP developed optic neuritis in addition to subacute LETM; this patient was AQP4-Ab negative as well. Patients were found to be predominantly female and of African descent both in the NMOSD and in the HAM/TSP group; Osame scale and expanded disability status scale scores did not differ significantly between the two groups.

Conclusions: Our results argue both against a role of antibodies to AQP4 in the pathogenesis of HAM/TSP and against an association between HTLV-1 infection and the development of AQP4-Ab. Moreover, the absence of HTLV-1 in all patients with NMOSD suggests that HTLV-1 is not a common trigger of acute attacks in patients with AQP4-Ab positive NMOSD in populations with high HTLV-1 seroprevalence.

Citation: von Glehn F, Jarius S, Penalva de Oliveira AC, Brandão CO, Farias AS, et al. (2012) Aquaporin-4 Antibodies Are Not Related to HTLV-1 Associated Myelopathy. PLoS ONE 7(7): e39372. doi:10.1371/journal.pone.0039372

Editor: Christoph Kleinschnitz, Julius-Maximilians-Universität Würzburg, Germany

Received April 9, 2012; **Accepted** May 20, 2012; **Published** July 10, 2012

Funding: This study received financial support from the Brazilian government agencies FAPESP (Fundação de Amparo à Pesquisa do Estado de São Paulo -www.fapesp.br/en) and CAPES (Coordenação de Aperfeiçoamento de Pessoal de Nível Superior - www.capes.gov.br). The work of S.J. and B.W. was supported by research grants from Bayer Schering Healthcare and from Merck Serono. The funders had no role in study design, data collection and analysis, decision to publish, or preparation of the manuscript.

Competing Interests: The work of S.J. and B.W. was supported by research grants from Bayer Schering Healthcare and from Merck Serono. A.C.P.O. received consulting fees from - Abbott & Bristol and speaking fees from Abbott & GSK. K.P.W. is an employee of Euroimmun, Luebeck, Germany. This does not alter the authors' adherence to all the PLoS ONE policies on sharing data and materials.

* E-mail: fglehn@terra.com.br (FvG); leonilda@unicamp.br (LMBS)

Introduction

Neuromyelitis optica (NMO) is an inflammatory disease of the central nervous system (CNS) of putative autoimmune aetiology, which is characterized by severe attacks of myelitis and optic neuritis (ON) [1,2]. In 60–80% of cases, NMO is associated with antibodies to aquaporin-4 (AQP4-Ab), the most abundant water channel in the CNS [3–4]. AQP4-Ab are also detectable in around 60% of patients with isolated longitudinally extensive transverse myelitis (LETM) [5] and in 5–25% of patients with recurrent, isolated ON [6–8], which are therefore considered *formes frustes* of NMO. NMO, LETM, and ON are often referred to as 'NMO spectrum disorders' (NMOSD) [9].

It is estimated that 15 to 20 million individuals are infected with the human T-cell leukemia virus type 1 (HTLV-1) worldwide [10].

HTLV-1 infection remains asymptomatic in the vast majority of cases, yet less than 5% of affected individuals will develop two major diseases: adult T-cell leukaemia/lymphoma (ATL) and HTLV-1 associated myelopathy or tropical spastic paraparesis (HAM/TSP) [11]. While HAM/TSP's pathogenesis is not fully understood, it is thought to be related to a high HTLV-1 provirus burden and an exaggerated proinflammatory cellular immune response, leading to a chronic extensive myelitis [12]. Some case reports have described an acute variant of HAM/TSP, characterized by longitudinally extensive transverse myelitis (LETM) on magnetic resonance imaging (MRI), a key feature of neuromyelitis optica (NMO), which may or may not be associated with ON [13–16].

There are few population-based epidemiological studies of NMOSD, but it seems that the disease is more prevalent in peoples of Asian, African-American or Hispanic background when compared with those of Northern European descent [17–19]. Accordingly, the proportion of NMOSD patients among all patients with CNS demyelinating disorders is high in Brazil [20]. At the same time, Brazil is among the countries with the highest prevalence of HTLV-1 infected individuals [12,21]. Moreover, both among patients with AQP4-Ab positive NMOSD and among patients with HAM/TSP an afrodescendant predilection was reported [12,22–24].

As testing for aquaporin-4 antibodies (AQP4-Ab) became available only few years ago, cases of AQP4-Ab positive LETM occurring in the context of HTLV-1 seropositivity might thus have been misdiagnosed as acute HAM/TSP in a subset of patients in the past. Furthermore, AQP4-Ab positive NMO was shown to be frequently preceded by viral or bacterial infections and HTLV-1 infection may act as a trigger of NMO in some cases [1–2].

This study aimed to determine the seroprevalence of antibodies to AQP4 in patients with HTLV-1 associated myelopathy (HAM/TSP) and that of HTLV-1 antibodies in patients with neuromyelitis optica spectrum disorders (NMOSD) and to compare the clinical characteristics of a HAM/TSP and NMOSD in Brazilian patients.

Patients and Methods

Patients

This is a cross-sectional study that included along with regular visits NMOSD patients who were followed-up at the neurological outpatient unit of the University of Campinas (UNICAMP) Hospital as well as HTLV-1 seropositive asymptomatic and HAM/TSP patients attending the outpatient clinic at the Emilio Ribas State Reference Institute of Infectious Diseases and at the UNICAMP Hospital, São Paulo, Brazil, during the period of January 2011 to January 2012.

At each appointment, demographic and clinical data were collected and the neurological statuses were evaluated by different scales, including the EDSS [25] and Osame scales [26]. We excluded from the study other causes of transverse myelitis, clinically and radiologically, such as spinal cord compression, infectious myelopathy, including parasitic etiology (e.g. *Schistosoma mansoni*, which is endemic in northeast Brazil) [27], spinal cord ischemia or bleeding, vitamin B12 and folate deficiency, among others. We also excluded patients co-infected with hepatitis C virus (HCV), hepatitis B virus (HBV), human immunodeficiency virus types 1 and 2 (HIV-1/2) and HTLV type 2 in the HTLV-1 seropositive group. We decided to exclude these potentially confounding factors, because these viruses co-infection could interact and transactivate each other, thus altering the clinical presentation of the myelopathy. Moreover, HIV itself may cause vacuolar myelopathy, which shares some neurological traits with HAM/TSP and could turn it difficult to determine which virus was causing the clinical myelopathy [28].

Peripheral blood samples were collected from patients diagnosed with HAM/TSP as defined by World Health Organization (WHO) criteria [29], from asymptomatic individuals with positive HTLV-1 serostatus, from patients diagnosed with NMO spectrum disorders (NMOSD) [30], and from healthy controls (HC) (Table 1). NMO was diagnosed according to Wingerchuk's revised 2006 criteria without the need for positive AQP4-Ab testing. LETM was defined as acute myelitis with spinal cord lesions extending over three or more vertebral segments on magnetic resonance imaging; the median time between onset of transverse myelitis symptoms and spinal MRI in the LETM group was 7 days (range, 5–25 days). ON was defined as the occurrence of at least two episodes of clinical optic neuritis, with an interval of more than 30 days between them, and of no brain lesions outside the optic nerves.

Ethics Statement

UNICAMP and Emilio Ribas Institute of Infectious Diseases Ethics Committees for Research approved the study and all patients provided informed written consent. On the behalf of the minors/children participants involved in our study, we obtained informed written consent from one of their parents.

Methods

We tested all peripheral blood samples for AQP4-Ab in a standardized cell based immunofluorescence assay (Figure 1) employing recombinant human AQP4 (Euroimmun AG, Germany) [31] at the Neuroimmunology Laboratory of the University of Campinas and for HTLV-1 in a commercial enzyme immunosorbent assay (ELISA) kit (HTLV-I/II ELISA 4.0, MP Diagnostics, Germany). When a serum sample tested positive, it was confirmed by a Western blot (WB) assay (HTLVblot 2.4, MP Diagnostics, Germany) at the Laboratory of Retrovirology of Emilio Ribas Institute of Infectious Diseases. Data were analyzed using GraphPad Prism 5. Statistical significance of differences was determined by Chi-square or Fisher's exact test for binominal outcomes and by ANOVAs without assuming Gaussian distribution (Kruskal-Wallis test) and subsequent Dunn's multiple comparison tests. Differences were considered statically significant with p values <0.05.

Results

Detection of AQP4-Ab in Serum of Patients with NMOSD, HAM/TSP and Healthy Control

Serum AQP4-Ab were detected in 20 out of 34 (59%) patients in the NMOSD group, which included patients with NMO (positive in 14/17 cases) and patients with syndromes considered to confer a high risk for conversion to NMO (recurrent ON or LETM; positive in 6/17 cases) (see Table 1 for details), but in none of the patients previously diagnosed with HAM/TSP (n = 23), in none of the patients with positive HTLV-1 serostatus but no neurological symptoms at the time of presentation (n = 20), and in none of the HCs (n = 23) ($p<0.0001$; Chi-square test). Moreover, while all patients previously diagnosed with HAM/TSP were positive for HTLV-1 antibodies, as detected by ELISA and confirmed by WB assay, all patients with NMOSD were negative.

During the study, we excluded two asymptomatic patients that turned out to be infected with HTLV type 2 after WB test and three HAM/TSP patients that were co-infected with HCV and/or HIV1/2. All of them tested negative for serum AQP4-Ab.

Table 1. Demographic and baseline clinical characteristics of patients and controls.

	Patients #	Age (years)*	Gender F/M	Time from first symptoms (years)*	EDSS**	Osame scale	Aqua4-Ab (%)	CSF Oligoclonal bands (%)***
NMOSD	34	38 (14–76)	26/8	4 (1–17)	4.5 (1–8.5)	3.5 (1–10)	20/34 (59%)	10/34 (29%)
NMO	17	38 (17–63)	15/2	5 (2–17)	5.5 (2.0–8.5)	3 (1–10)	14/17 (82%)	7/17 (41%)
HRS	17	38 (14–76)	11/6	1 (1–9)	3.0 (1.0–8.0)	1 (0–10)	6/17 (35%)	3/17 (18%)
LETM	11	43 (14–76)	8/3	1 (1–3)	5.5 (1.0–8.0)	4 (1–10)	4/11 (36%)	3/11 (27%)
ON	6	32 (16–49)	3/3	5 (1–9)	2.5 (1.0–3.0)	0 (0–0)	2/6 (33%)	0/6 (0%)
HAM/TSP	23	49 (22–83)	16/7	8 (4–21)	6.5 (2.0–7.5)	5 (1–9)	0/23 (0%)	N.d.
HTLV-1+ asymptomatic	20	51.5 (34–72)	17/3	N.a.	N.a.	N.a.	0/20 (0%)	N.a.
Normal controls	23	30 (21–61)	16/7	N.a.	N.a.	N.a.	0/23(0%)	N.a.

*Median (range); **EDSS = Expanded disability status scale score;
***CSF Oligoclonal bands = Two or more cerebrospinal fluid restricted IgG oligoclonal bands.
HRS = high risk syndromes (patients at high risk for conversion into NMO); N.a.= Not applicable; N.d.= Not done.
doi:10.1371/journal.pone.0039372.t001

Clinical Characteristics and Comparison of the Study Population

The demographic and baseline clinical characteristics of the study population are shown in Table 1. Most patients of the HAM/TSP group had progressive lower limb weakness and muscle spasticity, sensory disturbances, dorsal pain, neurogenic bladder, and bowel and sexual dysfunction. The patients with NMOSD usually presented severe attacks of ON, with poor recovery leading to low vision, with no or only light perception in one or both eyes, and/or myelitis with severe motor disability and deep sense and sphincters disturbance. Pain was also frequent, occurring in 8 out of 11 (73%) in the LETM group and in 12 out of 17 (71%) in the NMO group, and usually affected one or more areas of the chest, waist, legs, and back.

One patient developed an atypical form of HAM/TSP with relapsing subacute LETM and ON. HTLV-1 antibodies were detectable in serum and in the cerebrospinal fluid (CSF) of this patient by western blot analysis; by contrast, serum AQP4-Ab were negative. Moreover, *in vitro* culture of T-cells from this patient's peripheral blood mononuclear cells (PBMC) revealed an elevated spontaneous proliferative response when compared with a healthy control. After cells were cultured for 48h and pulsed with thymidine during 18h, the proliferative response were determinated by the mean incorporation of thymidine in DNA, and indicated as counts per minute (cpm). This spontaneous proliferation of PBMC *in vitro* is an immunopathologic characteristic of HTLV-1–infected individuals, driven by the HTLV-1-encoded TAX protein and indicate the exaggerated proinflammatory cellular immune response [12,32].

In the NMOSD group, no difference regarding gender was found between AQP4-Ab positive and negative patients ($p = 0.23$, Fisher's exact test). 15 out 32 (47%) patients self-reported their ethic origin as afrodescendant in the NMOSD group, 9 out of 17 (53%) in the HAM/TSP group, and 7 out 15 (47%) in the HTLV-1+ group.

Regarding the median degree of disability, as measured by Osame scale ($p = 0.47$) and EDSS ($p = 0.52$), there were no statistically significant differences between the three groups (Figure 2). An Osame scale score $>= 4$ (unilateral walking aid needed) was found in 80% of the HAM/TSP patients, in 47% of the NMO patients, and in 54% of the LETM patients. An EDSS score ≥ 6.5 (constant bilateral assistance needed to walk at least 20 meters without resting) had 60% of the HAM/TSP patients, 41% of the NMO patients, and 45% of the LETM patients.

Discussion

Our findings are relevant not only from a diagnostic but also from a pathophysiological point of view. HTLV-1 infection is highly prevalent among Brazilians, and patients with HAM/TSP can present with an acute/subacute form of longitudinally extensive myelitis, which can be confused with LETM lesions seen in NMOSD on MRI. Our results argue both against a role of antibodies to AQP4 in the pathogenesis of HAM/TSP and against an association between HTLV-1 infection and the development of AQP4-Ab. Moreover, the fact that antibodies to HTLV-1 were absent in all patients with NMOSD suggests that HTLV-1 is not a common trigger of acute attacks in patients with AQP4-Ab positive NMOSD, a disorder in which relapses are often preceded by infection, in populations with high HTLV-1 seroprevalence.

NMOSD and HAM/TSP are both highly prevalent in some global areas. In Japan and in Martinique, for example, NMOSD accounts for around 40% and 17.3% of cases of CNS demyelinating diseases, respectively, and these areas also feature a high prevalence of HTLV-

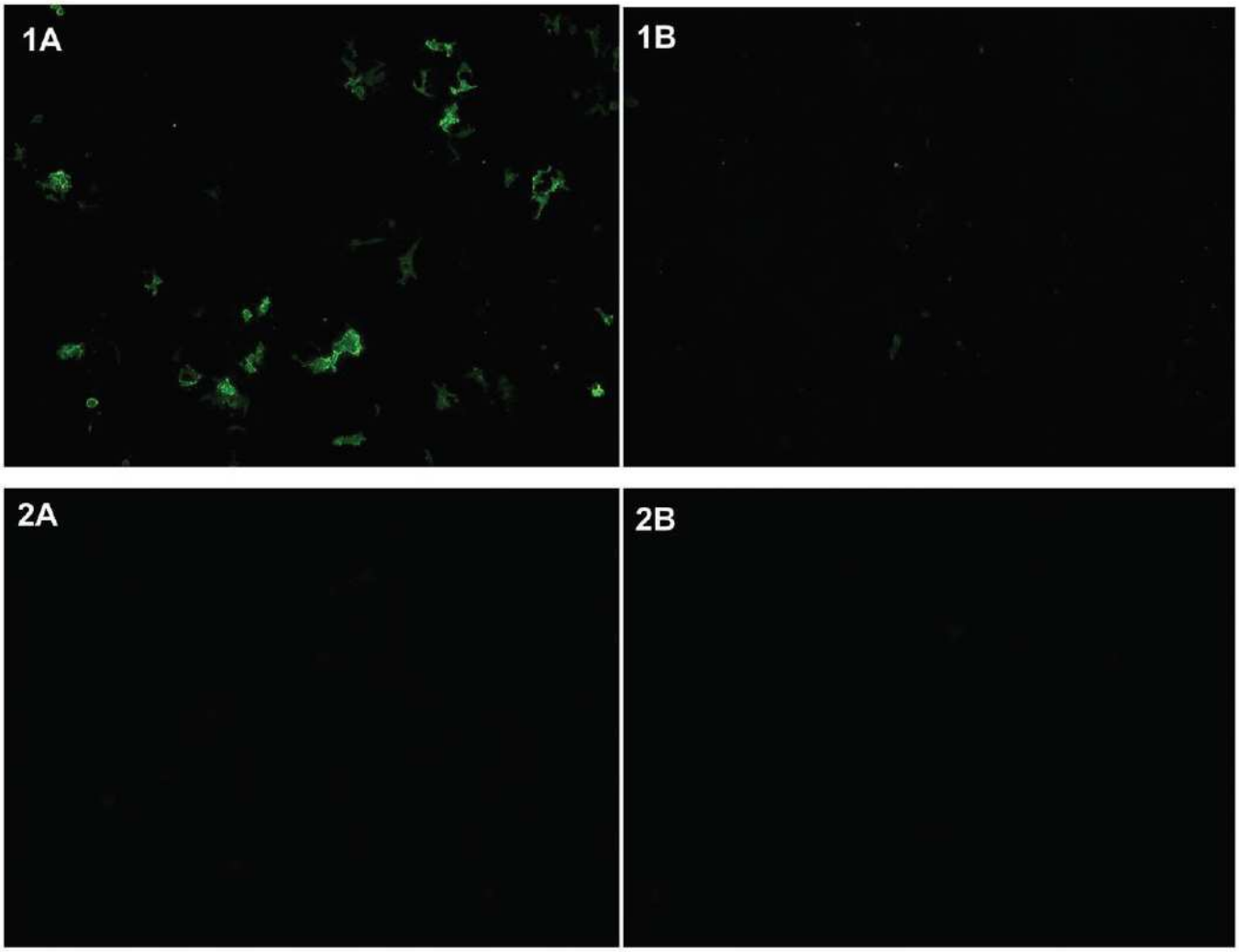

Figure 1. Cell based assay. Antibodies to aquaporin-4 (AQP4) as detected by binding of patient IgG to HEK293 cells transfected with human full length AQP4 (left column) but not to non-transfected control HEK293 cells (right column). **1A and B:** Positive AQP4-Ab test in a patient with NMO according to Wingerchuk's 2006 criteria [29]. **2A and B:** Negative AQP4-Ab test in a patient with HAM/TSP as defined by World Health Organization criteria [28].
doi:10.1371/journal.pone.0039372.g001

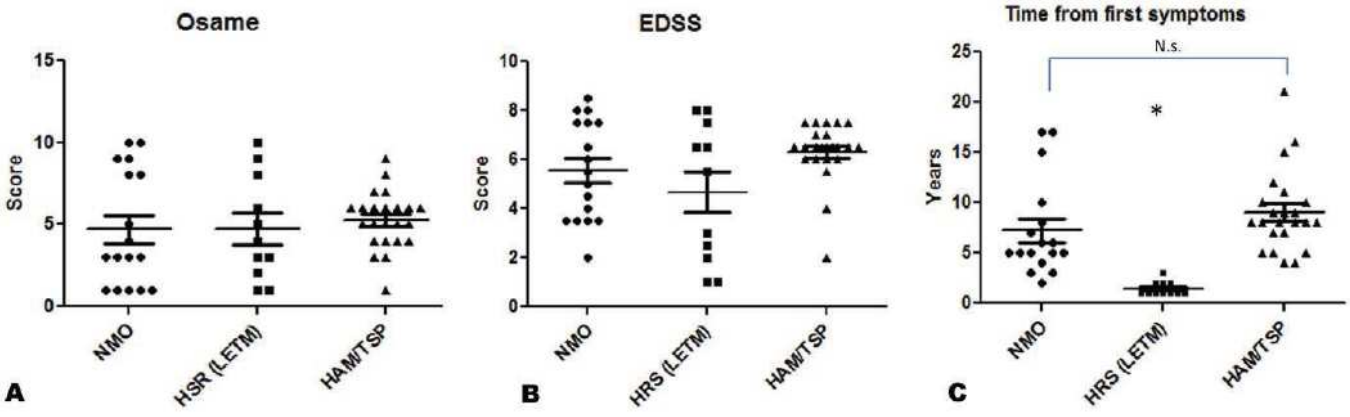

Figure 2. Disease duration and disability. (**A** and **B**) Disability scores as measured by the Osame scale ($p = 0.52$, Kruskal Wallis Test) and by the EDSS scores ($p = 0.35$, Kruskal Wallis Test) did not differ significantly between patients with established NMO, non-HTLV-1-associated LETM, and HAM/TSP. (**C**) The fact that the median Osame and EDSS scores did not differ between LETM and the other groups despite shorter disease duration in the LETM group reflects the rapid accumulation of disability in NMOSD as described before ($p < 0.0001$, Kruskal Wallis Test. Dunn's multiple comparison test did not demonstrate significant difference between NMO vs. HAM/TSP groups) [1,2].
doi:10.1371/journal.pone.0039372.g002

1 infection [12,18,19]. In Brazil, around 30% of patients with CNS demyelinating diseases present with optic spinal symptoms and around 12% with strict NMO [20]. The seroprevalence of HTLV-1 has been reported to be 0.45% among volunteer blood-donors in Brazil in a nationwide survey [21]. Epidemiological studies indicate that NMOSD more commonly affects patients of non-Caucasian background [17], as do HTLV-1 infection. Similarly, a higher proportion of afrodescendants and Asians than Caucasians has been found among Brazilian HTLV-1 patients [22]; the latter fact has been discussed to reflect the African origin of HTLV-1, which is thought to be derived from primate T-lymphotropic virus (PTLV) and later spreading with the old population's migratory pathway [12]. Accordingly, we found a high proportion of individuals with afrodescendant both in the NMOSD and in the HAM/TSP group in our study.

Regarding the patients' epidemiological data, we found an older median age at onset in the HAM/TSP group compared to the NMOSD group in accordance with the literature, possibly reflecting the long latency of HTLV-1 infection [9,29]. A female preponderance was found in all groups. While the higher proportion of females in the HAM/TSP group can be explained by the higher sexual transmission efficiency from men to women than from women to men [33], that observed in the NMOSD group is in line with the putative autoimmune aetiology of this disorder; female preponderance is a common characteristic of many autoimmune diseases [34].

The relative high EDSS and Osame scores in the NMOSD group as compared to the HAM/TSP group despite a shorter disease duration reflects the attack severity in NMOSD with poor recovery [1,2], which is in contrast with the mostly progressive course of disease in HAM/TSP. The frequency and distribution of pain symptoms in the NMOSD group is in line with the literature [2,35]. The relatively low frequency of CSF oligoclonal bands (29%) in our NMOSD patients is also in accordance with previous studies, which consistently demonstrated a lower frequency of CSF OCB when compared to multiple sclerosis patients [1,36,37].

In conclusion, our findings indicate that misdiagnosis of NMOSD as HAM/TSP is rare and support the view that LETM associated to either HAM/TSP or NMO are distinct disorders, which are likely to be pathogenetically unrelated.

Acknowledgments

The AQP4-Ab assay used in this study was kindly provided by Euroimmun AG, Luebeck, Germany.

Author Contributions

Conceived and designed the experiments: FvG SJ ACPdO LMBS. Performed the experiments: FvG ASF JC ALFL ASM. Analyzed the data: FvG SJ ACPdO COB ASF LMBS. Contributed reagents/materials/analysis tools: FvG COB AD BPD JC ACPdO KPW. Wrote the paper: FvG SJ COB LMBS. Involved in critical revision of the manuscript for important intellectual content: FvG SJ ACPdO COB AD JC KPW BPD BW LMBS. Read and approved the final version of the manuscript: FvG SJ ACPdO COB ASF AD JC ASM ALFL KPW BPD BW LMBS.

References

1. Wingerchuk DM, Hogancamp WF, O'Brien PC, Weinshenker BG (1999) The clinical course of neuromyelitis optica (Devic's syndrome). Neurology 53: 1107–1114.
2. Jarius S, Ruprecht K, Wildemann B, Kuempfel T, Ringelstein M, et al. (2012) Contrasting disease patterns in seropositive and seronegative neuromyelitis optica: A multicentre study of 175 patients. J Neuroinflammation 9: 14.
3. Lennon VA, Wingerschuk DM, Kryzer TJ, Pittock SJ, Lucchinetti CF, et al. (2004) A serum autoantibody marker of neuromyelitis optica: distinction from multiple sclerosis. Lancet 364: 2106–2112.
4. Jarius S, Wildemann B (2010) AQP4 antibodies in neuromyelitis optica: diagnostic and pathogenetic relevance. Nat Rev Neurol 6: 383–392.
5. Pittock SJ, Lennon VA, de Seze J, Vermersch P, Homburger HA, et al. (2008) Neuromyelitis optica and non-organ-specific autoimmunity. Arch Neurol 65: 78–83.
6. Matiello M, Lennon VA, Jacob A, Pittock SJ, Lucchinetti CF, et al. (2008) NMO-IgG predicts the outcome of recurrent optic neuritis. Neurology 70: 2197–2200.
7. Jarius S, Frederikson J, Waters P, Paul F, Akman-Demir G, et al. (2010) Frequency and prognostic impact of antibodies to aquaporin-4 in patients with optic neuritis. J Neurol Sci 298: 158–162.
8. Petzold A, Pittock S, Lennon V, Maggiore C, Weinshenker BG, et al. (2010) Neuromyelitis optica-IgG (aquaporin-4) autoantibodies in immune mediated optic neuritis. J Neurol Neurosurg Psychiatry 81: 109–111.
9. Wingerchuk DM, Lennon VA, Lucchinetti CF, Pittock SJ, Weinshenker BG (2007) The spectrum of neuromyelitis optica. Lancet Neurol 6: 805–815.
10. Matsuoka M, Jeang KT (2007) Human T-cell leukaemia virus type 1 (HTLV-1) infectivity and cellular transformation. Nat Rev Cancer 7: 270–280.
11. Kaplan JE, Osame M, Kubota H, Igata A, Nishitani H, et al. (1990) The risk of development of HTLV-I-associated myelopathy/tropical spastic paraparesis among persons infected with HTLV-I. J Acquir Immune Defic Syndr 3: 1096–1101.
12. Verdonck K, González E, Van Dooren S, Vandamme AM, Vanham G, et al. (2007) Human T-lymphotropic virus 1: recent knowledge about an ancient infection. Lancet Infectious Disease 7: 266–281.
13. Olindo S, Bonnan M, Merle H, Signate A, Smadja D, et al (2010) Neuromyelitis optica associated with subacute human T-lymphotropic virus type 1 infection. J Clin Neurosci 17: 1449–1451.
14. Kasahata N, Shiota J, Miyazawa Y, Nakano I, Murayama S (2003) Acute human T-lymphotropic virus type 1-associated myelopathy: a clinicopathologic study. Arch Neurol 60: 873–876.
15. Koga M, Takahashi T, Kawai M, Negoro K, Kanda T (2009) Neuromyelitis optica with HTLV-1 infection: different from acute progressive HAM? Intern Med 48: 1157–1159.
16. Yoshida Y, Saiga T, Takahashi H, Hara A (1998) Optic neuritis and human T-lymphotropic virus type 1-associated myelopathy: a case report. Ophthalmologica 212: 73–76.
17. Wingerchuk DM (2009) Neuromyelitis optica: effect of gender. J Neurol Sci 286: 18–23.
18. Kira JI (2003) Multiple sclerosis in the Japanese population. Lancet Neurol 2: 117–127.
19. Cabre P, Heinzlef O, Merle H, Buisson GG, Bera O, et al. (2001) MS and neuromyelitis optica in Martinique (French West Indies). Neurology 56: 507–514.
20. Lana-Peixoto MA, Lana Peixoto MI (1992) Is multiple sclerosis in Brazil and Asia alike? Arq Neuropsiquiatr 50: 419–425.
21. Galvão-Castro B, Loures L, Rodrigues LG, Sereno A, Ferreira Junior OC, et al. (1997) Distribution of human T-lymphotropic virus type I among blood donors: a nationwide Brazilian study. Transfusion 37: 242–243.
22. Kashima S, Alcantara LC, Takayanagui OM, Cunha MA, Castro BG,et al. (2006) Distribution of human T cell lymphotropic virus type 1 (HTLV-1) subtypes in Brazil: genetic characterization of LTR and tax region. AIDS Res Hum Retroviruses 22: 953–959.
23. Papais-Alvarenga RM, Miranda-Santos CM, Puccioni-Sohler M, de Almeida AM, Oliveira S, et al. (2002) Optic neuromyelitis syndrome in Brazilian patients. J Neurol Neurosurg Psychiatry 73: 429–435.
24. Adoni T, Lino AM, da Gama PD, Apóstolos-Pereira SL, Marchiori PE, et al. (2010) Recurrent neuromyelitis optica in Brazilian patients: clinical, immunological, and neuroimaging characteristics. Mult Scler 16: 81–86.
25. Kurtzke JF (1983) Rating neurologic impairment in multiple sclerosis: an expanded disability status scale (EDSS). Neurology 33: 1444–1452.
26. Osame M, Usuku K, Izumo S, Ijichi N, Amitani H, et al. (1986) HTLV-I associated myelopathy, a new clinical entity. Lancet 1: 1031–1032.
27. Brito JC, da Nóbrega PV (2003) Myelopathy: clinical considerations and etiological aspects. Arq Neuropsiquiatr 61: 816–821.
28. Casseb J, de Oliveira AC, Vergara MP, Montanheiro P, Bonasser F, et al. (2008) Presence of tropical spastic paraparesis/human T-cell lymphotropic virus type 1-associated myelopathy (TSP/HAM)-like among HIV-1-infected patients. J Med Virol 80: 392–398.
29. WHO (1989): Scientific Group on HTLV-I Infections and Associated Diseases, Kagoshima, Japan 10–15 December 1988: report. Manila, Philippines: World Health Organization Regional Office for the Western Pacific: 4–6.
30. Wingerchuk DM (2007) Diagnosis and treatment of neuromyelitis optica. Neurologist 13: 2–11.
31. Jarius S, Probst C, Borowski K, Franciotta D, Wildemann B, et al. (2010) Standardized method for the detection of antibodies to aquaporin-4 based on a highly sensitive immunofluorescence assay employing recombinant target antigen. J Neurol Sci 291: 52–56.

32. Matsumoto M, Sugimoto M, Nakashima H, Imamura F, Kawano O, et al. (1990) Spontaneous T cell proliferation and release of soluble interleukin-2 receptors in patients with HTLV-I-associated myelopathy. Am J Trop Med Hyg 42: 365–373.
33. Murphy EL, Figueroa JP, Gibbs WN, Brathwaite A, Holding-Cobham M, et al. (1989) Sexual transmission of human T-lymphotropic virus type I (HTLV-I). Ann Intern Med 111: 555–560.
34. Haines JL, Bradford Y, Garcia ME, Reed AD, Neumeister E, et al. (2002) Multiple susceptibility loci for multiple sclerosis. Hum Mol Genet 11: 2251–2256.
35. Kanamori Y, Nakashima I, Takai Y, Nishiyama S, Kuroda H, et al. (2011) Pain in neuromyelitis optica and its effect on quality of life: a cross-sectional study. Neurology 77: 652–658.
36. Jarius S, Paul F, Franciotta D, Ruprecht K, Ringelstein M, et al. (2011) Cerebrospinal fluid findings in aquaporin-4 antibody positive neuromyelitis optica: results from 211 lumbar punctures. J Neurol Sci 306: 82–90.
37. Bergamaschi R, Tonietti S, Franciotta D, Candeloro E, Tavazzi E, et al. (2004) Oligoclonal bands in Devic's neuromyelitis optica and multiple sclerosis: differences in repeated cerebrospinal fluid examinations. Mult Scler 10: 2–4.

Copyright – Autorização da revista PLoS ONE para inclusão do artigo na tese de doutorado.

-----Original Message-----
From: Anna O'Shea
Sent: Monday, April 08, 2013 18:29
To: fglehn@terra.com.br
Subject: Case: 01924194 "Permission [ref:_00DU0Ifis._500U07HeBq:ref]

Dear Dr. von Glehn,

Thank you for contacting PLOS ONE.

All PLOS content is open access. You can read about our open access license at http://www.plos.org/journals/license.html. This license allows you to download, reuse, reprint, modify, distribute, and/or copy articles or images in PLOS journals, so long as proper attribution is given to the original source (which you can easily do by including the article's citation and/or the image credit).

There are many ways to access our content, including HTML, XML, and PDF versions of each article. Higher resolution versions of figures can be downloaded directly from the article. Additionally, our articles are archived at PubMed Central (http://www.pubmedcentral.gov/), which offers a public FTP service from which you can download a complete site of files for each of our articles. See http://www.pubmedcentral.gov/about/openftlist.html for links to the FTP site, file list, and organizational directory.

Kind Regards,
Anna O'Shea
PLOS ONE

Case Number: 01924194
ref:_00DU0Ifis._500U07HeBq:ref

Capítulo 2

Artigo submetido em março de 2013 na revista Neurology.

Structural brain abnormalities are related to RNFL thinning, disease duration and AQP4ab in NMOSD

Felipe von Glehn MD, MSc[1,2 *]; Sven Jarius MD[3]; Rodrigo Pessoa Cavalcanti Lira MD, PhD[4]; Maria Carolina Alves Ferreira MD[4]; Fadua H. Ribeiro von Glehn MD[2]; Stella Maris Costa e Castro MSc[4]; Guilherme Coco Beltramini[2,5]; Felipe P.G. Bergo PhD[2]; Alessandro S. Farias PhD[1]; Carlos Otávio Brandão MD, PhD[1,2]; Brigitte Wildemann MD, PhD[3]; Benito P. Damasceno MD, PhD[2]; Fernando Cendes MD, PhD[2]; Leonilda M. B. Santos PhD[1*] and Clarissa Lin Yasuda MD, PhD[2]

(1) Neuroimmunology Unit, Department of Genetics, Evolution and Bioagents, University of Campinas, Campinas, Brazil; (2) Laboratory of Neuroimaging, Department of Neurology, University of Campinas, Campinas, Brazil; (3) Division of Molecular Neuroimmunology, Department of Neurology, University of Heidelberg, Heidelberg, Germany; (4) Department of Ophthalmology, University of Campinas, Campinas, Brazil; (5) Institute of Physics "Gleb Wataghin", University of Campinas, Campinas, Brazil.

[*] Corresponding authors: Felipe von Glehn, M.D., M.Sc., Leonilda M. B. Santos Ph.D. and Clarissa Lin Yasuda – Neuroimmunology Unit, Departamento de Genética, Evolução e Bioagentes - UNICAMP, Rua Monteiro Lobato, 255, Campinas, SP Brazil, CEP 13083-970, Phone: +55 (19) 3521-6263; FAX: +55 (19) 3521-6276, Email: fglehn@terra.com.br, leonilda@unicamp.br, yasuda.clarissa@gmail.com.

Running title: **Structural Brain abnormalities in NMOSD**

Keywords: Neuromyelitis optica; Devic's disease; longitudinally extensive transverse myelitis; optic neuritis; retinal nerve fiber layer atrophy; optical coherence tomography analysis; VBM analysis; gray matter atrophy; white matter atrophy.

Word and character count

Title (characters): 97; Running head (characters): 40;

Abstract (words): 250; Manuscript (words): 3162;

Tables, figures and references

Tables: 2; Figures: 3; References: 34; Supplementary Tables: 2 and figures: 1.

Abstract:

Although AQP4 is widely expressed in the human brain cortex, brain lesions are rare in neuromyelitis optica (NMO). Recently, however, several studies have demonstrated occult structural brain atrophy in NMO. **Objectives**: To investigate magnetic resonance imaging (MRI) patterns of gray matter (GM) and white matter (WM) abnormalities in patients with NMO and its incomplete forms, isolated longitudinally extensive transverse myelitis and optic neuritis, and to assess the prognostic impact of GM and WM abnormalities in these conditions. **Methods**: Thirty-four patients with NMO spectrum disorders (NMOSD) and 34 matched healthy controls underwent both 3T high-resolution T1-weighted and diffusion tensor MRI. Voxel-based morphometry (SPM8/MATLAB2012b), cortical analyses (Freesurfer), and diffusion tensor imaging analyses (TBSS-FSL) were used to investigate brain abnormalities. In addition, retinal nerve fiber layer measurement by optic coherence tomography (OCT) was performed. **Results**: We demonstrate that NMOSD is associated with GM and WM atrophy, that this atrophy encompasses more than the motor, sensory, and visual pathways, that it is more widespread in patients with NMO and LETM than in patients with ON, that the extent of GM atrophy correlates with disease duration, and that GM/WM atrophy in NMOSD is more pronounced in AQP4 antibody-seropositive than in -seronegative patients. Furthermore, we demonstrate for the first time a correlation between RNFL atrophy and GM atrophy in the occipital lobes as assessed by OCT. **Conclusion:** Our findings indicate a role for retrograde degeneration in GM atrophy in NMOSD and suggest that the extent of brain GM/WM atrophy may be of prognostic relevance in NMOSD.

Introduction

Neuromyelitis optica (NMO) is an inflammatory relapsing disease of the central nervous system (CNS) of putative autoimmune etiology which is characterized by severe attacks of myelitis and optic neuritis (ON)[1-2]. In 60-80% of cases, NMO is associated with antibodies to aquaporin-4 (AQP4ab), the most abundant water channel in the CNS, and its presence is related to a relapsing and often worse disease course[3-6]. AQP4ab are also detectable in around 60% of patients with isolated longitudinally extensive transverse myelitis (LETM)[7] and in 5-25% of patients with recurrent, isolated ON[6,8,9], which are therefore considered *formes frustes* of NMO[10].

Although AQP4 is also expressed widely in the human brain cortex[11], beyond the common sites of lesions in NMO, recent studies have found no MRI or histopathological evidence for cortical demyelination[11,12]. However, two independent neuroimaging studies demonstrated occult structural brain atrophy, predominantly involving regions connected with sensorimotor and visual systems[12-13].

Without signs of cortical demyelination or global atrophy, it was suggested that this focal cortical atrophy could be related to retrograde degeneration, triggered by lesions of the optic nerve and spinal cord[11-14]. Similarly, optical coherence tomography (OCT) studies have demonstrated a severe reduction in the thickness of the retinal nerve fiber layer (RNFL) in NMO, as a consequence of Wallerian degeneration following ON[15-18].

In this study, we used high-field MRI (3T) and applied a multiparametric neuroimaging approach to investigate the presence and extent of both gray matter (GM) and white matter (WM) abnormalities in patients with NMO spectrum disorders (NMOSD). Intrigued by the clear distinction of neurological manifestation between subgroups, we searched for differences in the pattern of abnormalities between the incomplete or inaugural

forms of NMO (LETM and ON) and established NMO. In addition, we explored possible associations between clinical and laboratory factors of known prognostic impact (AQP4ab seropositivity, RNFL atrophy, and disease duration) and the extent of GM/WM abnormalities.

Patients and Methods

Patients

This was a single-center, cross-sectional study including 34 consecutive patients [15 with NMO, 10 with LETM, and 9 with relapsing ON (rON)] and 34 healthy individuals matched for sex and age. Patients were stratified according to AQP4ab serostatus (19 seropositive, 15 seronegative patients) and disease duration [short duration (≤ 5 years): 22 patients; longer duration (> 5 years): 12 patients]. NMO and patients with syndromes considered to carry a high risk of conversion to NMO (AQP4ab seropositive ON; LETM) were classified as NMOSD[10]. All patients were recruited during regular follow-up visits at the neurological outpatient unit of the University of Campinas (UNICAMP) Hospital, São Paulo, Brazil, between January 2011 and October 2012.

UNICAMP Ethics Committees for Research approved the study, and informed written consent was obtained for all patients. For minors, consent was provided by their parents.

All patients were seronegative for anti-HIV and anti-HTLV1/2 antibodies[19]. All 19 AQP4ab-seropositive NMOSD patients were treated with immunosuppressive drugs (e.g. azathioprine, methotrexate, or rituximab). In the AQP4ab-seronegative subgroup, two patients with LETM and three with ON were not treated with immunosuppressive drugs, because of a long relapse-free period and no sign of inflammatory activity during the study. All OCT scans were performed more than 3 months after the most recent episode of ON to ensure that the results were not affected by acute optic disk swelling.

NMO was diagnosed according to Wingerchuk's revised 2006 criteria without the need for positive AQP4ab testing[20]. LETM was defined as acute myelitis with spinal cord lesions extending over three or more vertebral segments on MRI; rON as the occurrence of at least two episodes of clinical ON, with an interval of at least 30 days between them, and absence of brain lesions outside the optic nerves[20]. The rON patients with seronegative AQP4ab were studied as a separate group due to the low risk of conversion to NMO.

The expanded disability status scale (EDSS) was used as a measure of disease severity. In addition, serum samples were collected and both MRI acquisitions and OCT analysis were performed for each patient.

Methods

AQP4ab testing. We tested all peripheral blood samples for AQP4ab in a commercial, standardized cell-based immunofluorescence assay employing recombinant human full-length AQP4 (Euroimmun AG, Luebeck, Germany)[21] at the UNICAMP Neuroimmunology Laboratory.

Optical coherence tomography. All patients were scanned using the commercially available SOCT Spectralis OCT™ (Heidelberg Engineering, Heidelberg, Germany). The Spectralis software version was 5.0. This instrument uses a wavelength of 820nm in the near-infrared spectrum in the SLO mode. The light source of the SOCT is a superluminescent diode with a wavelength of 870nm. The OCT system simultaneously captures infrared fundus and spectral domain (SD) OCT images at 40,000 A-scans per second. A real-time eye-tracking system measures eye movements and provides feedback to the scanning mechanism, to stabilize the retinal position of the B-scan. This system thus enables sweep-verging at each B-scan location

to reduce speckle noise. The average number of scans to produce each circular B scan was nine. The RNFL Spectralis protocol generates a map showing the average thickness and six sector thicknesses (supero-nasal, nasal, infero-nasal, infero-temporal, temporal, and supero-temporal) in the clockwise direction for the right eye and counterclockwise for the left eye.

Magnetic resonance imaging. All patients and controls underwent MRI on a Phillips Achieva-Intera 3-T scanner at UNICAMP hospital. T1- and T2-weighted images were acquired in axial, coronal, and sagittal planes with thin cuts. All patients underwent a comprehensive MRI protocol for demyelinating disease (see details on supplementary material) which was evaluated by a certified radiologist (FHRvG). We also obtained two specific sequences that were later employed for voxel-based morphometry (VBM) and diffusion tensor imaging (DTI) analyses, respectively (see details on supplementary material).

VBM protocol and analysis. We used VBM8 (http://dbm.neuro.uni-jena.de/vbm) SPM8 (http://www.fil.ion.ucl.ac.uk/spm) running on MATLAB-R2012b to extract GM and WM maps from each subject and to perform statistical comparisons among different groups and controls. Regarding spatial normalization, we also applied a more sophisticated registration model (the DARTEL algorithm) that substantially reduces the imprecision of intersubject registration[22]. Processed images of patients and controls were compared using a voxelwise statistical analysis[23]. We exclusively reported clusters that survived an uncorrected threshold of $p<0.001$ with at least 30 contiguous voxels and a minimum statistical T=3.4. The results were not corrected for multiple comparisons due to the exploratory nature of this study. In order to display the results and pinpoint their anatomical location we used an additional SPM extension, XJVIEW (http://www.alivelearn.net/xjview) (see details on supplementary material).

DTI analyses. We processed the diffusion data with FSL software V.4.1.4[24], starting with FMRIB's Diffusion Toolbox (FDT) to perform head motion and eddy current correction, followed by Brain Extraction Tool[25] to extract non-brain voxels and create a brain mask. Fractional anisotropy (FA) maps in the subject native space were then obtained by fitting a tensor model to the raw diffusion data with DTIFIT.

Comparison of groups was then carried out with tract-based spatial statistics (TBSS), also part of the FSL software V.4.1.4[26], which involves some pre-processing steps before the final analyses. The voxelwise statistics employed a permutation test (n=5000) using the "program randomize" segment of FSL. The statistically significant voxels were identified with threshold-free cluster enhancement (TFCE) applying familywise error correction threshold (FWE) for multiple comparisons with the threshold of $p<0.05$. We used the Johns Hopkins WM DTI-based atlas within the FSL, localizing the areas with FA reduction resulting from statistical analyses (see details on supplementary material).

Cortical analyses. We used an automated brain segmentation software, Freesurfer image analysis suite v5.1.0 (http://surfer.nmr.mgh.harvard.edu), to obtain cortical thickness measurements and volumetric segmentation in groups of patients compared to paired controls[27]. Univariate correlations between continuous variables were assessed using the Pearson correlation coefficient and those including discrete variables with the Spearman rank correlation coefficient (r). Data were analyzed using GraphPad Prism 5. The statistical significance of differences was determined by Unpaired T Test with Welch's correction and by ANOVAs without assuming Gaussian distribution (Kruskal–Wallis test) and subsequent Dunn's multiple comparison tests. Differences with p values <0.05 were considered statistically significant.

Results

Demographic, clinical, and serological characteristics of the patients are given in Table 1.

There was a female preponderance in all groups, which is accordance with published data on the epidemiology of NMOSD[1,2,28]. The LETM group had shorter disease duration (1 year) than the others groups. Patients with AQP4ab-seropositive status and longer disease duration presented more relapses and worse EDSS scores than those with AQP4ab-seronegative status and shorter disease duration. As in previous studies[1,29], cerebrospinal fluid (CSF)-restricted IgG oligoclonal bands were detected in only few patients, with no significant difference regarding AQP4ab serostatus or disease duration **(Table 1).**

RNFL atrophy

OCT could not be performed in two patients in whom visual acuity was bilaterally reduced to perception of light. The overall average thickness and the thickness in almost all of the six sectors (supero-nasal, nasal, infero-nasal, infero-temporal, temporal, and supero-temporal) were significantly lower in both the NMO and the ON group than in the LETM group (**Table 1 and Figure 1**). Longer disease duration was associated with more severe RNFL atrophy than shorter duration. Overall average RNFL thickness did not differ between AQP4ab-positive and AQP4ab-negative patients; however, AQP4ab-positive patients presented more atrophy in the temporal RNFL sector (mean ± standard deviation: 43.24 ± 19.76µm vs. 53.93 ± 20.88µm, p=0.0445) and a tendency to more atrophy in the supero-nasal (p=0.0639) and infero-nasal sectors (p=0.0724) **(Table 1)**.

RNFL atrophy correlates with pericalcarine cortical thickness and EDSS score

To study the impact of RNFL atrophy in the visual system pathway we correlated the overall average RNFL from both eyes with the cortical thickness of the pericalcarine bilateral GM area. As both eyes of a given patient are at the same risk of relapse, and because subclinical episodes of ON may cause a small amount of retinal damage to the contralateral eye[18], we analyzed the mean of the bilateral RNFL of each patient. We found a positive correlation between RNFL thinning and cortical pericalcarine atrophy (r= 0.5299, r^2= 0.2451, p= 0.0031). We also observed a negative correlation between EDSS score and RNFL thinning (r= -0.5057, r^2= 0.2166, p= 0.0099) **(Figure 1).**

GM results

VBM analysis revealed significant GM volumetric reduction in some areas of the frontal, parietal, temporal, occipital, and limbic lobes and in the cerebellum in the NMOSD group and in the NMO and LETM subgroups compared to sex- and age-matched controls. The ON group showed atrophy restricted to the occipital lobe. Patients with longer duration of disease and those in the AQP4ab-positive group presented both larger and more abundant clusters (**Figure 2, Supplementary Table 1**).

To confirm these findings, we performed cortical thickness analyses (**Tables 2, Supplementary Figure 1**). These analyses revealed a more widespread pattern of cortical atrophy in the NMOSD group and in the NMO and LETM subgroups than in paired ON and controls, encompassing areas of the frontal, parietal, temporal, occipital, and limbic lobes and cerebellar cortex volume. However, cortical thinning in patients with ON was restricted principally to the visual pathways. With regard to AQ4ab serostatus and disease duration, direct comparison of both AQP4ab-positive vs. AQP4ab-negative groups and shorter duration vs. longer duration of disease showed no significant differences. When we compared each of

these four groups with normal controls, however, we detected significant cortical thinning encompassing areas of the frontal, parietal, occipital, and limbic lobes in all groups. The group with longer disease duration showed more areas of cortical thinning than the shorter duration group. AQP4-positive and AQP4-negative groups showed no difference regarding the number of areas affected (**Table 2, Supplementary Figure 1)**.

WM results

VBM identified several areas of WM volumetric reduction in areas of the brainstem, cerebellum, optic chiasm, and frontal, parietal, temporal, occipital, and limbic lobes in the NMOSD group and in the NMO and LETM subgroups compared to matched controls. The ON group demonstrated WM volumetric reduction restricted to the visual pathways . Patients with AQP4ab-positive serostatus showed more widespread WM atrophy (**Figure 2, Supplementary Table 1)**.

TBSS analysis performed to confirm the VBM findings revealed reduced FA involving diffuse subcortical white matter of the frontal, parietal, temporal, occipital, and limbic lobes, brainstem, and cerebellum in the NMOSD, NMO, and LETM subgroups. We detected a more restricted pattern of FA reduction in the ON group, encompassing exclusively the visual pathways. Patients with AQP4ab-positive serostatus demonstrated more widespread WM microstructural abnormalities than AQP4ab-negative patients **(Figure 3, Supplementary Table 2**).

Discussion

We have demonstrated (i) that NMOSD is associated with both GM and WM atrophy; (ii) that this atrophy is not restricted to the motor, sensory, and visual pathways; (iii) that the extent of

GM atrophy correlates with disease duration; and (iv) that GM and WM atrophy in NMOSD are more pronounced in AQP4ab-seropositive than in AQP4ab-seronegative patients. Furthermore, we have shown for the first time a correlation between RNFL atrophy and GM atrophy in the occipital lobes as assessed by OCT.

Correlation of RNFL atrophy with pericalcarine cortical thickness and EDSS score

We found severe RNFL reduction in the NMO group in almost all retinal areas studied; in contrast, the atrophy affects mainly the temporal RNFL in multiple sclerosis (MS)[16-18]. These findings provide further evidence for the notion that NMO and MS are distinct disease entities.

The marked reduction in the thickness of the RNFL following ON observed by us and others, which has been shown to be directly related to loss of retinal ganglion cell axons and optic nerve atrophy[16-18], matches clinical studies demonstrating more severe visual disability in NMO than in MS[18]. Merle et al. described an average time to blindness of just 2 years in the first eye and 13 years in the second eye[30]. Another study found that 18% of patients were functionally blind at last follow-up after a median disease duration of approximately 6 years[31].

As both eyes of any given patient are at the same risk of relapse attack, and because subclinical episodes of ON may cause a small amount of retinal damage to the contralateral eye[18], we analyzed the mean bilateral RNFL from each patient. By contrast, previous studies had analyzed only the eye previously affected by ON[17,18] or the left and the right eyes of each group separately[16]. This approach also permitted the correlation of RNFL with the mean occipital cortical thickness, as both sides receive input from both eyes, meaning that a unilateral optic nerve lesion could affect both sides of the visual pathway. In accordance with

the notion that ON attacks in NMOSD are more destructive and bear greater potential for causing visual disability than in MS, we detected a correlation between disability, as measured by EDSS score, and RNFL thickness, corroborating results from a previous study whose authors hypothesized that this finding could be related to widespread axonal damage in the central nervous system[16].

Our results revealed that more severe atrophy of cortical thickness and RNFL was associated with both AQP4ab seropositivity and longer disease duration in NMOSD. Initially, we hypothesized that this finding could be related to the fact that the group with shorter disease duration included all the patients with LETM, but even after removal of these patients from the analysis the difference remained statistically significant (65.77 ± 29.57µm vs. 49.91 ±29.59µm; p=0.0326).

WM and GM atrophy

WM atrophy was assessed by VBM, that provide a macroscopic map of atrophy and TBSS, that enable the identification of microstructural damage, therefore essentially complementary tools. We demonstrated restricted WM lesions encompassing the optic radiations in the ON group, while a more diffuse pattern was detected in the NMOSD and NMO groups. Even the LETM group, despite the shorter disease duration, demonstrated more widespread WM microstructural lesions than the ON and control groups as assessed by TBSS. AQP4ab-positive serostatus was related to more abnormalities, suggesting a pathogenic role for this antibody.

The cerebral cortex presented more focal areas of GM atrophy throughout the lobes in patients with NMO and LETM (**Figure 2, Supplementary Tables 1 and 2**), while patients

with isolated ON presented a more restricted pattern of cortical thinning limited mainly to the occipital lobes, arguing against major subclinical damage to the spinal cord in these patients. In contrast, no OCT abnormalities were present in the LETM group, suggesting that there was no subclinical optic nerve damage in these patients. Furthermore, we demonstrated GM volumetric reduction and cortical thinning in AQP4ab-seronegative and -seropositive patients but a more severe pattern in the seropositive ones, in accordance with the worse clinical evolution in these patients. Thus, the pattern of GM/WM atrophy observed in our patients with NMOSD is different from the pattern seen in patients with classical MS, which is characterized by extensive, diffuse cortical demyelination associated with global and more severe GM atrophy, as well as neuronal loss[12,32].

In accordance with two previous studies, our results revealed mild thinning in cortical areas (postcentral, precentral, and calcarine gyri) that are connected to the motor, sensory, and visual pathways as well as correlation with both disease duration and disability[12,33]. However, the cause of cortical atrophy in NMO is still not fully understood. Despite the fact that AQP4ab is widely expressed in the brain cortex, a neuropathological study of 19 autopsied patients disclosed signs of neither cerebral cortical demyelination nor disruption of the cortical distribution of AQP4[11], but rather revealed prominent astrogliosis, mostly involving interlaminar astrocytes. This would suggest that the GM/WM changes are somewhat related to retrograde degeneration of neurons after axonal transection in the spinal cord, optic nerves, and/or WM. The authors speculated that the absence of cortical inflammation in their study might have been due to specific characteristics of parenchymal organization of the brain cortex, such as blood–brain barrier permeability or astrocytic and microglial disposition[11]. Extending these previous findings, we demonstrate that RNFL atrophy is particularly

correlated with pericalcarine cortex thinning, which strongly suggests axonal damage and Wallerian degeneration across the visual pathway (**Figure 1).**

Nevertheless, a contribution of additional inflammatory damage to GM atrophy cannot be fully ruled out. In fact, a recent study demonstrated loss of AQP4 and glial fibrillary acidic protein in the WM of the temporal lobe associated with loss of AQP4 in the adjacent GM in a single AQP4ab-positive patient [34], and an earlier MRI study detected decreased magnetization transfer ratio (MTR) and increased mean diffusivity (MD) in the GM of patients with NMO, possibly indicating GM tissue damage[14]. Moreover, our results revealed that some areas of mild GM atrophy are present in almost all cerebral lobes, extending over the previously described areas associated with motor, sensory, and visual pathways (**Table 2, Supplementary Figure 1, Supplementary Tables 1 and 2).**

Importantly, both the localized pattern of GM/WM atrophy and the global retinal RNFL reduction, which are atypical for MS, were present not only in the AQP4ab-seropositive but also in the AQP4ab-seronegative group. This further supports the notion that seronegative NMO is not simply a special manifestation of MS, as already suggested by clinical, CSF, and spinal MRI data[2,10].

The relatively small number of individuals tested (n=68) is a potential limitation of our study. Nevertheless, NMO is a very rare disease and large-scale studies are therefore generally difficult to perform. To overcome the limitations of using a single imaging method, we used high-field MRI (3T) and applied different methods to evaluate both GM and WM abnormalities, including VBM (with the DARTEL algorithm), Freesurfer, and TBSS, three validated and unbiased methods.

In conclusion, the finding of a restricted pattern of cortical atrophy in ON and more widespread atrophy in both NMO and LETM suggests a possible involvement of retrograde degeneration in the mechanism of GM atrophy, a hypothesis supported by the fact that neuropathological studies did not identify cortical demyelination in most patients with NMO, despite wide distribution of APQ4 in the cerebral cortex. A more severe pattern of GM and WM abnormalities in AQP4ab-positive patients was expected, as these patients present more severe disease. The mechanisms that protect cortical AQP4 against antibody-dependent cytotoxicity remain to be elucidated.

Acknowledgements

The MRI gadolinium contrast medium (gadoteric acid) used in this study was kindly provided by Guerbet, Roissy CdG, France. The AQP4ab assay used in this study was kindly provided by Euroimmun AG, Luebeck, Germany.

References

1. Wingerchuk DM, Hogancamp WF, O'Brien PC, Weinshenker BG. The clinical course of neuromyelitis optica (Devic's syndrome). Neurology 1999; 53: 1107-1114.
2. Jarius S, Ruprecht K, Wildemann B, et al. Contrasting disease patterns in seropositive and seronegative neuromyelitis optica: A multicentre study of 175 patients. J Neuroinflammation 2012; DOI: 10.1186/1742-2094-9-14.
3. Lennon VA, Wingerschuk DM, Kryzer TJ, et al. A serum autoantibody marker of neuromyelitis optica: distinction from multiple sclerosis. Lancet 2004; 364: 2106-2112.
4. Jarius S, Wildemann B. AQP4 antibodies in neuromyelitis optica: diagnostic and pathogenetic relevance. Nat Rev Neurol 2010; 6: 383-392.
5. Akman-Demir G, Tüzün E, Waters P, et al. Prognostic implications of aquaporin-4 antibody status in neuromyelitis optica patients. J Neurol. 2011; 258: 464-470.

6. Jarius S, Frederikson J, Waters P, et al. Frequency and prognostic impact of antibodies to aquaporin-4 in patients with optic neuritis. J Neurol Sci 2010; 298: 158-162.
7. Pittock SJ, Lennon VA, de Seze J, et al. Neuromyelitis optica and non-organ-specific autoimmunity. Arch Neurol 2008; 65: 78-83.
8. Matiello M, Lennon VA, Jacob A, et al. NMO-IgG predicts the outcome of recurrent optic neuritis. Neurology 2008; 70: 2197-2200.
9. Petzold A, Pittock S, Lennon V, et al. Neuromyelitis optica-IgG (aquaporin-4) autoantibodies in immune mediated optic neuritis. J Neurol Neurosurg Psychiatry 2010; 81: 109-111.
10. Wingerchuk DM, Lennon VA, Lucchinetti CF, et al. The spectrum of neuromyelitis optica. Lancet Neurol 2007; 6: 805-815.
11. Popescu BF, Parisi JE, Cabrera-Gómez JA, et al. Absence of cortical demyelination in neuromyelitis optica. Neurology 2010; 75: 2103-2109.
12. Calabrese M, Oh MS, Favaretto A, et al. No MRI evidence of cortical lesions in neuromyelitis optica. Neurology 2012; 79: 1671-1676.
13. Pichiecchio A, Tavazzi E, Poloni G, et al. Advanced magnetic resonance imaging of neuromyelitis optica: a multiparametric approach. Mult Scler 2012;18: 817-824.
14. Rocca MA, Agosta F, Mezzapesa DM, et al. Magnetization transfer and diffusion tensor MRI show gray matter damage in neuromyelitis optica. Neurology. 2004; 62: 476-478.
15. Merle H, Olindo S, Donnio A, et al. Retinal peripapillary nerve fiber layer thickness in neuromyelitis optica. Invest Ophthalmol Vis Sci 2008; 49: 4412-4417.
16. de Seze J, Blanc F, Jeanjean L, et al. Optical coherence tomography in neuromyelitis optica. Arch Neurol 2008; 65: 920-923.
17. Green AJ, Cree BA. Distinctive retinal nerve fibre layer and vascular changes in neuromyelitis optica following optic neuritis. J Neurol Neurosurg Psychiatry 2009; 80: 1002-1005.
18. Ratchford JN, Quigg ME, Conger A, et al. Optical coherence tomography helps differentiate neuromyelitis optica and MS optic neuropathies. Neurology 2009; 73: 302-308.

19. von Glehn F, Jarius S, Penalva de Oliveira AC, et al. Aquaporin-4 antibodies are not related to HTLV-1 associated myelopathy. PLoS One 2012; DOI:10.1371/ journal.pone.0039372.
20. Wingerchuk DM. Diagnosis and treatment of neuromyelitis optica. Neurologist 2007; 13: 2-11.
21. Jarius S, Probst C, Borowski K, et al. Standardized method for the detection of antibodies to aquaporin-4 based on a highly sensitive immunofluorescence assay employing recombinant target antigen. J Neurol Sci 2010; 291: 52-56.
22. Ashburner JA. A fast diffeomorphic image registration algorithm. NeuroImage 2007; 38: 95-113.
23. Ashburner J, Friston KJ. Voxel-based morphometry—the methods. NeuroImage 2000; 11: 805-821.
24. Smith SM, Jenkinson M, Woolrich MW, et al. Advances in functional and structural MR image analysis and implementation as FSL. Neuroimage 2004; 23 (Suppl 1): S208–219.
25. Smith SM. Fast robust automated brain extraction. Hum Brain Mapp 2002; 17: 143-155.
26. Smith SM, Jenkinson M, Johansen-Berg H, et al. Tract-based spatial statistics: voxelwise analysis of multi-subject diffusion data. Neuroimage 2006; **31**: 1487-1505.
27. Fischl B. FreeSurfer. Neuroimage 2012; 62: 774-781.
28. Wingerchuk DM. Neuromyelitis optica: effect of gender. J Neurol Sci 2009; 286: 18-23.
29. Jarius S, Paul F, Franciotta D, et al. Cerebrospinal fluid findings in aquaporin-4 antibody positive neuromyelitis optica: results from 211 lumbar punctures. J Neurol Sci 2011; 306: 82-90.
30. Merle H, Olindo S, Bonnan M, et al. Natural history of the visual impairment of relapsing neuromyelitis optica. Ophthalmology 2007; 114: 810-805.
31. Kitley J, Leite MI, Nakashima I, et al. Prognostic factors and disease course in aquaporin-4 antibody-positive patients with neuromyelitis optica spectrum disorder from the United Kingdom and Japan. Brain 2012; 135: 1834-1849.
32. Magliozzi R, Howell OW, Reeves C, et al. A Gradient of neuronal loss and meningeal inflammation in multiple sclerosis. Ann Neurol 2010; 68: 477-493.
33. Ciccarelli O. Do cortical lesions help us to distinguish MS from NMO? Neurology 2012; 79: 1630-1631.

34. Yaguchi H, Yabe I, Takai Y, et al. Pathological study of subacute autoimmune encephalopathy with anti-AQP4 antibodies in a pregnant woman. Mult Scler 2012; 18: 683-687.

Table legends

Table 1. Demographic, baseline clinical characteristics and OCT analysis of the RNFL by clinical presentations, AQP4ab serostatus, and disease duration.

Table 2. Brain structures volumetric reduction and areas of cortical thinning (mean left and right hemispheres) in NMOSD patients, comparing its clinical presentations, AQP4ab serostatus and length of disease duration to normal controls.

Figure legends

Figure 1. Retinal nerve fiber layer atrophy associated with EDSS score and pericalcarine cortical thinning. (**A**) An example of OCT analysis: the affected left eye of a NMO patient. Note the RNFL thinning in all sectors, indicating diffuse and severe axonal loss. (**B**) Pronounced RNFL atrophy in the NMO and ON groups compared with the LETM group (Kruskal–Wallis test with Dunn's multiple comparison, p = 0.0016). (**C**) Pronounced RNFL atrophy related to disease duration, in patients with more than 5 years of disease (Mann–Whitney test. p=0.0034). The differences in AQP4ab serostatus did not reach statistical significance. (**D**) RNFL thinning correlates with EDSS score (r= -0.5057, r^2= 0.2166, p= 0.0099). Each plot represents the correlation of the means of global right and left eye RNFL thickness and the EDSS score from each NMOSD patient. (**E**) RNFL atrophy correlates with pericalcarine cortical thickness (r= 0.5299, r^2= 0.2451, p= 0.0031). Each plot represents the correlation of the means of global right and left eye RNFL thickness and the means of right and left pericalcarine cortical thickness from each patient.

Figure 2. Voxel-based morphometry of cerebral gray matter (GM) and white matter (WM) in NMOSD patients, comparing its clinical presentations, AQP4ab serostatus and length of disease duration to controls. Results of voxelwise analysis showing areas of GM and WM volumetric reduction in patients with NMOSD, NMO, LETM, and ON (**A**) and in

the AQP4ab-positive group, the AQP4ab-negative group, patients with disease duration ≤ 5 years, and patients with disease duration > 5 years **(B)** after comparison with age- and sex-matched controls. Note the GM volumetric reduction in some areas of the frontal, parietal, temporal, occipital, and limbic lobes and also cerebellum in the NMOSD group and in the NMO and LETM subgroups. ON group showed a restricted atrophy to the occipital lobe. Note the greater GM and WM atrophy in the AQP4ab-positive subgroup. In the subgroup with longer disease duration, GM atrophy was more pronounced after 5 years. Shorter disease duration presented more WM volumetric reduction. The results are shown on the MNI152 1 mm template. MNI z axis coordinates are shown (in mm) above each image. The color-coded bars represent the T score. The red bar relates to GM, the blue bar to WM.

Figure 3. White matter microstructural abnormalities demonstrated by tract based spatial statistics in NMOSD patients, comparing its clinical presentations, AQP4ab serostatus and length of disease duration to controls. Voxelwise analysis showing areas of reduced fractional anisotropy (FA) in patients of the NMOSD group, the NMO group, the LETM group, and ON group (**A**), and the AQP4ab-positive group, those of the AQP4ab-negative group, those with disease duration ≤ 5 years, and those with disease duration > 5 years (**B**) after comparison with age- and sex-matched controls. Areas with reduced FA are shown in yellow–red and represent cluster-based values (p<0.05, corrected with familywise error correction). The results are shown on the MNI152 1 mm template. MNI z axis coordinates are shown (in mm) above each image. The color-coded bar represents p values ranging from 0.05 to <0.001.

Supplementary Tables legends

Supplementary Table 1. Results of voxel-based morphometry of cerebral gray matter (GM) and white matter (WM) in NMOSD patients, comparing its clinical presentations, AQP4ab serostatus and length of disease duration to controls.

Supplementary Table 2. Results of tract-based spatial statistics voxelwise analysis of FA in NMOSD patients, comparing its clinical presentations, AQP4ab serostatus and length of disease duration to controls.

Supplementary Figure legends

Supplementary Figure 1. Cortical thickness decreases in NMOSD patients. Spatial distribution of cortical thickness thinning in NMOSD patients, comparing its clinical presentations, AQP4ab serostatus and length of disease duration to controls. Hotter colors indicate reduced cortical thickness in patients with NMOSD (**A**), NMO (**B**), LETM (**C**), ON (**D),** and in the AQP4ab**-**positive group **(E),** the AQP4ab-negative group **(F),** patients with disease duration ≤ 5 years **(G),** and patients with disease duration > 5 years **(H)** after comparison with age- and sex-matched controls. The color-coded bar represents the T score.

Table 1. Demographic, baseline clinical characteristics and OCT analysis of the RNFL by clinical presentations, AQP4ab serostatus, and disease duration.

	NMOSD	NMO	LETM	ON	*p* value†	< = 5 years	> 5 years	*p* value‡	AQP4ab +	AQP4ab -	*p* value‡
Patients #	27	15	10	9		22	12		19	15	
Age (years)*	42 (14-76)	38 (17-63)	49 (14-76)	28 (16-49)	0.0769	40 (14-76)	38 (17-63)	0.9856	38 (14-63)	39 (16-76)	0.9585
Gender F / M	24 / 3	15 / 0	7 / 3	6 / 3	0.0658	18 / 4	10 / 2	1	17 / 2	11 / 4	0.3696
Time from first symptoms (years)*	5 (0.9-19)	6 (2-19)	1 (0.9-3)	5 (0.9-9)	0.0012	2 (0.9-5)	8.5 (6-19)	P<0.0001	5 (1-19)	2.0 (0.9-9)	0.0615
Number of relapses*	3 (1-15)	5 (3-15)	2 (1-3)	4 (2-9)	0.001	3 (1-6)	8.5 (2-15)	0.002	4 (2-15)	2.0 (1-9)	0.0012
EDSS*	4 (1-8.5)	5 (2-8.5)	2.5 (1-7)	3 (1-4)	0.0315	3 (1-8.5)	4 (1-8)	0.1017	4.5 (1.5-8.5)	3 (1-6.5)	0.0373
AQP4ab (%)	19/27 (70%)	13/15 (87%)	4/10 (40%)	2/9 (22%)		11/22 (50%)	8/12 (67%)		19 /19(100%)	0/15 (0%)	
CSF oligoclonal bands (%)**	11/27 (41%)	6/15 (40%)	3/10 (30%)	2/9 (22%)	0.7377	6/22 (27%)	6/12 (50%)	0.2655	8/19(42%)	4/15 (27%)	0.4764
Overall average RNFL thickness (µm)¶	69.65 ± 30.76	58.62 ± 30.34	91.72 ± 18.84	56.72 ± 31.12	0.0034	77.45 ± 28.22	49.91 ± 29.59	0.003	62.29 ± 31.76	74.21 ± 30.27	0.151
Inferior nasal RNFL thickness (µm)¶	85.52 ± 45.73	72.88 ± 43.15	113.1 ± 39.66	69.78 ± 39.21	0.0068	98.1 ± 40.9	57.36 ± 39.43	P<0.0001	76.65 ± 45.85	92.14 ± 42.34	0.0724
Superior nasal RNFL thickness (µm)¶	81.56 ± 39.72	68.23 ± 39.24	107.4 ± 29.87	64.28 ± 34.11	0.0031	90.18 ± 35.44	57.14 ± 38.04	0.0009	70.59 ± 39.35	88 ± 38.05	0.0639
Nasal RNFL thickness (µm)¶	49.69 ± 28.05	39.65 ± 28.56	68.61 ± 16.06	37.06 ± 26.95	0.0016	56.68 ± 24.48	30.27 ± 27.12	0.0003	43.50 ± 30.12	51.93 ± 25.59	0.2548
Inferior temporal RNFL thickness (µm)¶	94.48 ± 44.53	84.50 ± 46.08	118.8 ± 30.96	85.22 ± 49.32	0.055	106.4 ± 42.37	73.32 ± 43.62	0.0042	87.38 ± 47.58	103.5 ± 41.64	0.1337
Superior temporal RNFL thickness (µm)¶	95.98 ± 42.09	80.54 ± 38.55	127.6 ± 27.24	73.78 ± 44.71	0.0005	106 ± 41.28	67.23 ± 36.61	0.0008	87.82 ± 41.51	97.57 ± 46.18	0.5812
Temporal RNFL thickness (µm)¶	49.17 ± 20.38	41.77 ± 18.54	64.61 ± 12.83	40.61 ± 21.78	0.0009	52.63 ± 19.69	39.77 ± 20.64	0.0149	43.24 ± 19.76	53.93 ± 20.88	0.0445

Abbreviations: NMOSD= neuromyelitis optica spectrum disorders; LETM= longitudinal extensive transverse myelitis; ON= optic neuritis;

AQP4ab+= seropositivity for anti-AQP4 antibody; AQP4ab-= seronegativity for anti-AQP4 antibody; EDSS= expanded disability status scale

***Median (range); **CSF Oligoclonal bands= Two or more cerebrospinal fluid restricted IgG oligoclonal bands**

¶Mean ± (SD); †Kruskal-Wallis with Dunn's Multiple Comparison Test; ‡Mann Whitney test

Table 2. Brain structures volumetric reduction and areas of cortical thinning (mean left and right hemispheres) in NMOSD patients, comparing its clinical presentations, AQP4ab serostatus and length of disease duration to normal controls.

Gray matter area	NC	NMOSD	*p* value¥	NMO	LETM	ON	*p* value†	AQP4ab +	AQP4ab -	*p* value¥	= < 5 years	> 5 years	*p* value¥
Total cortex volume	438 ± 56.3	406.1 ± 85.9	0.0809	391.9 ± 76.5	383.2 ± 94.1	459.3 ± 75.4	0.027	403.1 ± 84.8	409.4 ± 89.01	0.1438	417.5 ± 89.2	380.9 ± 74.6	0.2407
Brain stem	20.24 ± 2.91	19.22 ± 4.57	0.2902	17.68 ± 3.58	20.62 ± 5.85	20.17 ± 4.04	0.1504	18.9 ± 5.43	19.6 ± 3.51	0.214	19.8 ± 4.55	17.9 ± 4.56	0.278
Optic quiasm	0.21 ± 0.09	0.22 ± 0.08	0.6228	0.19 ± 0.08	0.24 ± 0.08	0.25 ± 0.09	0.4451	0.20 ± 0.08	0.24 ± 0.09	0.5691	0.23 ± 0.08	0.19 ± 0.08	0.1824
Cerebellar cortex	91.51 ± 10.7	88.95 ± 24.8	0.5918	79.64 ± 16.4	93.07 ± 32.1	100.1 ± 23.6	0.0663	87.3 ± 26	90.9 ± 24.1	0.3077	93.3 ± 26.9	79.5 ± 16.7	0.0884
Thalamus	6.62 ± 0.97	6.54 ± 1.37	0.7043	6.43 ± 1.31	6.14 ± 1.45	7.25 ± 1.18	0.0343	6.49 ± 1.27	6.6 ± 1.5	0.546	6.72 ± 1.32	6.16 ± 1.44	0.1499
Pericalcarine	1.62 ± 0.13	1.55 ± 0.16	0.0058	1.53 ± 0.15 *	1.57 ± 0.17	1.57 ± 0.17	0.0296	1.56 ± 0.15	1.54 ± 0.17 *	0.4856	1.56 ± 0.15	1.52 ± 0.17 *	0.3447
Lingual	2.04 ± 0.15	1.97 ± 0.17	0.0066	1.90 ± 0.12 **	1.97 ± 0.20	2.07 ± 0.17	0.0004	1.94 ± 0.16 *	1.99 ± 0.18	0.6473	1.98 ± 0.17	1.94 ± 0.17	0.4269
Cuneus	1.88 ± 0.13	1.80 ± 0.18	0.009	1.75 ± 0.13 **	1.84 ± 0.17	1.85 ± 0.23	0.0058	1.79 ± 0.15	1.82 ± 0.20	0.9063	1.81 ± 0.17	1.79 ± 0.20	0.6222
Pre-cuneus	2.38 ± 0.16	2.30 ± 0.19	0.0075	2.24 ± 0.13 **	2.32 ± 0.23	2.37 ± 0.20	0.0034	2.32 ± 0.18	2.27 ± 0.20 *	0.4285	2.32 ± 0.20	2.25 ± 0.15 *	0.1215
Fusiform	2.76 ± 0.17	2.75 ± 0.19	0.7292	2.71 ± 0.19	2.76 ± 0.20	2.82 ± 0.18	0.3437	2.76 ± 0.19	2.74 ± 0.19	0.6904	2.77 ± 0.19	2.71 ± 0.19	0.2429
Paracentral lobule	2.37 ± 0.18	2.21 ± 0.19	P<0.0001	2.16 ± 0.16 **	2.16 ± 0.23 *	2.34 ± 0.15	P<0.0001	2.21 ± 0.19 **	2.21 ± 0.20 **	0.5804	2.23 ± 0.21 **	2.17 ± 0.15 **	0.2018
Superior frontal	2.64 ± 0.20	2.48 ± 0.22	P<0.0001	2.46 ± 0.20 **	2.42 ± 0.24 **	2.59 ± 0.22	P<0.0001	2.51 ± 0.20 *	2.45 ± 0.25 **	0.7144	2.49 ± 0.24 **	2.46 ± 0.19 **	0.582
Frontal pole	2.75 ± 0.35	2.62 ± 0.33	0.0282	2.60 ± 0.33	2.54 ± 0.32	2.73 ± 0.32	0.0544	2.60 ± 0.27	2.63 ± 0.39	0.739	2.64 ± 0.32	2.58 ± 0.36	0.5171
Medial orbito-frontal	2.54 ± 0.20	2.40 ± 0.29	0.0024	2.43 ± 0.27	2.27 ± 0.33 **	2.50 ± 0.25	0.0006	2.45 ± 0.27	2.33 ± 0.31 **	0.5072	2.4 ± 0.32 *	2.39 ± 0.21	0.8177
Cingulate rostral anterior	2.99 ± 0.30	2.82 ± 0.36	0.0056	2.86 ± 0.36	2.67 ± 0.39 **	2.94 ± 0.30	0.003	2.87 ± 0.37	2.77 ± 0.36	0.7871	2.81 ± 0.39	2.85 ± 0.32	0.6651
Cingulate caudal anterior	2.68 ± 0.27	2.51 ± 0.30	0.0008	2.54 ± 0.30	2.45 ± 0.29 **	2.53 ± 0.32	0.0053	2.51 ± 0.32 *	2.50 ± 0.28 *	0.8974	2.50 ± 0.28 **	2.52 ± 0.36	0.8127
Cingulate posterior	2.65 ± 0.18	2.48 ± 0.23	P<0.0001	2.40 ± 0.17 **	2.49 ± 0.29 *	2.57 ± 0.21	P<0.0001	2.47 ± 0.23 **	2.48 ± 0.23 **	0.5172	2.51 ± 0.24 **	2.4 ± 0.17 **	0.0554
Cingulate isthmus	2.62 ± 0.24	2.51 ± 0.29	0.0275	2.45 ± 0.24	2.47 ± 0.37	2.65 ± 0.23	0.0121	2.5 ± 0.24	2.52 ± 0.35	0.8813	2.52 ± 0.30	2.48 ± 0.27	0.5708
Parahippocampal	2.91 ± 0.31	2.90 ± 0.37	0.7774	2.8 ± 0.42	2.90 ± 0.32	3.05 ± 0.29	0.1297	2.82 ± 0.42	2.98 ± 0.29	0.2447	2.85 ± 0.37	3.01 ± 0.35	0.1229
Entorhinal	3.58 ± 0.29	3.60 ± 0.40	0.7752	3.56 ± 0.37	3.50 ± 0.42	3.81 ± 0.38	0.0728	3.59 ± 0.38	3.61 ± 0.43	0.932	3.58 ± 0.43	3.65 ± 0.32	0.4924
Temporal pole	3.78 ± 0.47	3.87 ± 0.30	0.2016	3.90 ± 0.23	3.79 ± 0.38	3.92 ± 0.32	0.4472	3.96 ± 0.24	3.77 ± 0.33	0.1506	3.86 ± 0.31	3.9 ± 0.29	0.6132
Temporal inferior	2.84 ± 0.17	2.85 ± 0.22	0.7502	2.83 ± 0.18	2.85 ± 0.22	2.89 ± 0.27	0.7726	2.89 ± 0.22	2.80 ± 0.20	0.1138	2.89 ± 0.22	2.76 ± 0.19	0.0154
Temporal middle	2.87 ± 0.18	2.87 ± 0.23	1	2.82 ± 0.21	2.87 ± 0.23	2.96 ± 0.25	0.1991	2.89 ± 0.23	2.85 ± 0.22	0.4371	2.91 ± 0.25	2.79 ± 0.18	0.0442
Temporal superior	2.84 ± 0.18	2.75 ± 0.24	0.0201	2.73 ± 0.21	2.64 ± 0.25 *	2.89 ± 0.21	0.0003	2.76 ± 0.22	2.74 ± 0.26	0.9826	2.74 ± 0.25	2.77 ± 0.21	0.6598
Temporal transverse	2.38 ± 0.24	2.32 ± 0.34	0.2689	2.32 ± 0.29	2.15 ± 0.32	2.51 ± 0.37	0.0028	2.34 ± 0.33	2.3 ± 0.36	0.9756	2.32 ± 0.35	2.33 ± 0.35	0.9139
Frontal rostral-middle	2.25 ± 0.18	2.15 ± 0.17	0.001	2.15 ± 0.17	2.12 ± 0.18 *	2.18 ± 0.16	0.0077	2.16 ± 0.18	2.14 ± 0.15 *	0.8221	2.16 ± 0.17	2.12 ± 0.16 *	0.357
Frontal caudal-middle	2.40 ± 0.16	2.27 ± 0.18	P<0.0001	2.31 ± 0.18	2.21 ± 0.19 **	2.32 ± 0.16	0.0001	2.31 ± 0.19	2.25 ± 0.17 **	0.5061	2.27 ± 0.20 **	2.30 ± 0.15	0.5686
Frontal lateral-orbito	2.71 ± 0.20	2.63 ± 0.26	0.0412	2.64 ± 0.28	2.54 ± 0.20 *	2.71 ± 0.26	0.0327	2.66 ± 0.23	2.59 ± 0.29 *	0.5706	2.64 ± 0.26	2.6 ± 0.26	0.5511
Pre-central	2.48 ± 0.15	2.37 ± 0.16	0.0002	2.35 ± 0.16 *	2.33 ± 0.18 *	2.47 ± 0.09	0.0007	2.37 ± 0.16 *	2.38 ± 0.17	0.9751	2.37 ± 0.18	2.38 ± 0.10	0.9416
Post-central	1.99 ± 0.14	1.91 ± 0.16	0.0022	1.89 ± 0.15 **	1.89 ± 0.20	1.98 ± 0.13	0.0034	1.91 ± 0.15 *	1.92 ± 0.18	0.2163	1.94 ± 0.18	1.86 ± 0.11 **	0.042
Parietal superior	2.17 ± 0.16	2.05 ± 0.14	P<0.0001	2.02 ± 0.10 **	2.07 ± 0.20	2.08 ± 0.10	0.0003	2.08 ± 0.14	2.03 ± 0.14 **	0.4232	2.07 ± 0.15	2.02 ± 0.09 **	0.1065
Supramarginal	2.53 ± 0.17	2.37 ± 0.19	P<0.0001	2.35 ± 0.14 **	2.31 ± 0.24 **	2.49 ± 0.16	P<0.0001	2.4 ± 0.19 **	2.35 ± 0.19 **	0.9375	2.38 ± 0.22 **	2.36 ± 0.11 **	0.716
Parietal inferior	2.46 ± 0.19	2.33 ± 0.20	0.0002	2.29 ± 0.14 **	2.32 ± 0.27	2.42 ± 0.19	P<0.0001	2.35 ± 0.19 *	2.32 ± 0.22 *	0.5686	2.35 ± 0.22 *	2.29 ± 0.14 **	0.1308
Occipital lateral	2.19 ± 0.17	2.13 ± 0.15	0.06	2.09 ± 0.13	2.16 ± 0.17	2.17 ± 0.16	0.0565	2.11 ± 0.14	2.16 ± 0.16	0.3353	2.15 ± 0.14	2.09 ± 0.19	0.2267
Insula	3.04 ± 0.17	2.92 ± 0.23	0.0005	2.87 ± 0.21 **	2.87 ± 0.21 *	3.06 ± 0.23	P<0.0001	2.90 ± 0.20 **	2.94 ± 0.25	0.5156	2.94 ± 0.23	2.87 ± 0.22 **	0.2918

Abbreviations: NC= normal control; NMOSD= neuromyelitis optica spectrum disorders; LETM= longitudinal extensive transverse myelitis; ON= optic neuritis;

Mean ± SD of cortical thickness reported for each area in millimeters. For cerebellar cortex, thalamus, optic quiasm, brain stem and total cortex, the volume (in cm3) is reported and normalized for Intracranial Volume.

†Kruskal-Wallis with Dunn's Multiple Comparison Test; ¥Unpaired T Test with Welch's correction; * p< 0.05 compared to NC; ** p< 0.001 compared to NC.

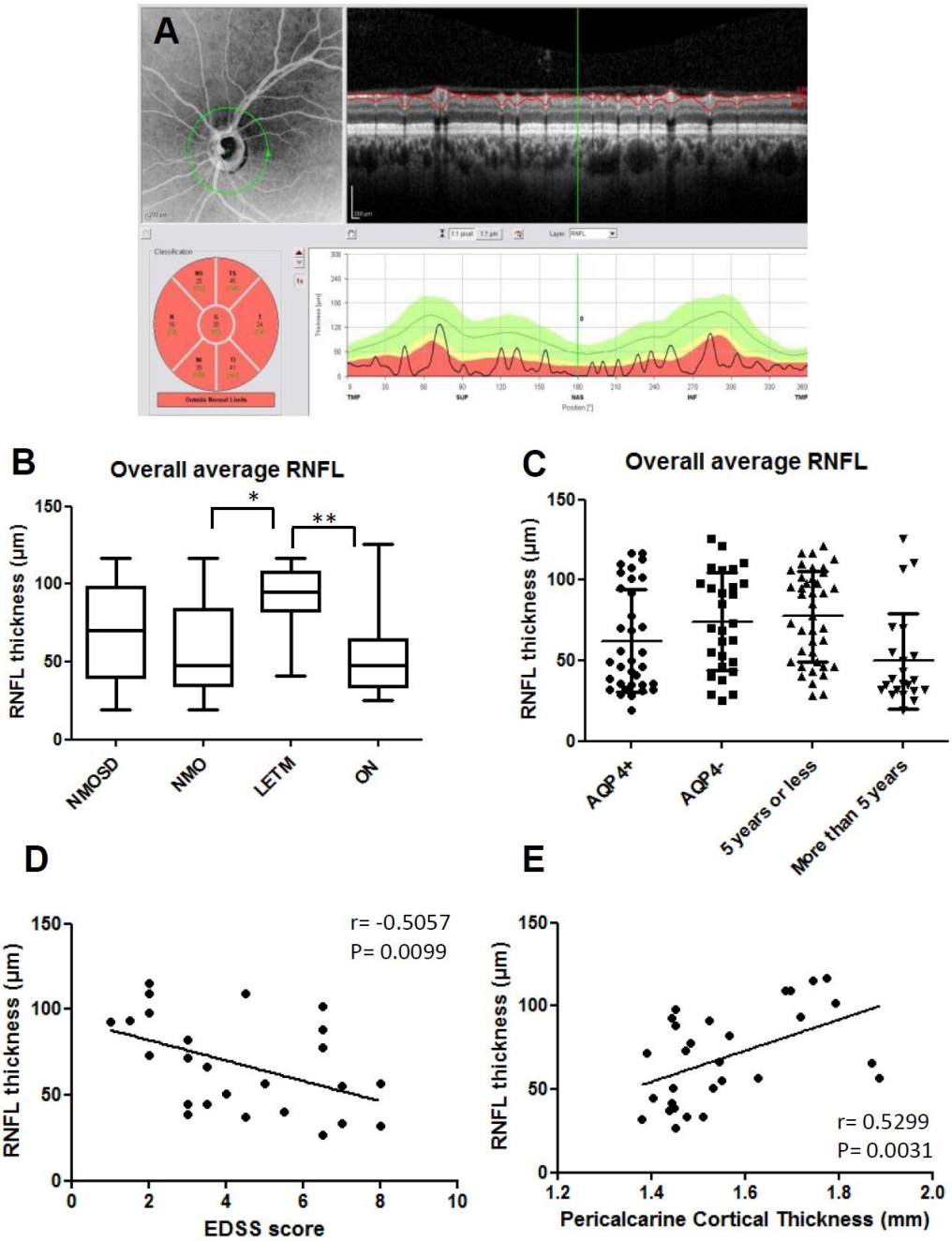

Figure 1. Retinal nerve fiber layer atrophy associated with EDSS score and pericalcarine cortical thinning. (**A**) An example of OCT analysis: the affected left eye of a NMO patient. Note the RNFL thinning in all sectors, indicating diffuse and severe axonal loss. (**B**) Pronounced RNFL atrophy in the NMO and ON groups compared with the LETM group (Kruskal–Wallis test with Dunn's multiple comparison, $p = 0.0016$). (**C**) Pronounced RNFL atrophy related to disease duration, in patients with more than 5 years of disease (Mann–Whitney test. $p=0.0034$). The differences in AQP4ab serostatus did not reach statistical significance. (**D**) RNFL thinning correlates with EDSS score ($r= -0.5057$, $r^2= 0.2166$, $p= 0.0099$). Each plot represents the correlation of the means of global right and left eye RNFL thickness and the EDSS score from each NMOSD patient. (**E**) RNFL atrophy correlates with pericalcarine cortical thickness ($r= 0.5299$, $r^2= 0.2451$, $p= 0.0031$). Each plot represents the correlation of the means of global right and left eye RNFL thickness and the means of right and left pericalcarine cortical thickness from each patient.

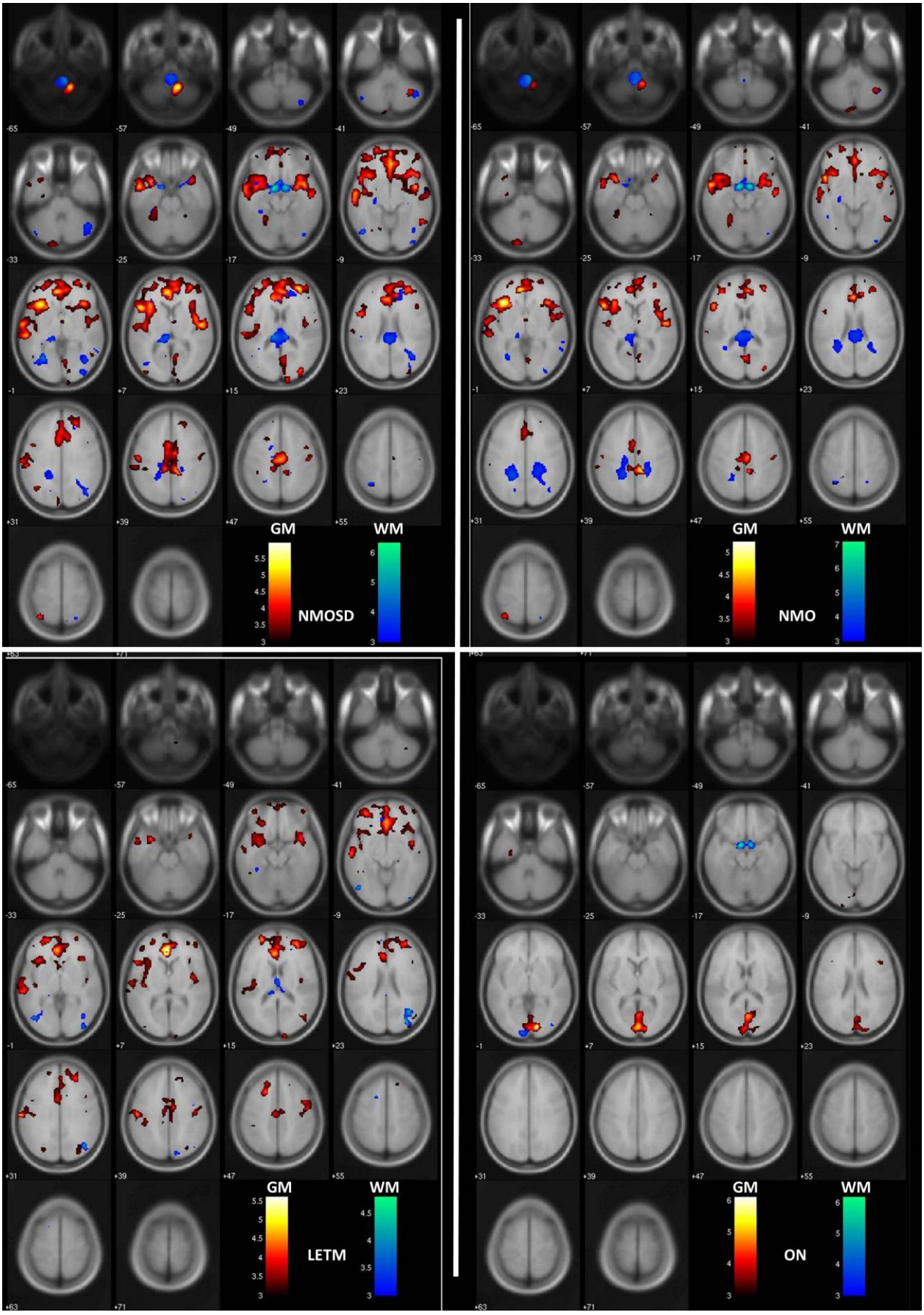

Figure 2A.

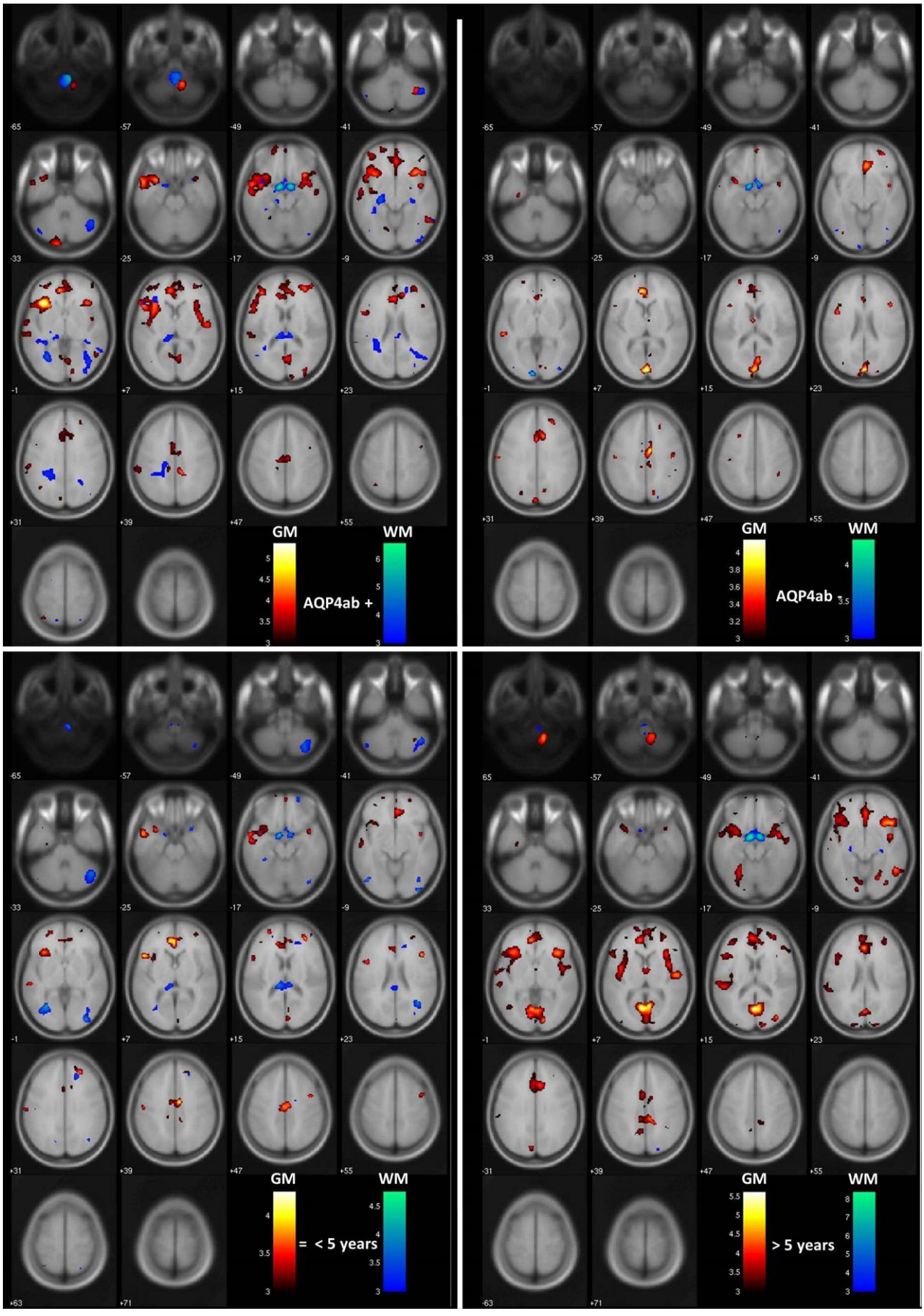

Figure 2B.

Figure 2. Voxel-based morphometry of cerebral gray matter (GM) and white matter (WM) in NMOSD patients, comparing its clinical presentations, AQP4ab serostatus and length of disease duration to controls. Results of voxelwise analysis showing areas of GM and WM volumetric reduction in patients with NMOSD, NMO, LETM, and ON (**A)** and in the AQP4ab**-**positive group**,** the AQP4ab-negative group**,** patients with disease duration ≤ 5 years**,** and patients with disease duration > 5 years **(B)** after comparison with age- and sex-matched controls. Note the GM volumetric reduction in some areas of the frontal, parietal, temporal, occipital, and limbic lobes and also cerebellum in the NMOSD group and in the NMO and LETM subgroups. ON group showed a restricted atrophy to the occipital lobe. Note the greater GM and WM atrophy in the AQP4ab-positive subgroup. In the subgroup with longer disease duration, GM atrophy was more pronounced after 5 years. Shorter disease duration presented more WM volumetric reduction. The results are shown on the MNI152 1 mm template. MNI z axis coordinates are shown (in mm) above each image. The color-coded bars represent the T score. The red bar relates to GM, the blue bar to WM.

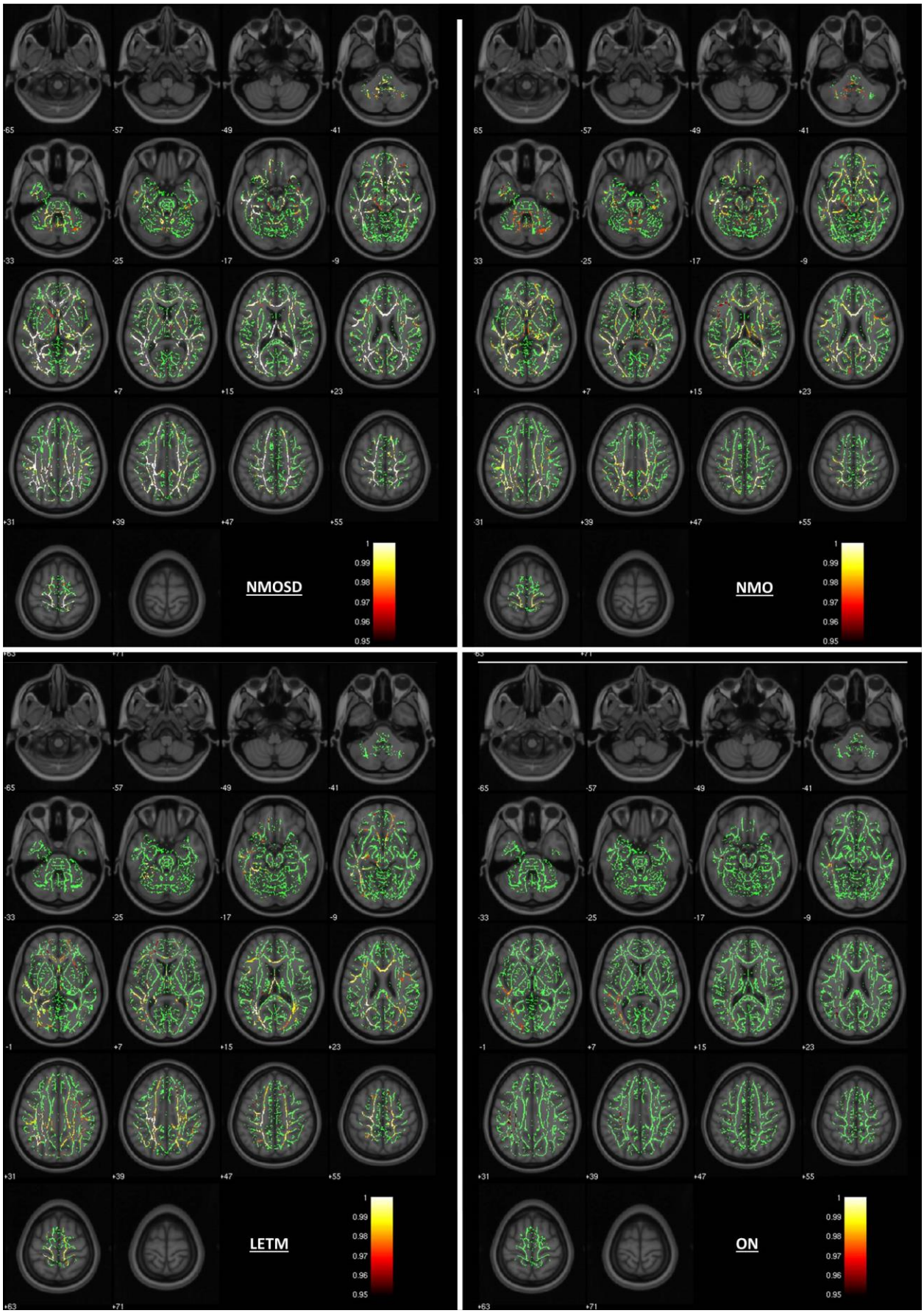

Figure 3A.

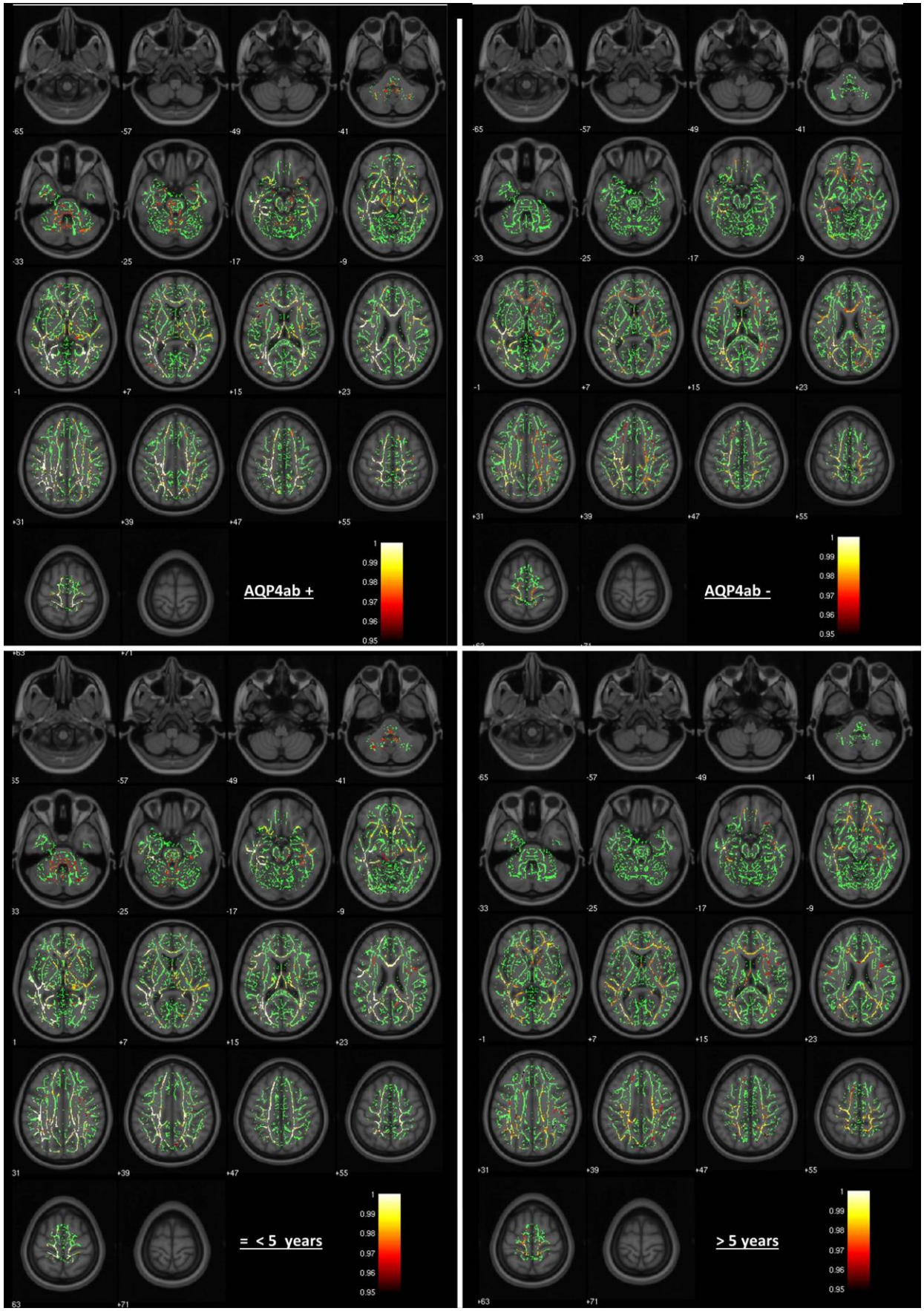

Figure 3B.

Figure 3. White matter microstructural abnormalities demonstrated by tract based spatial statistics in NMOSD patients, comparing its clinical presentations, AQP4ab serostatus and length of disease duration to controls. Voxelwise analysis showing areas of reduced fractional anisotropy (FA) in patients of the NMOSD group, the NMO group, the LETM group, and ON group (**A**), and the AQP4ab-positive group, those of the AQP4ab-negative group, those with disease duration ≤ 5 years, and those with disease duration > 5 years (**B**) after comparison with age- and sex-matched controls. Areas with reduced FA are shown in yellow–red and represent cluster-based values (p<0.05, corrected with familywise error correction). The results are shown on the MNI152 1 mm template. MNI z axis coordinates are shown (in mm) above each image. The color-coded bar represents p values ranging from 0.05 to <0.001.

Supplementary data

Comprehensive MRI protocol for demyelinating disease

MRI protocol. All individuals underwent a comprehensive MRI protocol for demyelinating disease which would enable us to disclose any MS like lesions. This protocol included MRI encompassing brain, cervical and thoracic spine, with the following sequences:

Brain

1. T2-weighted TSE images acquired in the axial plane with 4mm slice thickness (TR=2581.9ms, TE= 80ms, matrix= 560 x 560mm, field of view= 505 x 554mm).
2. T2-weighted FLAIR images acquired in the axial plane with 4mm slice thickness (TR= 12000ms, TE= 140ms, matrix= 448x 448, field of view= 1145 x 554mm).
3. Volumetric (three-dimensional) T2-weighted FLAIR images were acquired in the sagittal plane with 1mm slice thickness (TR= 5000ms, TE= 334ms, matrix= 240 x 240, field of view=1145 x 554mm).
4. T1-weighted MT images acquired in the axial plane with 4mm slice thickness (TR= 636.5ms, TE= 10ms, matrix= 512 x 512mm, field of view= 505 x 554mm), before and after intravenous infusion of paramagnetic contrast agent.
5. T2-weighted STIR images acquired in the axial plane with 4mm slice thickness (TR= 3555.4ms, TE= 40ms, matrix= 560 x 560, field of view= 505 x 554mm).
6. Diffusion echoplanar images acquired in the axial plane with 4mm slice thickness (TR= 4080.4ms, TE= 74.4ms, matrix= 256 x 256, field of view= 1145 x 554mm).
7. Volumetric (three-dimensional) T1-weighted MT images were acquired in the sagittal plane with 2mm slice thickness (TR= 15ms, TE= 1.7ms, matrix= 240 x 240, field of view= 505 x 554mm), after intravenous infusion of paramagnetic contrast agent.

Spine

1. T2-weighted TSE images acquired in the sagittal plane with 3mm slice thickness (TR= 2898.9ms, TE= 120ms, matrix= 560 x 560, field of view= 505 x 554mm).

2. T2-weighted TSE with fat suppression images acquired in the sagittal plane with 3 mm slice thickness (TR= 3530.3ms, TE= 120ms, matrix= 560 x 560, field of view= 1145 x 554mm).
3. T1-weighted TSE images acquired in the sagittal plane with 3mm slice thickness (TR= 584ms, TE= 7.3ms, matrix= 512 x 512, field of view= 1145x 554mm), before and after intravenous infusion of paramagnetic contrast agent.
4. Proton density images acquired in the sagittal plane with 3mm slice thickness (TR= 1500ms, TE= 8ms, matrix=512 x 512, field of view= 504 x 554mm).
5. T2-weighted TSE images acquired in the axial plane with 4mm slice thickness (TR= 3143.7ms, TE= 120ms, matrix= 512 x 512, field of view= 505 x 512mm).
6. T2-weighted VISTA images were acquired in the sagittal plane with 3,2mm slice thickness (TR= 1800ms, TE= 149.4ms, matrix= 512 x 512, field of view= 505 x 554mm).

VBM and DTI. We also obtained two specific sequences that were later employed for voxel-based morphometry (VBM) and diffusion tensor imaging (DTI) analyses, respectively.

Volumetric (three-dimensional) T1-weighted gradient echo images were acquired in the sagittal plane with 1 mm slice thickness (flip angle=35°, TR=7.1 ms, TE=3.2 ms, matrix=240 × 240, field of view=240 × 240 mm). DTI was undertaken via a 32-direction non-collinear echo planar sequence (flip angle=90°, voxel size=2×2×2 mm^3, TR=8500 ms, TE=61 ms, matrix=128 × 128, field of view=256 × 256 mm, 70 slices with 3 mm thickness, b value =1000).

VBM protocol and analysis. We used VBM8 (http://dbm.neuro.uni-jena.de/vbm) SPM8 (http://www.fil.ion.ucl.ac.uk/spm) running on MATLAB-R2012b to extract GM and WM maps from each subject and to perform statistical comparisons among different groups and controls. This process includes spatial normalization of all image data to the same stereotaxic space; segmentation and tissue extraction; spatial smoothing; and correction for volume changes induced by spatial normalization (modulation). Regarding spatial

normalization, we also applied a more sophisticated registration model (the DARTEL algorithm) that substantially reduces the imprecision of intersubject registration[22].

Processed images of patients and controls were compared using a voxelwise statistical analysis[23]. We used full factorial design from SPM to investigate patterns of WM and GM atrophy in the stratified subgroups [clinical (NMOSD, NMO, LETM, and ON), serum positivity (AQP4ab+ and AQP4ab–) and disease duration (<= 5 years and >5 years)] in comparison to healthy controls. We exclusively reported clusters that survived an uncorrected threshold of $p<0.001$ with at least 30 contiguous voxels and a minimum statistical T=3.4. The results were not corrected for multiple comparisons due to the exploratory nature of this study. In order to display the results and pinpoint their anatomical location we used an additional SPM extension, XJVIEW (http://www.alivelearn.net/xjview).

DTI analyses. We processed the diffusion data with FSL software V.4.1.4[24], starting with FMRIB's Diffusion Toolbox (FDT) to perform head motion and eddy current correction, followed by Brain Extraction Tool[25] to extract non-brain voxels and create a brain mask. Fractional anisotropy (FA) maps in the subject native space were then obtained by fitting a tensor model to the raw diffusion data with DTIFIT.

Comparison of groups was then carried out with tract-based spatial statistics (TBSS), also part of the FSL software V.4.1.4[26], which involves some pre-processing steps before the final analyses. All FA images are initially aligned to a standard space using the non-linear registration. The next step involves the creation of a mean FA template, which then enables the generation of the mean FA skeleton. Thereafter, each patient's aligned FA map is projected over this skeleton; this is an essential step in the processing algorithm because it removes the effect of cross-subject spatial variability. These final data are then used for voxelwise cross-subject statistics. The voxelwise statistics employed a permutation test (n=5000) using the "program randomize" segment of FSL. The statistically significant voxels were identified with threshold-free cluster enhancement (TFCE) applying familywise error correction threshold (FWE) for multiple comparisons with the threshold of $p<0.05$. We used the Johns Hopkins WM DTI-based atlas within the FSL, localizing the areas with FA reduction resulting from statistical analyses.

Supplementary Table 1. Results of voxel-based morphometry of cerebral gray matter (GM) and white matter (WM) in NMOSD patients, comparing its clinical presentations, AQP4ab serostatus and length of disease duration to controls.

Supplementary Table 1. Results of voxel-based morphometry of cerebral gray matter (GM) and white matter (WM) in NMOSD patients, comparing its clinical presentations, AQP4ab serostatus and length of disease duration to controls.

NMOSD					
Cluster	**Cluster size (voxels)**	***p* value**	**T**	**Peak MNI coordinates: x, y, z {mm}**	**Anatomic location**
GM					
1	53	p<0.001	3.61	45, 19.5, 24	R. frontal lobe, middle frontal gyrus
2	80	p<0.001	3.93	42, 3, 49.5	R. frontal lobe, middle frontal gyrus
3	236	p<0.001	3.84	48, -13.5, 46.5	R. frontal lobe, precentral gyrus
4	24	p<0.001	3.4	-21, 18, 48	L. frontal lobe, middle frontal gyrus
5	33741	p<0.001	5.65	-34.5, 22.5, 1.5	L. frontal lobe, medial frontal gyrus, limbic lobe, cingulate gyrus and insula
6	14	p<0.001	3.24	-45, -19.5, 27	L. parietal lobe, postcentral gyrus
7	10	p<0.001	3.45	-37.5, -36, 45	L. parietal lobe, inferior parietal lobule
8	84	p<0.001	3.95	-39, -61.5, 33	L. parietal lobe, angular gyrus
9	245	p<0.001	4.5	-34.5, -58.5, 61.5	L. parietal lobe, superior parietal lobule
10	6466	p<0.001	5.78	42, 1.5, -12	R. temporal lobe, superior temporal gyrus
11	234	p<0.001	4.36	54, -57, -7.5	R. temporal lobe, inferior temporal gyrus
12	352	p<0.001	5	34.5, -82.5, 13.5	R. occipital lobe,middle occipital gyrus
13	25	p<0.001	3.24	25.5, -91.5, 27	R. occipital lobe, cuneus
14	6	p<0.001	3.24	25.5, -81, 27	R. occipital lobe, precuneus
15	373	p<0.001	4.15	12, -100.5, 13.5	R. occipital lobe, cuneus
16	54	0.001	3.67	-39, -88.5, 7.5	L. occipital lobe, middle occipital gyrus
17	28	p<0.001	3.3	-6, -84, 30	L. occipital lobe, cuneus
18	9	p<0.001	3.64	-13.5, -69, -6	L. occipital lobe, lingual gyrus
19	15	p<0.001	3.61	30, -9, -6	R. Lentiform Nucleus
20	708	p<0.001	4.12	7.5, -64.5, 12	R. limbic lobe, posterior cingulate
21	1307	p<0.001	5.96	15, -49.5, -61.5	R. cerebellum posterior lobe
22	189	p<0.001	4.04	33, -57, -40.5	R. cerebellum posterior lobe and cerebellar Tonsil
23	193	p<0.001	3.64	-12, -94.5, -34.5	L. cerebellum posterior lobe and uvula
24	480	p<0.001	3.85	-27, -48, -21	L. cerebellum anterior lobe and Culmen
WM					
1	358	P<0.001	3.83	18, 40.5, 19.5	R. frontal lobe, medial frontal gyrus and limbic lobe, anterior cingulate
2	37	P<0.001	3.86	24, -61.5, 61.5	R. parietal lobe, superior parietal lobule
3	344	P<0.001	3.86	-30, -55.5, 54	L. parietal lobe, superior parietal lobule
4	32	P<0.001	3.87	58.5, -52.5, -4.5	R. temporal lobe, middle temporal gyrus

5	668	P<0.001	4.37	39, -61.5, 27	R. temporal lobe, middle temporal gyrus
6	64	P<0.001	3.64	-31.5, -39, -21	L. temporal lobe, fusiform gyrus
7	292	P<0.001	3.94	39, -70.5, -1.5	R. occipital lobe, sub-gyral, middle occipital gyrus
8	237	P<0.001	4.79	36, -90, 1.5	R. occipital lobe, middle occipital gyrus
9	822	P<0.001	4.93	-43.5, -73.5, -10.5	L. occipital lobe, middle occipital gyrus and lingual gyrus
10	31	P<0.001	3.39	-16.5, -24, 36	L. limbic lobe, cingulate gyrus
11	30	P<0.001	3.38	-15, 4.5, 48	L. limbic lobe, cingulate gyrus
12	1649	P<0.001	6.32	-10.5, -1.5, -19.5	L. limbic lobe, parahippocampal gyrus and uncus
13	2386	P<0.001	4.72	-9, -30, 13.5	L. sub-lobar, extra-nuclear, corpus callosum
14	367	P<0.001	3.93	43.5, -60, -37.5	R. cerebellum posterior lobe, tuber and cerebellar tonsil
15	60	P<0.001	3.54	-46.5, -69, -39	L. cerebellum posterior lobe, tuber

Abbreviations: NMOSD= neuromyelitis optica spectrum disorders; WM= white matter; GM=gray matter
Results reported on height threshold: T = > 3.0

NMO

Cluster	Cluster size (voxels)	*p* value	T	Peak MNI coordinates: x, y, z {mm}	Anatomic location
GM					
1	3563	p<0.001	4.51	51, -10.5, 7.5	R. frontal lobe, precentral gyrus
2	523	p<0.001	4.14	33, 46.5, 16.5	R. frontal lobe, middle frontal gyrus
3	68	p<0.001	3.75	46.5, -15, 48	R. frontal lobe, precentral gyrus
4	89	p<0.001	3.7	-22.5, 55.5, 3	L. frontal lobe, superior frontal gyrus
5	275	p<0.001	4.05	-36, 42, 13.5	L. frontal lobe, middle frontal gyrus
6	59	p<0.001	3.69	-46.5, 9, 27	L. frontal lobe, inferior frontal gyrus
7	32	p<0.001	3.6	-52.5, -13.5, 40.5	L. frontal lobe, precentral gyrus
8	107	p<0.001	3.68	-21, 61.5, -9	L. frontal lobe, superior frontal gyrus
9	300	p<0.001	4.01	51, -12, -16.5	R. temporal lobe, middle temporal gyrus
10	522	p<0.001	3.92	52.5, -54, -9	R. temporal lobe, inferior temporal gyrus
11	7167	p<0.001	5.24	-34.5, 24, 1.5	L. insula, inferior frontal gyrus, superior temporal gyrus
12	102	p<0.001	3.7	-43.5, -10.5, 6	L. insula and precentral gyrus
13	56	p<0.001	3.5	4.5, -70.5, -1	R. occipital lobe, lingual gyrus
14	330	p<0.001	4.15	1.5, -69, 18	R. occipital lobe, precuneus
15	105	p<0.001	4.4	33, -82.5, 13.5	R. occipital lobe, middle occipital gyrus
16	628	p<0.001	5.07	9, -37.5, 42	R. limbic lobe, cingulate gyrus
17	213	p<0.001	3.87	-7.5, -33, 43.5	L. limbic lobe, cingulate gyrus
18	5422	p<0.001	4.81	-1.5, 31.5, 25.5	L. limbic lobe, anterior cingulate and medial frontal gyrus
19	32	0.001	3.41	-10.5, -60, 4.5	L. limbic lobe, posterior cingulate
20	178	p<0.001	3.7	34.5, -60, -43.5	R. cerebellum posterior lobe, cerebellar tonsil
21	565	p<0.001	4.39	13.5, -48, -60	R. cerebellum posterior lobe

22	292	p<0.001	3.58	-24, -52.5, -18	L. cerebellum anterior lobe, culmen
23	275	p<0.001	3.72	-12, -94.5, -34.5	L. cerebellum posterior lobe
WM					
1	2120	P<0.001	4.21	-19.5, -45, 33	L. parietal lobe, sub-gyral and cingulate gyrus
2	68	P<0.001	4.18	58.5, -52.5, -4.5	R. temporal lobe, middle temporal gyrus
3	3759	P<0.001	4.35	-7.5, -30, 13.5	L. sub-lobar, extra-nuclear and corpus callosum
4	1193	P<0.001	7.09	-9, -1.5, -18	L. limbic lobe, parahippocampal gyrus
5	76	P<0.001	4	34.5, -88.5, 1.5	R. occipital lobe, middle occipital gyrus
6	109	P<0.001	3.86	-28.5, -64.5, -4.5	L. occipital lobe, lingual gyrus
7	1692	P<0.001	5.23	6, -39, -63	Medulla

Abbreviations: NMO= neuromyelitis optica; WM= white matter; GM=gray matter
Results reported on height threshold: T = > 3.0

LETM

Cluster	Cluster size (voxels)	*p* value	T	Peak MNI coordinates: x, y, z {mm}	Anatomic location
GM					
1	94	p<0.001	3.67	43.5, 55.5, -15	R. frontal lobe, middle frontal gyrus
2	181	p<0.001	3.77	27, 58.5, -4.5	R. frontal lobe, superior frontal gyrus
3	723	p<0.001	4.19	48, -7.5, 45	R. frontal lobe, precentral gyrus
4	454	p<0.001	4.27	-19.5, 21, 48	L. frontal lobe, superior frontal gyrus
5	101	p<0.001	3.56	-39, 40.5, 12	L. frontal lobe, inferior frontal gyrus
6	192	p<0.001	3.67	-42, 9, 24	L. frontal lobe, inferior frontal gyrus
7	53	0.001	3.4	-12, 51, 25.5	L. frontal lobe, superior frontal gyrus
8	118	p<0.001	3.46	31.5, -73.5, 36	R. parietal lobe, precuneus
9	136	p<0.001	3.76	-36, -27, 37.5	L. parietal lobe, inferior parietal lobule
10	936	p<0.001	4.71	-64.5, -18, 33	L. parietal lobe, postcentral gyrus
11	1292	p<0.001	4.75	42, 1.5, -12	R. temporal lobe, superior temporal gyrus
12	146	p<0.001	3.84	43.5, -73.5, 18	R. temporal lobe, middle temporal gyrus
13	173	p<0.001	3.8	-51, 1.5, -27	L. temporal lobe, middle temporal gyrus
14	4309	p<0.001	4.52	-58.5, -18, -6	L. temporal lobe, middle temporal gyrus and superior temporal gyrus
15	287	p<0.001	3.95	40.5, -6, 9	R. insula
16	815	p<0.001	4.04	9, -4.5, 40.5	R. limbic lobe, cingulate gyrus
17	10034	p<0.001	5.6	-1.5, 40.5, 7.5	L. limbic lobe, anterior cingulate
18	136	p<0.001	3.75	10.5, -103.5, 15	R. occipital lobe, cuneus
WM					
1	45	P<0.001	3.65	27, 42, 18	R. frontal lobe, superior and middle frontal gyrus
2	50	P<0.001	3.53	-15, 10.5, 52.5	L. frontal lobe, medial frontal gyrus
3	773	P<0.001	4.79	33, -78, 22.5	R. temporal lobe, sub-gyral, midle temporal gyrus, parietal lobe and angular gyrus
4	33	P<0.001	3.5	-33, -42, -21	L. temporal lobe, fusiform gyrus,

5	52	0.001	3.45	-10.5, -30, 13.5	L. sub-lobar, extra-nuclear
6	141	P<0.001	3.75	0, -15, 13.5	Inter-hemispheric, corpus callosum
7	105	0.001	3.83	39, -87, 1.5	R. occipital lobe, middle occipital gyrus
8	44	P<0.001	3.6	39, -70.5, -1.5	R. occipital lobe, sub-gyral
9	331	P<0.001	4.23	-46.5, -73.5, -12	L. occipital lobe, middle occipital gyrus

Abbreviations: LETM= longitudinal extensive transverse myelitis; WM= white matter; GM=gray matter
Results reported on height threshold: T = > 3.0

ON

Cluster	Cluster size (voxels)	*p* value	T	Peak MNI coordinates: x, y, z {mm}	Anatomic location
GM					
1	69	p<0.001	3.58	43.5, 19.5, 21	R. frontal lobe, middle frontal gyrus
2	56	p<0.001	3.6	-30, -15, -34.5	L. limbic lobe, uncus
3	4010	p<0.001	6.1	13.5, -87, -1	R. occipital lobe, lingual gyrus and cuneus
WM					
1	228	P<0.001	5.35	7.5, 0, -16.5	R. frontal lobe, subcallosal gyrus
2	285	P<0.001	6.16	-9, -1.5, -18	L. limbic lobe, parahippocampal gyrus
3	32	P<0.001	3.74	37.5, -84, 1.5	R. occipital lobe, middle occipital gyrus
4	229	P<0.001	4.36	-9, -97.5, -1.5	L. occipital lobe, cuneus and lingual gyrus

Abbreviations: ON= optic neuritis; WM= white matter; GM=gray matter
Results reported on height threshold: T = > 3.0

AQP4ab positive

Cluster	Cluster size (voxels)	*p* value	T	Peak MNI coordinates: x, y, z {mm}	Peak MNI coordinate region
GM					
1	47	p<0.001	4.52	40.5, 3, 51	R. frontal lobe, middle frontal gyrus
2	31	0.001	3.43	45, 55.5, 1.5	R. frontal lobe, middle frontal gyrus
3	753	p<0.001	4.29	33, 46.5, 15	R. frontal lobe, middle frontal gyrus
4	8419	p<0.001	5.36	-34.5, 24, 1.5	L. frontal lobe (inferior frontal gyrus) and temporal lobe (superior temporal gyrus)
5	235	p<0.001	3.66	-18, 55.5, -15	L. frontal lobe, superior frontal gyrus
6	68	p<0.001	3.66	-34.5, -58.5, 60	L. parietal Lobe, superior parietal lobule
7	257	p<0.001	3.6	-60, -28.5, 34.5	L. parietal lobe, inferior parietal lobule
8	41	0.001	3.41	51, -12, -16.5	R. temporal lobe, middle temporal gyrus
9	277	p<0.001	3.96	49.5, -58.5, 1.5	R. temporal lobe, middle temporal gyrus
10	125	p<0.001	3.57	-63, -7.5, -2.8	L. temporal lobe, superior temporal gyrus
11	107	p<0.001	3.66	-58.5, -25.5, 13.5	L. temporal lobe, superior temporal gyrus
12	2778	p<0.001	4.54	31.5, 18, -15	R.insula, frontal lobe, inferior frontal gyrus
13	774	p<0.001	4.06	6, -64.5, 12	R. limbic lobe, posterior cingulate
14	200	p<0.001	4.48	13.5, -40.5, 40.5	R. limbic lobe, cingulate gyrus
15	104	p<0.001	3.6	-10.5, -30, 43.5	L. limbic lobe, cingulate gyrus

16	4208	p<0.001	4.52	-9, 45, 1.5	L. limbic lobe, anterior cingulate
17	88	p<0.001	3.7	13.5, -87, -1	R. occipital lobe, lingual gyrus
18	78	p<0.001	3.75	-12, -70.5, -6	L. occipital lobe, lingual gyrus
19	75	p<0.001	3.66	12, -96, 12	R. occipital lobe, middle occipital gyrus
20	149	p<0.001	4.11	33, -84, 13.5	R. occipital lobe, middle occipital gyrus
21	584	p<0.001	4.45	13.5, -48, -60	R. cerebellum posterior lobe
22	273	p<0.001	4.07	33, -58.5, -42	R. cerebellar tonsil
23	387	p<0.001	4.07	-12, -94.5, -34.5	L. cerebellum posterior lobe
WM					
1	73	p<0.001	3.63	18, 46.5, 24	R. frontal lobe, superior frontal gyrus
2	46	p<0.001	3.6	-51, 21, 3	L. frontal lobe, inferior frontal gyrus
3	99	p<0.001	3.88	-34.5, 31.5, 10.5	L. frontal lobe, sub-gyral and inferior frontal gyrus
4	773	p<0.001	3.63	-31.5, -40.5, 34.5	L. parietal lobe, sub-gyral, inferior parietal lobule
5	36	p<0.001	3.48	30, -25.5, -9	R. temporal lobe, sub-gyral, hippocampus
6	104	p<0.001	4.36	57, -52.5, -4.5	R. temporal lobe, middle temporal gyrus
7	445	p<0.001	4.22	46.5, -63, 27	R. temporal lobe, superior temporal gyrus and middle temporal gyrus
8	75	p<0.001	3.59	9, -28.5, 15	R. sub-lobar, extra-nuclear
9	147	p<0.001	3.68	-31.5, -40.5, -3	L. sub-lobar, temporal lobe
10	445	p<0.001	3.86	-9, -30, 13.5	L. sub-lobar, extra-nuclear and corpus callosum
11	109	p<0.001	3.6	-16.5, -25.5, 36	L. limbic lobe, cingulate gyrus
12	1690	p<0.001	6.55	-10.5, -1.5, -19.5	L. limbic lobe, parahippocampal gyrus and sub-lobar, extra-nuclear
13	180	p<0.001	3.85	39, -72, -1.5	R. occipital lobe, middle occipital gyrus and inferior temporal gyrus
14	135	p<0.001	3.96	34.5, -88.5, 1.5	R. occipital lobe, middle occipital gyrus
15	338	p<0.001	4.39	-28.5, -64.5, -1.5	L. occipital lobe, lingual gyrus and middle occipital gyrus
16	506	p<0.001	4.2	42, -60, -37.5	R. cerebellum posterior lobe, tuber and cerebellar tonsil
17	74	p<0.001	3.5	-45, -69, -37.5	L. cerebellum posterior lobe, tuber
18	1535	p<0.001	5.53	7.5, -39, -64.5	Medulla

Abbreviations: AQP4ab+= seropositivity for anti-AQP4 antibody; WM= white matter; GM=gray matter.
Results reported on height threshold: T = > 3.0

AQP4ab negative

Cluster	Cluster size (voxels)	*p* value	T	Peak MNI coordinates: x, y, z {mm}	Peak MNI coordinate region
GM					
1	130	p<0.001	3.88	31.5, 52.5, -7.5	R. frontal lobe, middle frontal gyrus
2	72	p<0.001	3.62	45, 19.5, 24	R. frontal lobe, middle frontal gyrus
3	110	p<0.001	3.64	28.5, 40.5, 28.5	R. frontal lobe, superior frontal gyrus
4	55	p<0.001	3.46	43.5, -15, 40.5	R. frontal lobe, precentral gyrus

5	118	p<0.001	4.06	-42, 6, 25.5	L. frontal lobe, inferior frontal gyrus
6	70	p<0.001	3.66	12, -73.5, 36	R. parietal lobe, precuneus
7	53	p<0.001	3.69	39, -48, 42	R. parietal lobe,inferior parietal lobule
8	33	p<0.001	3.57	-51, -16.5, 40.5	L. parietal lobe, postcentral gyrus
9	125	p<0.001	4.15	42, 3, -12	R. temporal lobe, superior temporal gyrus
10	77	0.001	3.43	-31.5, 7.5, -18	L. temporal lobe, superior temporal gyrus
11	127	p<0.001	3.8	-55.5, -28.5, -3	L. temporal lobe, middle temporal gyrus
12	289	p<0.001	3.67	10.5, 18, 33	R. limbic lobe, cingulate gyrus
13	354	p<0.001	4.08	6, -6, 42	R. limbic lobe, cingulate gyrus
14	1000	p<0.001	4.08	-7.5, 42, 6	L. limbic lobe,anterior cingulate
15	67	p<0.001	3.67	-3, -6, 13.5	L. sub-lobar, thalamus
16	112	p<0.001	3.59	0, 13.5, 31.5	Inter-Hemispheric, limbic lobe, cingulate gyrus
17	1415	p<0.001	4.06	3, -87, 7.5	R. occipital lobe,cuneus
WM					
1	122	p<0.001	4.13	6, 4.5, -16.5	R. frontal lobe, subcallosal gyrus
2	169	p<0.001	4.34	-10.5, 2, -18	L. limbic lobe, parahippocampal gyrus
3	39	p<0.001	3.71	40.5, -72, -12	R. occipital lobe, middle occipital gyrus
4	56	p<0.001	4.05	37.5, -87, 1.5	R. occipital lobe, middle occipital gyrus
5	151	p<0.001	4.27	-6, -96, -3	L. occipital lobe, lingual gyrus and cuneus

Abbreviations: AQP4ab-= seronegativity for anti-AQP4 antibody; WM= white matter; GM=gray matter.

Results reported on height threshold: T = > 3.0

Longer Disease Duration

Cluster	Cluster size (voxels)	*p* value	T	Peak MNI coordinates: x, y, z {mm}	Peak MNI coordinate region
GM					
1	493	p<0.001	4.2	25.5, 52.5, 12	R. frontal lobe,middle frontal gyrus
2	103	p<0.001	3.75	46.5, 28.5, 10.5	R. frontal lobe, inferior frontal gyrus
3	4969	p<0.001	4.35	-36, 25.5, -1.5	L. frontal lobe, inferior frontal gyrus
4	173	p<0.001	3.88	-31.5, 46.5, 10.5	L. frontal lobe, middle frontal gyrus
5	151	p<0.001	3.76	-9, -54, 37.5	L. parietal lobe, precuneus
6	3810	p<0.001	5.06	54, -13.5, 9	R. temporal lobe, superior temporal gyrus
7	85	p<0.001	3.5	54, -7.5, -18	R. temporal lobe, middle temporal gyrus
8	317	p<0.001	4.49	51, -54, -9	R. temporal lobe, inferior temporal gyrus
9	100	p<0.001	3.7	-58.5, -28.5, -1.5	L. temporal lobe, superior temporal gyrus
10	107	p<0.001	3.54	-64.5, -9, -1.5	L. temporal lobe, superior temporal gyrus
11	36	p<0.001	3.49	-42, -63, 1.5	L. temporal lobe, middle temporal gyrus
12	4960	p<0.001	5.6	0, -67.5, 15	Inter-hemispheric, limbic lobe, posterior cingulate
13	627	p<0.001	5.06	15, -42, 42	R. limbic lobe, cingulate gyrus
14	40	p<0.001	3.56	10.5, 1.5, 39	R. limbic lobe, cingulate gyrus
15	4518	p<0.001	5.02	-1.5, 31.5, 25.5	L. limbic lobe, anterior cingulate
16	299	p<0.001	3.9	1.5, -4.5, 4.5	R. Sub-lobar, thalamus

17	197	p<0.001	4.01	21, -70.5, -7.5	R. occipital lobe, lingual gyrus
18	51	p<0.001	4.84	34.5, -78, -7.5	R. occipital lobe, inferior occipital gyrus
19	239	p<0.001	3.82	15, -93, 13.5	R. occipital lobe, middle occipital gyrus
20	139	p<0.001	4.84	34.5, -81, 13.5	R. occipital lobe, middle occipital gyrus
21	32	p<0.001	3.46	-21, -94.5, 21	L. occipital lobe, cuneus
22	102	p<0.001	3.92	-13.5, -85.5, -12	L. occipital lobe, lingual gyrus
23	1111	p<0.001	4.71	13.5, -52.5, -61.5	R. cerebellum posterior lobe
WM					
1	11	p<0.001	3.38	21, -81, 37.5	R. parietal lobe, precuneus
2	5	p<0.001	3.42	60, -54, -4.5	R. temporal lobe, middle temporal gyrus
3	36	0.001	3.41	0, -48, -60	Inter-hemispheric, limbic lobe
4	5	p<0.001	3.3	28.5, -24, -9	R. limbic lobe, parahippocampal gyrus
5	1255	p<0.001	8.36	-9, -1.5, -18	L. limbic lobe, parahippocampa gyrus and subcallosal gyrus
6	5	p<0.001	3.38	36, -88.5, 1.5	R. occipital lobe, middle occipital gyrus
7	50	0.001	3.41	6, -36, -61.5	Medulla

Abbreviations: WM=white matter, GM=gray matter

Results reported on height threshold: T = > 3.0

Shorter Disease Duration

Cluster	Cluster size (voxels)	*p* value	T	Peak MNI coordinates: x, y, z {mm}	Peak MNI coordinate region
GM					
1	42	p<0.001	3.47	24, 57, -6	R. frontal lobe, superior frontal gyrus
2	96	p<0.001	3.87	45, 19.5, 24	R. frontal lobe, middle frontal gyrus
3	213	p<0.001	3.94	25.5, 42, 27	R. frontal lobe, superior frontal gyrus
4	53	p<0.001	3.69	1.5, 58.5, -15	R. frontal lobe, medial frontal gyrus
5	142	p<0.001	3.83	33, 46.5, 15	R. frontal lobe, middle frontal gyrus
6	159	p<0.001	4.27	40.5, 3, 49.5	R. frontal lobe, middle frontal gyrus
7	49	p<0.001	3.6	-25.5, 57, 15	L. frontal lobe, middle frontal gyrus
8	827	p<0.001	4.03	-51, 18, 9	L. frontal lobe, precentral gyrus
9	52	p<0.001	3.69	-51, -15, 40.5	L. frontal lobe, precentral gyrus
10	65	p<0.001	3.58	-24, 55.5, 1.5	L. frontal lobe, superior frontal gyrus
11	143	p<0.001	4.25	42, 3, -12	R. temporal lobe, superior temporal gyrus
12	666	p<0.001	3.95	-51, 4.5, -22.5	L. temporal lobe, middle temporal gyrus
13	319	p<0.001	3.84	-31.5, 9, -24	L. temporal lobe, superior temporal gyrus
14	71	p<0.001	3.63	-57, -28.5, -1.5	L. temporal lobe, superior temporal gyrus
15	629	p<0.001	4.31	7.5, -6, 40.5	R. limbic lobe, cingulate gyrus
16	1275	p<0.001	4.15	-7.5, 42, 6	L. limbic lobe, anterior cingulate
17	64	0.001	3.44	-1.5, 13.5, 33	L. limbic lobe, cingulate gyrus
18	71	p<0.001	3.49	4.5, -85.5, 18	R. occipital lobe, cuneus
WM					
1	35	p<0.001	3.64	27, 40.5, 18	R. frontal lobe, sub-gyral

2	134	p<0.001	3.74	21, 37.5, 34.5	R. frontal lobe, medial frontal gyrus and anterior cingulate
3	48	p<0.001	3.51	21, 58.5, -18	R. frontal lobe, superior frontal gyrus
4	351	p<0.001	4.31	39, -60, 25.5	R. temporal lobe, superior temporal gyrus and middle temporal gyrus
5	32	p<0.001	3.51	-33, -40.5, -16.5	L. temporal lobe, fusiform gyrus
6	361	p<0.001	4.17	10.5, 1.5, -18	R. limbic lobe, parahippocampal gyrus and uncus
7	321	p<0.001	4.75	-10.5, -1.5, -19.5	L. limbc lobe, parahippocampal gyrus
8	576	p<0.001	3.89	-7.5, -30, 12	L. sub-lobar, extra-nuclear, corpus callosum
9	418	p<0.001	4.17	36, -87, 1.5	R. occipital lobe, middle occipital gyrus and inferior occipital gyrus
10	675	p<0.001	4.41	-46.5, -75, -12	L. occipital lobe, middle occipital gyrus and lingual gyrus
11	445	p<0.001	3.85	30, -69, -52.5	R. cerebellum posterior lobe, inferior semi-lunar lobule
12	572	p<0.001	4.05	43.5, -61.5, -37.5	R. cerebellum posterior lobe,tuber
13	49	p<0.001	3.46	-45, -69, -39	L. cerebellum posterior lobe, tuber

Abbreviations: WM=white matter, GM=gray matter

Results reported on height threshold: T = > 3.0

Supplementary Table 2. Results of tract-based spatial statistics voxelwise analysis of FA in NMOSD patients, comparing its clinical presentations, AQP4ab serostatus and length of disease duration to controls.

Supplementary Table 2. Results of tract-based spatial statistics voxelwise analysis of FA in NMOSD patients, comparing its clinical presentations, AQP4ab serostatus and length of disease duration to controls.

NMOSD

Cluster	Cluster size (voxels)	*p* value*	Peak MNI coordinates: x, y, z {mm}	Anatomic location
WM				
1	65330	P<0.001	-38, -49, -6	L. and R. Sagittal stratum (include inferior longitudinal fasciculus and inferior fronto-occipital fasciculus); Middle cerebellar peduncle; Genu, body and splenium of corpus callosum; R. and L. Anterior, superior and posterior corona radiata; L. and R. Posterior thalamic radiation (include optic radiation); R. and L. external capsule; R. and L. Superior longitudinal fasciculus; R. and L. Medial lemniscus; R. and L. Inferior and superior cerebellar peduncle; R. and L. Cerebral peduncle; R. and L. Anterior, posterior limb and retrolenticular part of internal capsule; R. and L. Cingulum (cingulate gyrus and hippocampus); R. and L. Fornix / Stria terminalis.

Abbreviations: NMOSD= neuromyelitis optica spectrum disorders; WM= white matter
*** two sample t test with family wise error correction**

NMO

Cluster	Cluster size (voxels)	*p* value*	Peak MNI coordinates: x, y, z {mm}	Anatomic location
WM				
1	51444	0.002	-34, -60, -3	L. and R. Posterior thalamic radiation (include optic radiation); Genu, body and splenium of corpus callosum; Middle cerebellar peduncle; R. and L. Inferior and superior cerebellar peduncle; R. and L. Anterior, superior and posterior corona radiata; R. and L. External capsule; R. and L. Anterior, posterior limb and retrolenticular part of internal capsule; R. and L. Cerebral peduncle; R. and L. Sagittal stratum (include inferior longitudinal fasciculus and inferior fronto-occipital fasciculus); R. and L. Superior longitudinal fasciculus; R. and L. Fornix / Stria terminalis; R. and L. Cingulum (cingulate gyrus and hippocampus).

Abbreviations: NMO= neuromyelitis optica; WM= white matter
*** two sample t test with family wise error correction**

LETM

Cluster	Cluster size (voxels)	*p* value*	Peak MNI coordinates: x, y, z {mm}	Anatomic location
WM				
1	77	0.047	31, -24, -7	R. Fornix / Stria terminalis; R. Retrolenticular part of internal capsule.
2	34697	0.001	-30, -22, 33	Genu, body and splenium of corpus callosum; R. and L. Posterior thalamic radiation (include optic radiation); R. and L. Superior longitudinal fasciculus; L. Retrolenticular part of internal capsule; R. and L. Anterior, superior and posterior corona radiata.

Abbreviations: LETM= longitudinal extensive transverse myelitis; WM= white matter;

*** two sample t test with family wise error correction**

ON

Cluster	Cluster size (voxels)	*p* value*	Peak MNI coordinates: x, y, z {mm}	Anatomic location
WM				
1	660	0.04	-32, -60, 22	L. Posterior corona radiata; L. Superior longitudinal fasciculus.
2	877	0.036	-42, -17, 28	L. Superior longitudinal fasciculus; L. Superior corona radiata.
3	2901	0.015	-41, -30, -15	L. Posterior thalamic radiation (include optic radiation); L. Retrolenticular part of internal capsule; L. Sagittal stratum (include inferior longitudinal fasciculus and inferior fronto-occipital fasciculus); L. Superior longitudinal fasciculus; L. External capsule; L. Posterior limb of internal capsule.

Abbreviations: ON= optic neuritis; WM= white matter;
*** two sample t test with family wise error correction**

AQP4ab positive

Cluster	Cluster size (voxels)	*p* value*	Peak MNI coordinates: x, y, z {mm}	Peak MNI coordinate region
WM				Middle cerebellar peduncle; Genu, body and splenium of corpus callosum; R. and L. Fornix / Stria terminalis, L. and R. Corticospinal tract; R. and L. Medial lemniscus; R. and L. Inferior and superior cerebellar peduncle;
1	57397	0.001	-40, -31, -16	R. and L. Cerebral peduncle; R. and L. Anterior, posterior limb and retrolenticular part of internal capsule; R. and L. Anterior, superior and posterior corona radiata; L. and R. Posterior thalamic radiation (include optic radiation); R. and L. External capsule; R. and L. Superior longitudinal fasciculus; L. and R. Sagittal stratum (include inferior longitudinal fasciculus and inferior fronto-occipital fasciculus); R. and L. Cingulum (hippocampus); L. Cingulum (cingulate gyrus).

Abbreviations: AQP4ab+= seropositivity for anti-AQP4 antibody; WM= white matter.
*** two sample t test with family wise error correction**

AQP4ab negative

Cluster	Cluster size (voxels)	*p* value*	Peak MNI coordinates: x, y, z {mm}	Peak MNI coordinate region
WM				Genu, body and splenium of corpus callosum; R. and L. anterior, superior and posterior corona radiata; L. and R. Posterior thalamic radiation (include optic radiation); L. and R. Sagittal stratum (include inferior longitudinal fasciculus and inferior fronto-occipital fasciculus);
1	35112	0.002	-40, -33, 0	R. and L. external capsule; L. and R. Superior longitudinal fasciculus; L. and R. Fornix / Stria terminalis; L. and R. Cingulum (cingulate gyrus); L. Cingulum (hippocampus); R. anterior limb of internal capsule; R. and L. posterior limb and retrolenticular part of internal capsule;

Abbreviations: AQP4ab-= seronegativity for anti-AQP4 antibody; WM= white matter
*** two sample t test with family wise error correction**

Shorter Disease Duration

Cluster	Cluster size (voxels)	*p* value*	Peak MNI coordinates: x, y, z {mm}	Peak MNI coordinate region
WM				
1	50143	0.001	-37, -34, -18	Genu, body and splenium of corpus callosum; Middle cerebellar peduncle; R. and L. Inferior and superior cerebellar peduncle; R. and L. Cerebral peduncle; L. and R. Posterior thalamic radiation (include optic radiation); L. and R. Sagittal stratum (include inferior longitudinal fasciculus and inferior fronto-occipital fasciculus); R. and L. external capsule; R. and L. Superior longitudinal fasciculus; R. and L. Fornix / Stria terminalis; R. and L. Cingulum (cingulate gyrus and hippocampus); R. and L. anterior, superior and posterior corona radiata; R. and L. anterior, posterior limb and retrolenticular part of internal capsule; R. and L. Medial lemniscus; R. and L. corticospinal tract; Pontine crossing tract (a part of MCP)

Abbreviations: WM=white matter

*** two sample t test with family wise error correction**

Longer Disease Duration

Cluster	Cluster size (voxels)	*p* value*	Peak MNI coordinates: x, y, z {mm}	Peak MNI coordinate region
WM				
1	182	0.048	35, -48, 31	R. Superior longitudinal fasciculus
2	15106	0.002	-30, -66, 0	L. Posterior thalamic radiation (include optic radiation); L. Superior longitudinal fasciculus; L. Fornix / Stria terminalis; L. External capsule; L. Sagittal stratum (include inferior longitudinal fasciculus and inferior fronto-occipital fasciculus); L. Superior and posterior corona radiata; L. Posterior limb and retrolenticular part of internal capsule; Body and splenium of corpus callosum; L. Cingulum (hippocampus).
3	19979	0.008	38, -50, -5	Genu, body and splenium of corpus callosum; R. anterior, posterior limb and retrolenticular part of internal capsule; R. and L. anterior and superior corona radiata; R. posterior corona radiata; R. Posterior thalamic radiation (include optic radiation); R. Sagittal stratum (include inferior longitudinal fasciculus and inferior fronto-occipital fasciculus); R. and L. External capsule; R. Superior longitudinal fasciculus; R. Fornix / Stria terminalis;

Abbreviations: WM=white matter

*** two sample t test with family wise error correction**

Supplemental Figure 1. Cortical thickness decreases in NMOSD patients.

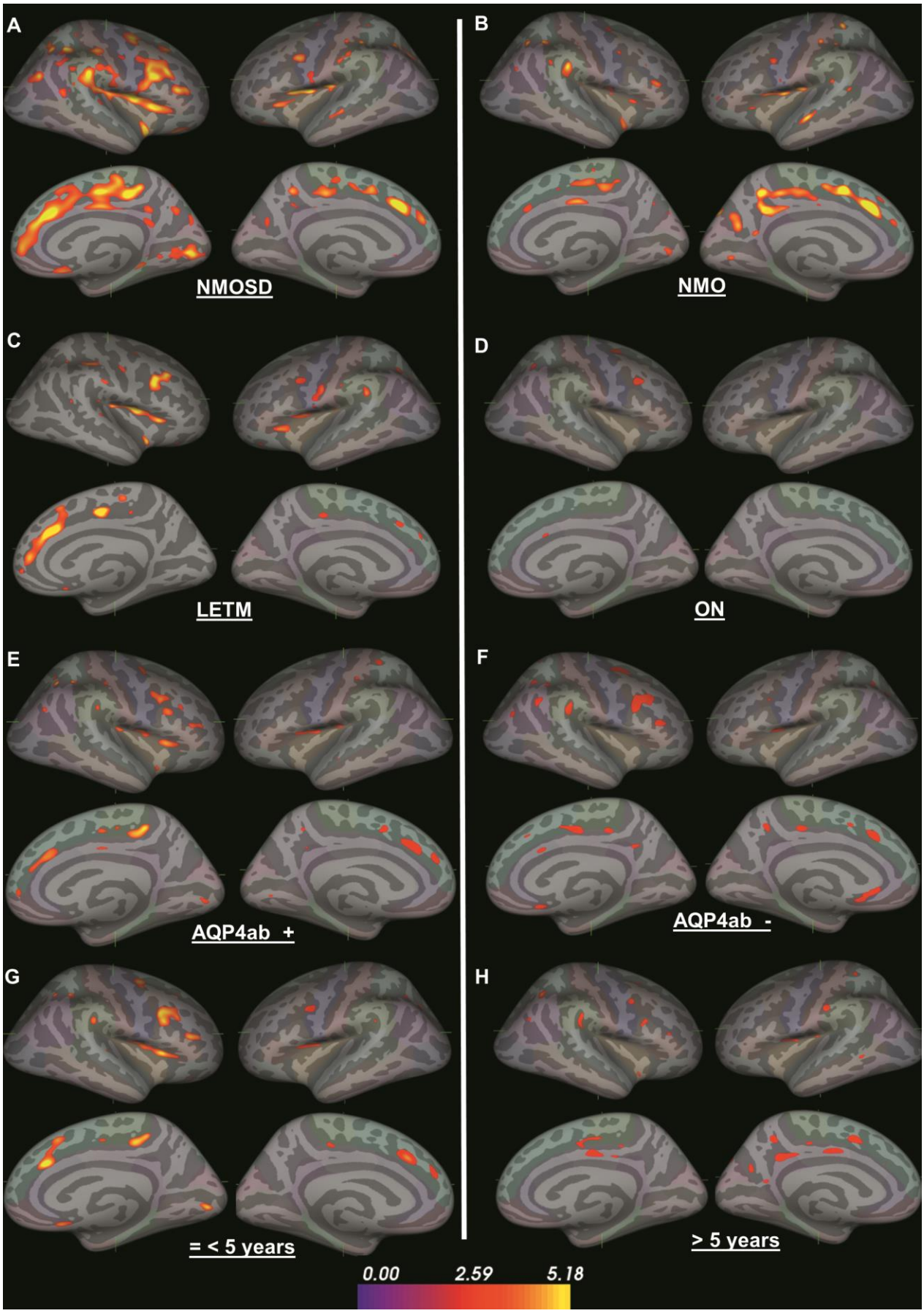

Discussão Geral

Conforme descrito no capítulo 1, para verificar se o HTLV-1 poderia agir como desencadeador do DENMO, foi investigada a presença de anticorpos anti-AQP4 em 22 indivíduos portadores assintomáticos de HTLV-1 e 26 com HAM/TSP, sendo que 3 deles eram co-infectados com HIV e/ou vírus da hepatite C. Um paciente apresentou HAM/TSP agudo, com história de NO de repetição e mielite transversa. Não foi detectado anti-AQP4 nos casos estudados. Foi feita também a pesquisa de anticorpo anti-HTLV-1 em um grupo de pacientes com diagnóstico de DENMO clínico e soropositivo para anti-AQP4 e nenhum destes pacientes apresentou anticorpo anti-HTLV-1 detectável. Esses achados sugerem que o HTLV-1 não parece ser um agente viral comum desencadeador do DENMO; que anti-AQP4 não está comumente envolvido na fisiopatogenia da mielopatia associada ao HTLV-1; que em áreas com alta prevalência de infecção pelo HTLV-1 e casos de DENMO, como o Brasil, pacientes com quadro clínico atípico de HAM/TSP deveriam ser investigados para presença do anticorpo anti-AQP4 para melhor definição diagnóstica e proposta terapêutica adequada.

Os dados apresentados sugerem que o HTLV-1 não seja um desencadeador do DENMO, uma doença autoimune, porém a coexistência das duas doenças poderia alterar a evolução natural delas, piorando a sua apresentação clínica. Em dois únicos relatos de casos na literatura sobre HAM/TSP aguda, os quais apresentavam anti-AQP4 positivo, este anticorpo foi titulado em altos níveis, ultrapassando o limite máximo de titulação do método utilizado (38,51). Níveis elevados de anti-AQP4 estão associados a pior evolução

clínica e riscos de surtos de mielite e/ou NO (2,20). Além disso, estes dois pacientes apresentavam múltiplas lesões desmielinizantes na substância branca encefálica vista na RNM de crânio (38,51). Estes níveis elevados de anti-AQP4 poderiam estar relacionados à estimulação de linfócitos B por células T infectadas pelo HTLV-1, o que levaria a maior produção de anticorpos derivados das células B estimuladas (52). Entretanto, mais estudos são necessários para definir se a infecção pelo HTLV-1 alteraria a evolução natural do DENMO, apresentando-se como um fator de pior prognóstico para os pacientes.

No capítulo 2, para verificar se a apresentação da doença (NMO, MTLE, NO), tempo de doença (5 anos ou menos do primeiro surto ou mais de 5 anos de duração) e detecção sérica do anticorpo anti-AQP4 (seropositivo ou seronegativo) resultariam em alterações estruturais da substância cinzenta e substância branca encefálica, foram analisadas as imagens de RNM de alto campo (3T) de 34 pacientes com DENMO e 34 controles sadios pareados por sexo e idade, bem como empregados métodos automatizados e sofisticados de computação (VBM, Freesurfer, TBSS) (31-33). Esta análise demonstrou que o DENMO está associado à atrofia de estruturas das substâncias cinzenta e branca cerebrais; que a atrofia não se limita apenas às áreas das vias sensorial, motora e visual, mas é mais difusa; e que quanto maior o tempo de doença e a presença do anticorpo anti-AQP4, maior é o grau de atrofia cortical.

Além disso, a OCT com espectro de dominância mostrou a presença de atrofia na camada de fibras nervosas retinianas, a qual foi maior nos casos de NO recorrente, NMO e mais de 5 anos de doença. Não foram detectadas lesões subclínicas nos pacientes que só apresentavam a forma de MTLE na nossa

casuística. Para estudar o provável mecanismo de degeneração retrógrada e/ou anterógrada após lesões axonais nos nervos ópticos, bem como seu efeito na via visual, foi demonstrada pela primeira vez uma correlação positiva entre atrofia retiniana e atrofia do sulco pericalcarino, a qual foi maior nos casos de NO recorrente e NMO. Houve também uma correlação da atrofia retiniana com a escala de incapacidade funcional expandida (EDSS), corroborando com o achado de atrofia mais difusa das estruturas da substância cinzenta e branca.

O número pequeno de pacientes avaliados (n=34) pode ser considerado um limitador ao estudo. Entretanto, a NMO é uma doença mais rara, principalmente quando se compara com a EMRR, e por isso, estudos envolvendo um único centro se tornam mais difícil de realizar. Por isso, para atenuar esta limitação, foram utilizadas neuroimagens adquiridas em RNM de alto campo (3T) e análises em três programas independentes, automatizados e validados na literatura, reduzindo as chances de vieses.

Apesar da ampla expressão de AQP4 no córtex cerebral, não foram constatados infiltrados inflamatórios ou lesões desmielinizantes que costumam ocorrer na EMRR e determinam, nesta doença, pontos de atrofia cortical mais intensa do que a observada no DENMO (23,24). A causa da atrofia cortical na NMO ainda não está completamente elucidada, mas a degeneração retrograda neuronal após lesões axonais na medula, nervos ópticos e substância branca profunda parece exercerem um importante papel. Mais estudos são necessários para explicar a aparente proteção da AQP4 cortical contra a citotoxicidade mediada por anticorpos e inflamação resultante observada nos sítios lesionais típicos do DENMO.

Conclusão Geral

Nossas observações permitem concluir que:

1. A mielopatia associada à variante aguda da HAM/TSP e aquela associada ao anticorpo anti-AQP4 são entidades clínicas distintas, e provalvemente, não interrelaciodas de forma patogênica.
2. Os pacientes com DENMO não apresentaram níveis detectáveis de anticorpos contra o HTLV-1.
3. A presença do anticorpo anti-AQP4 na NMO e NO, e mais de 5 anos de doença podem ser considerados fatores de pior prognóstico para atrofia da camada de fibras nervosas retinianas.
4. A NMO com o anticorpo anti-AQP4 e mais de 5 anos de doença podem ser considerados fatores de alto risco para atrofia do córtex e substância branca cerebral.
5. O padrão de atrofia do cortex cerebral encontrado, associado à correlação positiva entre atrofia da camada de fibras nervosas retinianas e atrofia pericalcarina, além da escala de incapacidade funcional expandida EDSS, sugere que a degeneração neuronal retrograda e/ou anterógrada do tipo Walleriana é um importante causador da atrofia cortical no DENMO.

Referências Bibliográficas

1. Wingerchuk DM, Hogancamp WF, O'Brien PC, Weinshenker BG. The clinical course of neuromyelitis optica (Devic's syndrome). Neurology 1999; 53: 1107-1114.
2. Jarius S, Ruprecht K, Wildemann B, et al. Contrasting disease patterns in seropositive and seronegative neuromyelitis optica: A multicentre study of 175 patients. J Neuroinflammation 2012; 9: 14. Acesso em (10/12/2012).
3. Jarius S, Paul F, Franciotta D, Waters P, et al. Mechanism of Disease: aquaporin-4 antibodies in neuromyelites optica. Nat Cl Pract Neurol 2008; 4: 202-214.
4. Wingerchuk DM. Diagnosis and treatment of neuromyelitis optica. Neurologist. 2007,13:2-11.
5. Devic E. Myelite aigue compliquee de nevrite optique. Bull Med (Paris) 8: 1033-1034.
6. Lennon VA, Wingerschuk DM, Kryzer TJ, Piltock SJ, et al. A serum autoantibody marker of neuromyelitis optica: distinction from multiple sclerosis. Lancet 2004; 364: 2106-2112.
7. Lennon VA, Kryzer TJ, Pittock SJ, Verkman AS, et al. IgG marker of optic-spinal multiple sclerosis binds to the aquaporin-4 water channel. J Exp Med 2005; 202: 473-477.
8. Jung JS, Bhat RV, Preston GM, Guggino WB, et al. Molecular characterization of an aquaporin cDNA from brain: candidate osmoreceptor and regulator of water balance. Proc Natl Acad Sci U S A; 91: 13052-13056.

9. Yukutake Y and Yasui M. Regulation of water permeability through aquaporin-4. Neuroscience 2010; 168: 885-891.
10. Lucchinetti CF, Mandler RN, McGavern D, et al. A role for humoral mechanisms in the pathogenesis of Devic's neuromyelitis optica. Brain 2002; 125: 1450-1461.
11. Wingerchuk DM, Lennon VA, Lucchinetti CF, Pittock SJ, et al. The spectrum of neuromyelitis optica. Lancet Neurol. 2007, 6: 805-815.
12. Matsushita T, Isobe N, Matsuoka T, Shi N, et al. Aquaporin-4 autoimmune syndrome and anti-aquaporin-4 antibody-negative opticospinal multiple sclerosis in Japanese. Mult Scler 2009;15: 834-847.
13. Matsuoka, T. Matsushita and Y. Kawano. Heterogeneity of aquaporin-4 autoimmunity and spinal cord lesions in multiple sclerosis in Japanese. Brain 2007; 130: 1206–1223.
14. Pittock SJ, Lennon VA, de Seze J, et al. Neuromyelitis optica and non-organ-specific autoimmunity. Arch Neurol 2008; 65: 78-83.
15. Matiello M, Lennon VA, Jacob A, et al. NMO-IgG predicts the outcome of recurrent optic neuritis. Neurology 2008; 70: 2197-2200.
16. Jarius S, Frederikson J, Waters P, et al. Frequency and prognostic impact of antibodies to aquaporin-4 in patients with optic neuritis. J Neurol Sci 2010; 298: 158-162.
17. Petzold A, Pittock S, Lennon V, et al. Neuromyelitis optica-IgG (aquaporin-4) autoantibodies in immune mediated optic neuritis. J Neurol Neurosurg Psychiatry 2010; 81: 109-111.

18. Adoni T, Lino AM, Marchiori PE, Kok F, et al.Seroprevalence of NMO-IgG antibody in Brazilian patients with neuromyelitis optica. Arq Neuropsiquiatr 2008, 66: 295-297.
19. Cayrol R, Saikali P, Vincent T. Effector functions of antiaquaporin-4 autoantibodies in neuromyelitis optica. Ann N Y Acad Sci 2009; 1173: 478-486.
20. Jarius S, Aboul-Enein F, Waters P, et al. Antibody to aquaporin-4 in the long-term course of neuromyelitis optica. Brain 2008; 131: 3072-3080.
21. Roemer SF, Parisi JE, Lennon VA, et al. Pattern-specific loss of aquaporin-4 immunoreactivity distinguishes neuromyelitis optica from multiple sclerosis. Brain 2007; 130: 1194-1205.
22. Lassman H. Cortical lesions in multiple sclerosis: inflammation versus neurodegeneration. Brain 2012; 135: 2904-2905.
23. Calabrese M, Oh MS, Favaretto A, et al. No MRI evidence of cortical lesions in neuromyelitis optica. Neurology 2012; 79: 1671-1676.
24. Popescu BF, Parisi JE, Cabrera-Gómez JA, et al. Absence of cortical demyelination in neuromyelitis optica. Neurology 2010; 75: 2103-2109.
25. Pichiecchio A, Tavazzi E, Poloni G, et al. Advanced magnetic resonance imaging of neuromyelitis optica: a multiparametric approach. Mult Scler 2012;18: 817-824.
26. Rocca MA, Agosta F, Mezzapesa DM, et al. Magnetization transfer and diffusion tensor MRI show gray matter damage in neuromyelitis optica. Neurology. 2004; 62: 476-478.

27. Merle H, Olindo S, Donnio A, Richer R, et al. Retinal peripapillary nerve fiber layer thickness in neuromyelitis optica. Invest Ophthalmol Vis Sci 2008; 49: 4412-4417.
28. de Seze J, Blanc F, Jeanjean L, et al. Optical coherence tomography in neuromyelitis optica. Arch Neurol 2008; 65: 920-923.
29. Green AJ, Cree BA. Distinctive retinal nerve fibre layer and vascular changes in neuromyelitis optica following optic neuritis. J Neurol Neurosurg Psychiatry 2009; 80: 1002-1005.
30. Ratchford JN, Quigg ME, Conger A, et al. Optical coherence tomography helps differentiate neuromyelitis optica and MS optic neuropathies. Neurology 2009; 73: 302-308.
31. Ashburner J, Friston KJ. Voxel-based morphometry—the methods. NeuroImage 2000; 11: 805-821.
32. Smith SM, Jenkinson M, Johansen-Berg H, et al. Tract-based spatial statistics: voxelwise analysis of multi-subject diffusion data. Neuroimage 2006; **31**: 1487-1505.
33. Fischl B. FreeSurfer. Neuroimage 2012; 62: 774-781.
34. Heerlein K, Jarius S, Jacobi C, Rohde S, at al. Aquaporin-4 antibody positive longitudinally extensive transverse myelitis following varicella zoster infection. J Neurol Sci 2009; 276: 184-186.
35. Yoshida Y, Saiga T, Takahashi H, Hara A. Optic neuritis and human T-lymphotropic virus type 1-associated myelopathy: a case report. Ophthalmologica 1998; 212: 73-76.

36. Kasahata N, Shiota J, Miyazawa Y, Nakano I, et al. Acute human T-lymphotropic virus type 1-associated myelopathy: a clinicopathologic study. Arch Neurol 2003; 60: 873-876.
37. Puccioni-Sohler M, Chimelli L, Merçon M, et al. Pathological and virological assessment of acute HTLV-I-associated myelopathy complicated with encephalopathy and systemic inflammation. J Neurol Sci 2003; 207: 87-93.
38. Koga M, Takahashi T, Kawai M, Negoro K, et al. Neuromyelitis optica with HTLV-1 infection: different from acute progressive HAM? Intern Med 2009; 48: 1157-1159.
39. Olindo S, Bonnan M, Merle H, et al. Neuromyelitis optica associated with subacute human T-lymphotropic virus type 1 infection. J Clin Neurosci 2010; 17: 1449-1451.
40. Verdonck K, González E, Van Dooren S, et al. Human T-lymphotropic virus 1: recent knowledge about an ancient infection. Lancet Infectious Disease 2007; 7: 266–281.
41. Gessain A and Cassar O. Epidemiological Aspects and World Distribution of HTLV-1 Infection. Front Microbiol 2012; 3: 388. Acesso em (01/02/2013).
42. Galvão-Castro B, Loures L, Rodrigues LG, et al. Distribution of human T-lymphotropic vírus type I among blood donors: a nationwide Brazilian study. Transfusion 1997; 37: 242-243.
43. Araujo AQ-C, Ali A, Newell A, Dalgleish AG, Rudge P. HTLV-I infection and neurologycal disease in Rio de Janeiro. J Neurol Neurosurg Psych 1992; 55: 153-155.

44. Araujo AQ, Silva MT. The HTLV-1 neurological complex. Lancet Neurol 2006; 5: 1068-1076.
45. Catalan-Soares B, Carneiro-Proietti AB, Proietti FA; Interdisciplinary HTLV Research Group. Heterogeneous geographic distribution of human T-cell lymphotropic viruses I and II (HTLV-I/II): serological screening prevalence rates in blood donors from large urban areas in Brazil. Cad Saude Publica 2005; 21: 926-931.
46. Lana-Peixoto MA, Lana Peixoto MI. Is multiple sclerosis in Brazil and Asia alike? Arq Neuropsiquiatr 1992; 50: 419-425.
47. Papais-Alvarenga RM, Miranda-Santos CM, Puccioni-Sohler M, et al. Optic neuromyelitis syndrome in Brazilian patients. J Neurol Neurosurg Psychiatry 2002; 73: 429-435.
48. Adoni T, Lino AM, da Gama PD, et al. Recurrent neuromyelitis optica in Brazilian patients: clinical, immunological, and neuroimaging characteristics. Mult Scler 2010; 16: 81-86.
49. Waters PJ, McKeon A, Leite MI, Rajasekharan S, et al. Serologic diagnosis of NMO: a multicenter comparison of aquaporin-4-IgG assays. Neurology 2012; 28; 78: 665-671.
50. Jarius S, Probst C, Borowski K, Franciotta D, at al. Standardized method for the detection of antibodies to aquaporin-4 based on a highly sensitive immunofluorescence assay employing recombinant target antigen. J Neurol Sci 2010, 291: 52-56.

51. Symmonds M, Nirmalananthan N, Taylor GP, Bridges LR, et al. Devastating aquaporin-4 and HTLV-1-associated necrotizing encephalopathy. J Neurol 2012; 259: 2732-2735.

52. Higuchi M, Nagasawa K, Horiuchi T, Oike M, et al. Membrane tumor necrosis factor-alpha (TNF-alpha) expressed on HTLV-I-infected T cells mediates a costimulatory signal for B cell activation--characterization of membrane TNF-alpha. Clin Immunol Immunopathol 1997; 82: 133-140.

Anexos

Anexo 1: Parecer do Comitê de Ética em Pesquisa aprovando o trabalho.

FACULDADE DE CIÊNCIAS MÉDICAS
COMITÊ DE ÉTICA EM PESQUISA

www.fcm.unicamp.br/pesquisa/etica/index.html

CEP, 28/01/11
(Grupo III)

PARECER CEP: N° 1274/2010 (Este n° deve ser citado nas correspondências referente a este projeto).
CAAE: 1002.0.146.000-10

I - IDENTIFICAÇÃO:

PROJETO: **"NEUROMIELITE ÓPTICA X MIELOPATIA ASSOCIADA AO HTLV-I: CARACTERIZAÇÃO DO ANTICORPO ANTI-AQUAPORINA 4 NA DOENÇA AUTO-IMUNE E NA INFECÇÃO VIRAL".**
PESQUISADOR RESPONSÁVEL: Felipe von Glehn Silva
INSTITUIÇÃO: Hospital das Clínicas/UNICAMP
APRESENTAÇÃO AO CEP: 13/12/2010
APRESENTAR RELATÓRIO EM: 28/01/12 (O formulário encontra-se no *site* acima).

II - OBJETIVOS

Determinar a presença de anticorpos anti-Aquaporina 4 no soro de pacientes com Neuro-Mielite Optica (NMO), com Mielopatia associada ao HTLV-1 (HAM), com sorologia positiva para HTLV-1 e em indivíduos normais, correlacionando com a gravidade da doença; correlacionar os títulos com a função de linfócitos B e T; correlacionar com achados da ressonância magnética;acompanhar a evolução das lesões medulares e comparar com os níveis de anti-Aqua 4.

III - SUMÁRIO

Trata-se de um estudo observacional descritivo e comparativo onde serão avaliados pacientes com NMO, HAM e pacientes soropositivos para HTLV-1 acompanhados no ambulatório de Esclerose Multipla e Neuroinfectologia do HC da Unicamp. A quantificação do anticorpo anti-Aqua 4 será feita através de imunofluorescencia indireta recombinante. Sua avaliação auxilia o diagnostico da NMO e será usada na comparação entre as patologias e com as imagens de ressonância para acompanhamento das lesões. Em conjunto serão avaliados os linfócitos B e T através de imunofenotipagem. As amostras serão coletadas no momento da inclusão no estudo, após 6 e 12 meses. Serão incluídos 25 pacientes com NMO, 25 com HAM, 25 pacientes assintomáticos com sorologia positiva para HTLV-1 e 25 controles sadios. Serão excluídos os pacientes com outras doenças auto-imunes além da NMO, com outras infecções além do HTLV-1 ou que recusarem participar. Alem das amostras de sangue será coletado liquor dos pacientes, mas não dos controles. Será feito comparação entre os níveis de ACS dos 4 grupos.

IV - COMENTÁRIOS DOS RELATORES

Comitê de Ética em Pesquisa - UNICAMP
Rua: Tessália Vieira de Camargo, 126
Caixa Postal 6111
13083-887 Campinas – SP

FONE (019) 3521-8936
FAX (019) 3521-7187
cep@fcm.unicamp.br

Após respostas às pendências, o projeto encontra-se adequadamente redigido e de acordo com a Resolução CNS/MS 196/96 e suas complementares, bem como o Termo de Consentimento Livre e Esclarecido.

V - PARECER DO CEP

O Comitê de Ética em Pesquisa da Faculdade de Ciências Médicas da UNICAMP, após acatar os pareceres dos membros-relatores previamente designados para o presente caso e atendendo todos os dispositivos das Resoluções 196/96 e complementares, resolve aprovar sem restrições o Protocolo de Pesquisa, bem como ter aprovado o Termo do Consentimento Livre e Esclarecido, assim como todos os anexos incluídos na Pesquisa supracitada.

O conteúdo e as conclusões aqui apresentados são de responsabilidade exclusiva do CEP/FCM/UNICAMP e não representam a opinião da Universidade Estadual de Campinas nem a comprometem.

VI - INFORMAÇÕES COMPLEMENTARES

O sujeito da pesquisa tem a liberdade de recusar-se a participar ou de retirar seu consentimento em qualquer fase da pesquisa, sem penalização alguma e sem prejuízo ao seu cuidado (Res. CNS 196/96 – Item IV.1.f) e deve receber uma cópia do Termo de Consentimento Livre e Esclarecido, na íntegra, por ele assinado (Item IV.2.d).

Pesquisador deve desenvolver a pesquisa conforme delineada no protocolo aprovado e descontinuar o estudo somente após análise das razões da descontinuidade pelo CEP que o aprovou (Res. CNS Item III.1.z), exceto quando perceber risco ou dano não previsto ao sujeito participante ou quando constatar a superioridade do regime oferecido a um dos grupos de pesquisa (Item V.3.).

O CEP deve ser informado de todos os efeitos adversos ou fatos relevantes que alterem o curso normal do estudo (Res. CNS Item V.4.). É papel do pesquisador assegurar medidas imediatas adequadas frente a evento adverso grave ocorrido (mesmo que tenha sido em outro centro) e enviar notificação ao CEP e à Agência Nacional de Vigilância Sanitária – ANVISA – junto com seu posicionamento.

Eventuais modificações ou emendas ao protocolo devem ser apresentadas ao CEP de forma clara e sucinta, identificando a parte do protocolo a ser modificada e suas justificativas. Em caso de projeto do Grupo I ou II apresentados anteriormente à ANVISA, o pesquisador ou patrocinador deve enviá-las também à mesma junto com o parecer aprovatório do CEP, para serem juntadas ao protocolo inicial (Res. 251/97, Item III.2.e)

Relatórios parciais e final devem ser apresentados ao CEP, de acordo com os prazos estabelecidos na Resolução CNS-MS 196/96.

VII- DATA DA REUNIÃO

Homologado na I Reunião Ordinária do CEP/FCM, em 18 de janeiro de 2011.

Prof. Dr. Carlos Eduardo Steiner
PRESIDENTE do COMITÊ DE ÉTICA EM PESQUISA
FCM / UNICAMP

Anexo 2- Termo de Consentimento Livre e Esclarecido (TCLE), conforme resolução 196/96.

Projeto: Neuromielite Óptica x Mielopatia associada ao HTLV-I: caracterização do anticorpo anti-Aquaporina 4 na doença auto-imune e na infecção viral.

Pesquisador Responsável: Felipe von Glehn Data:_____

Justificativa e Objetivos: A Neuromielite Óptica (NMO) é uma doença inflamatória auto-imune, que acomete adultos jovens. A incidência de tal doença em nosso meio vem aumentando, causando preocupação nos especialistas. Acredita-se atualmente que as lesões causadas pela Neuromielite Óptica sejam resultadas de uma agressão de um anticorpo contra o próprio organismo, gerando os surtos e a piora da doença. Este processo de auto-agressão, por que ele ocorre e quais células de defesa estão alteradas, é pouco compreendido. Por esta razão, estamos realizando este trabalho de pesquisa, para estudar que células estão envolvidas e por quê este auto anticorpo se forma, estudando o processo inflamatório no líquor e sangue dos pacientes que aceitarem a participação. Os resultados podem ajudar na criação futura de novos métodos diagnósticos e tratamentos.

Os pacientes serão estudados durante o acompanhamento normal que já realiza no ambulatório de EM.

Procedimentos: O paciente durante procedimento diagnóstico no ambulatório de neurologia da UNICAMP / HC será perguntado da autorização para coleta de 10ml do líquor (obtida pela punção lombar) e 10ml do sangue para os estudos. Não é necessário estar em jejum e nem interromper medicações utilizadas.

Risco e Desconforto: A coleta do líquor será realizada nas costas (região lombar). A dor que acompanha a punção lombar é semelhante aquela da coleta de sangue. O desconforto será mínimo, pois será realizada com anestesia local por profissional treinado e devidamente habilitado para a realização de punção lombar. Após submeter-se a punção lombar, o paciente deverá permanecer em repouso em casa, por 24 horas, e aumentar a ingestão de líquidos. Este repouso é importante para evitar dor de cabeça após a punção, impossibilitando a realização das atividades habituais. Se houver dor, mesmo com o repouso, o paciente deverá permanecer por mais alguns dias sem atividades e ingerir a medicação prescrita pelo seu médico. Este tipo de dor de cabeça não traz qualquer prejuízo ao paciente, mas necessita de repouso para desaparecer.

A coleta do líquor por utilizar agulha apresenta os riscos inerentes ao procedimento. São descritas, raramente, intercorrências da punção, como dormências transitórias, dor local e infecção. Entretanto, a incidência destas complicações é baixa . O material é descartável e as agulhas atuais (modelo 22Gx 3.5 = 70x7) são mais finas e de excelente qualidade. Caso ocorra qualquer desconforto após o procedimento, o paciente deverá contatar a equipe de atendimento do HC - UNICAMP e a equipe de pesquisa, que orientarão as medidas a serem tomadas para aliviar os sintomas, sem nenhum custo.

Benefícios: Melhor entendimento da Neuromielite Óptica para ajudar na criação futura de novos métodos diagnósticos e terapêuticos. Não existe benefício imediato para o paciente.

Esclarecimento: Todas as dúvidas e perguntas do paciente quanto aos assuntos relacionados com a pesquisa e o tratamento serão esclarecidas pelos pesquisadores.

Recusa ou descontinuação da participação: Durante o decorrer do estudo informaremos ao paciente o andamento da pesquisa, podendo este deixar de participar da pesquisa a qualquer momento, sem prejuízo no atendimento que recebe pelo HC – UNICAMP, caso decida não colaborar com a equipe, pois a participação do paciente é voluntária.

Sigilo: As informações recebidas durante e depois do estudo e a privacidade dos pacientes serão mantidas em sigilo. Os resultados serão sempre analisados em grupo, estatisticamente, não sendo possível identificar de forma individual qualquer paciente. Caso tenha alguma dúvida deverá procurar a Dr. Felipe von Glehn no telefone (19) 3521-6263, (19) 9769-0777

Gastos adicionais: Se houverem gastos adicionais (seringas, agulhas descartáveis, material de curativo...) estes serão absorvidos pelo orçamento da pesquisa.

Armazenamento de Material Biológico: Após o estudo realizado, geralmente sobra alguma quantidade de líquor e soro, que tem a capacidade de ser avaliada em novas pesquisas futuras, sem a necessidade de realizar procedimentos de punção, com todos os seus riscos e desconfortos. Eu □□ **autorizo** □□ **não autorizo** o estoque de meu material biológico para estudos futuros aprovados pelo Comitê de Ética da UNICAMP.

Eu confirmo que Felipe von Glehn me explicou o objetivo do estudo, os procedimentos aos quais serei submetido e os riscos, desconforto e possíveis vantagens advindas desse projeto de pesquisa. Eu li, e/ou me foi explicado, assim como compreendi e recebi uma cópia deste formulário de consentimento e estou de pleno acordo em participar do estudo.

Paciente ou Responsável:_____ Idade:
RG:

Endereço:

Assinatura : _____

Responsabilidade do pesquisador. Eu expliquei a _____ o objetivo do estudo, os procedimentos requeridos e os possíveis riscos e vantagens que poderão advir do estudo, usando o melhor do meu conhecimento. Eu me comprometo a fornecer uma cópia desse formulário de consentimento ao participante ou responsável.

Felipe von Glehn CRM-SP: 114233
Email.: fglehn@terra.com.br Tel.: (19) 9769-0777 / 3521-7754

Outros Membros da Equipe:
1) Carlos Otávio Brandão - Tel:(19) 3521-7754 2) Benito Damasceno - Tel:(19) 3521-7754
3) Leonilda dos Santos - Tel:(19) 3521-6263 4) Augusto César Penalva de Oliveira
5) Comitê de Ética em Pesquisa Tel:(19) 3521-8936

Email.: cep@fcm.unicamp.br
Rua Tessália Vieira de Camargo, 126 – Caixa Postal 6111
13083-887 Campinas-SP

Qualquer intercorrências médicas, ligar para qualquer um dos membros da equipe.